Molecular mechanisms controlling extracellular matrix remodeling and cellular responses to injury.

A dissertation

submitted by

Tatiana N. Demidova-Rice

In partial fulfillment of the requirements

for the degree of

Doctor of Philosophy

in

Cell, Molecular and Developmental Biology

TUFTS UNIVERSITY

Sackler School of Graduate Biomedical Sciences

February 2011

ADVISERS:

IRA M. HERMAN, PhD

MICHAEL R. HAMBLIN, PhD

Abstract

Cutaneous wound healing is a well-orchestrated process leading to re-establishment of normal function of skin within few weeks. However, in diabetic and elderly patients, this process is compromised leading to development of non-healing ulcers. Despite the introduction of numerous treatment modalities, chronic wounds remain a significant healthcare problem. This dissertation is focused on development of innovative approaches for stimulation of cutaneous wound healing. Specifically, we use Low Level Light Therapy (LLLT) and novel bioactive extracellular matrix protein fragments. LLLT is known for over 40 years but its efficacy remains controversial and the mechanisms of its activity are poorly understood. Our work in mouse models of cutaneous wound healing demonstrates that both coherent and non-coherent light can stimulate cellular responses to injury, identifies the most effective wavelength of light (820 nm) and establishes that there are significant variations in response to treatment between different strains of mice. We demonstrate that LLLT fosters fibroblast to myofibroblast transition and promotes wound contraction. While contraction is an important part of the healing process, its stimulation in human subjects might not be desirable as excessive contraction can lead to reduction of skin elasticity and loss of function. Therefore, next we focused on development of wound healing modalities that could enhance wound healing without stimulation of contraction. Previously it has been shown that collagenase from *Clostridium histolyticum* promotes cellular responses to injury both in vitro and in vivo. We hypothesize that stimulation of repair occurs via collagenase-mediated release of matrix-associated bioactive moieties. We used endothelial ECM degraded by bacterial collagenase and immunoprecipitated with anti-collagen antibodies to identify these biologically active peptides. We isolated several fragments of collagen IV, fibrillin 1, tenascin X and created a novel peptide as a combination between fibrillin 1 and tenascin X. The peptides increase rates of microvascular endothelial cell proliferation by 50% and in vitro angiogenesis by 200% when compared to serum-stimulated controls. Moreover, we demonstrate that combinatorial peptide, applied into the wound bed of healing impaired cyclophosphamide treated mice enhances responses to injury. Current studies are aimed at revealing the molecular mechanisms regulating peptide-induced wound healing.

Acknowledgements.

I would like to thank many wonderful people that made this work possible.

I am very grateful to my two scientific mentors that were helping me during my work in Russia Dr. Zinaida S. Donetz, Dr. Igor A. Evlanov. Especially I would like to thank my dissertation advisors - Dr. Michael R. Hamblin and Dr. Ira M. Herman: thank you for helping me to become a scientist!

I would like to thank all the members of CMDB program at Tufts, especially our Program Director and my thesis committee chair Dr. John Castellot. My successful graduation would be much more difficult without his help.

I would also like to recognize the members of my research committee, Irene Kochevar and Jonathan Garlick: thank you for your constant support and for helping me to achieve my goal.

At Tufts Physiology my friends and labmates have been extremely helpful: Jennifer Durham, Jeffry Deckenback and Anita Geevarghese, thank you very much for your help, support and companionship. Thank you Tufts University Core facility members for identification of ECM fragments and peptide sythesis.

Thank you my friends and colleagues from the Wellman Center for Photomedicine for support and Photopathology Team - Jenny Zhao, Peggy Sherwood and Elena V. Salomatina for terrific help with histology.

I would like to thank my parents for everything they have done to help me to get to where I wanted to be and my extended family for their support and understanding.

Finally, I would like to send my special thanks to Dr. William L. Rice for many fruitful discussions, care and help with image analysis. And to our son Alexander W. Rice for being a good boy, and for sleeping so well at night during the time I was writing my dissertation.

Table of contents

List of tables

List of figures

Molecular mechanisms controlling extracellular matrix remodeling and cellular responses to injury

Chapter 1. Background and significance.

1.1 Significance of wound healing research.

Skin is the largest organ of human body. Its primary function is to provide a protective barrier from the environment and prevent invasion of outside elements. In addition, skin plays critical role thermoregulation, metabolism and sensory awareness (Rosdahl and Kowalski, 2008). Mechanical (wounding) or thermal (burning) damage and loss of skin continuity is harmful for human health and may lead to severe disabilities or even death. Therefore, the capacity to re-establish the skin's physical and mechanical integrity is crucial for organism's well-being and survival. The process of restoration of skin function after injury is achieved via well-organized and complex process termed wound healing.

Depending on the depth of the injury, wounds and burns can be classified into superficial, partial thickness and full thickness wounds. The later extend through epidermis, dermis and subcutaneous tissues, are most detrimental and often require medical attention (Sussman and Bates-Jensen, 2007). Cutaneous injuries can also be classified in respect to their age or time to healing. According to this classification, wounds that resolve within a few weeks are considered acute (normal), while wounds that persist for over 3 months (sometime several years) are called chronic (Werdin et al., 2008). Chronic wounds are further classified into vascular wounds, diabetic ulcers, and pressure sores (Harding et al., 2002).

In recent years considerable progress has been achieved in our understanding of the process of acute and chronic injury repair and in the

development of wound healing therapeutics. Nonetheless, both acute and chronic wounds remain a significant healthcare problem. Combined, these full thickness cutaneous injuries affect over 20 million people in the United States alone and represent a significant burden on healthcare system (Singer and Clark, 1999; Singer and Dagum, 2008). Therefore, research aimed at better understanding of the mechanisms of acute and chronic wound healing as well as the improvement of accelerants of healing is critically important.

1.2. Mechanisms of acute wound healing.

Typically, acute wound healing is a well-organized process leading to predictable tissue repair where platelets, keratinocytes, immune surveillance cells, microvascular cells and fibroblasts play key roles in the restoration of tissue integrity (Falanga, 2005; Singer and Clark, 1999). The wound repair process can be divided into four overlapping phases - coagulation, inflammation, formation of granulation tissue (proliferative phase) and remodeling or scar formation phase (Figure 1.1).

1.2.1. Coagulation/Inflammatory Phase.

Immediately after injury platelets adhere to damaged blood vessels, initiate a release reaction and begin a hemostatic reaction giving rise to a blood-clotting cascade that prevents excessive bleeding and provides provisional protection for the wounded area (Figure 1.2). As has been well studied, blood platelets release well over a dozen growth factors, cytokines and other survival or apoptosis-inducing agents (Weyrich and Zimmerman, 2004). Key components of

the platelet release reaction include platelet-derived growth factor (PDGF), and transforming growth factors β1 and 2 (TGF-β1 and 2), which attract inflammatory cells – leukocytes, neutrophils and macrophages (Singer and Clark, 1999). As leukocytes are phagocytic cells, they release reactive oxygen species (ROS) that are anti-microbial, and proteases that clear the wound of foreign bodies and bacteria. Resolution of the inflammatory phase is accompanied by apoptosis of inflammatory cells, which occurs gradually within a few days post-wounding. The exact mechanism through which resolution of inflammation occurs during

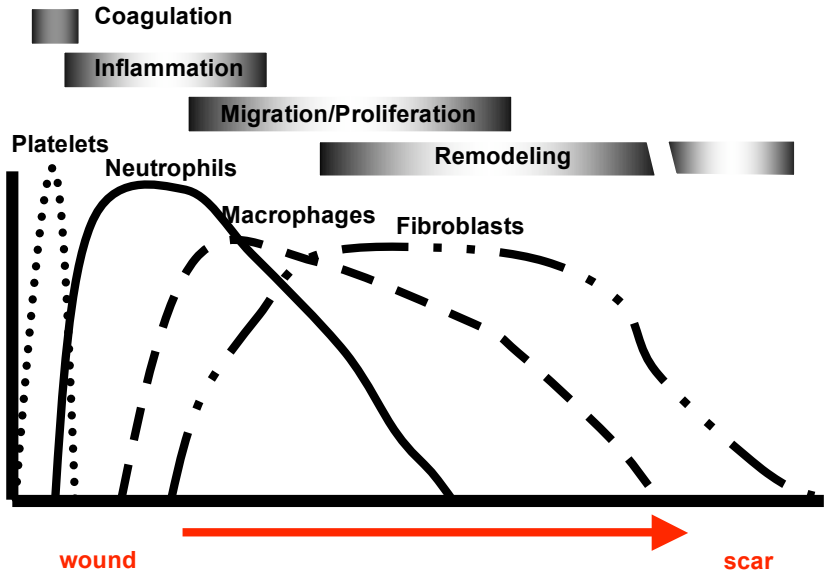

Figure 1.1. Phases of wound healing.

The phases of wound healing include coagulation, inflammatory phase, granulation tissue formation, and remodeling (scar formation). Platelets, neutrophils, macrophages and fibroblasts all contribute to repair process at different stages of healing.

cutaneous wound healing is not completely understood. However, it has been suggested that anti-inflammatory cytokines such as TGF-β1 and IL-1, and bioactive lipids - cyclopentenone prostaglandin, lipoxins and resolvins also take part in this process (Eming et al., 2007;Gilroy et al., 2004). The exact role of these entities during inflammatory phase resolution represents an active area of investigation.

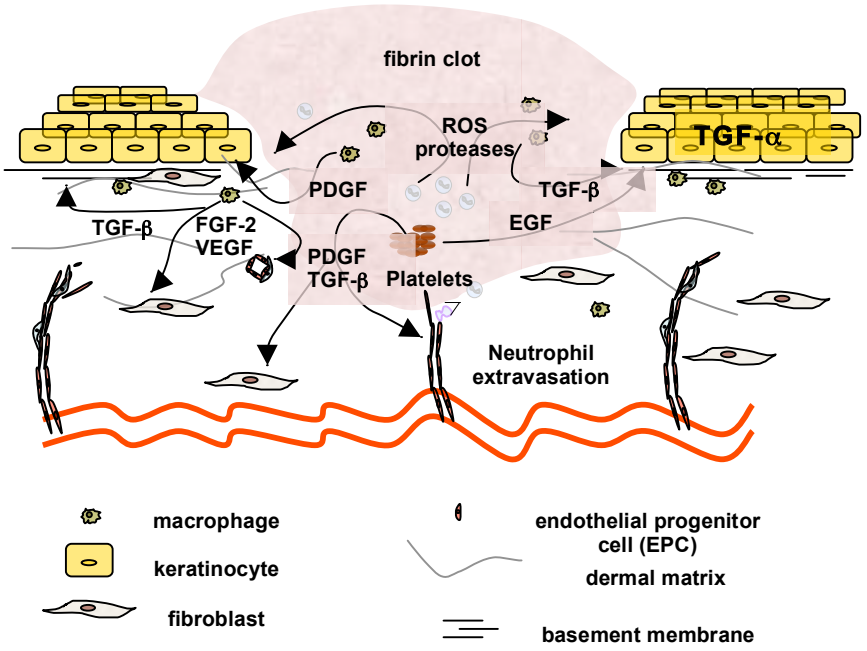

Figure 1.2. Coagulation and inflammatory phase of wound healing.

During this phase of the healing cascade, blood-borne cells - neutrophils, macrophages, as well as platelets play critical roles. These cells provide growth factors and provisional matrices that are necessary for recruitment of epidermal and dermal cells into the wound bed.

1.2.2. Proliferative Phase: Granulation tissue formation.

As the inflammatory phase subsides, the proliferative phase of repair begins (Figure 3). At this stage, growth factors produced by remaining

inflammatory cells, migrating epidermal and dermal cells act in autocrine, paracrine and juxtacrine fashion to induce and maintain cellular proliferation while initiating cellular migration: all events required for the formation of granulation tissue while supporting epithelialization (Falanga, 2005;Singer and Clark, 1999). As dermal and epidermal cells migrate and proliferate within the wound bed, there is a frank requirement for an adequate blood supply for nutrient delivery, gas and metabolite exchange. Therefore, for wound healing to progress normally, a robust angiogenic response must be initiated and sustained.

Wound healing angiogenesis begins immediately after injury when local hypoxia, secondary to injury-induced blood vessel disruption occurs. This event fosters the production of pro-angiogenic factors. Vascular endothelial growth factor (VEGF), fibroblast growth factor-2 (FGF-2) and PDGF (Humar et al., 2002) initially released by platelets and, then, by resident cells within the wound bed, are all central mediators of injury-induced angiogenic induction. In response, endothelial cells degrade basement membrane, migrate toward the wound site, proliferate, form cell-cell contacts and eventually, new blood vessels (Folkman and Klagsbrun, 1987; Singer and Clark, 1999). More recently, it has been revealed that endothelial progenitor cells (EPC) are also required for vascular restoration (Asahara et al., 1997;Leone et al., 2009; Liu and Velazquez, 2008). This process, called vasculogenesis, requires recruitment of EPC. Normally, EPC reside in the bone marrow, and are recruited into the circulation in response to injury. Subsequently, EPC are engrafted into the remodeling microvasculature, taking residence adjacent to endothelial cells bordering the injury site. EPC

mobilization is mediated by nitric oxide, VEGF and matrix metalloproteinases (MMP), particularly MMP-9 (Leone et al., 2009); EPC engraftment and possibly differentiation occurs in response to stromal cell derived factor 1α (SDF-1α) and, as has become apparent more recently, insulin-like growth factor (IGF) (Maeng et al., 2009). While more research needs to be done to further elucidate the mechanisms of EPC recruitment and homing, it is clear that these progenitor cells are necessary for normal wound healing-associated neovasculogenesis and injury repair.

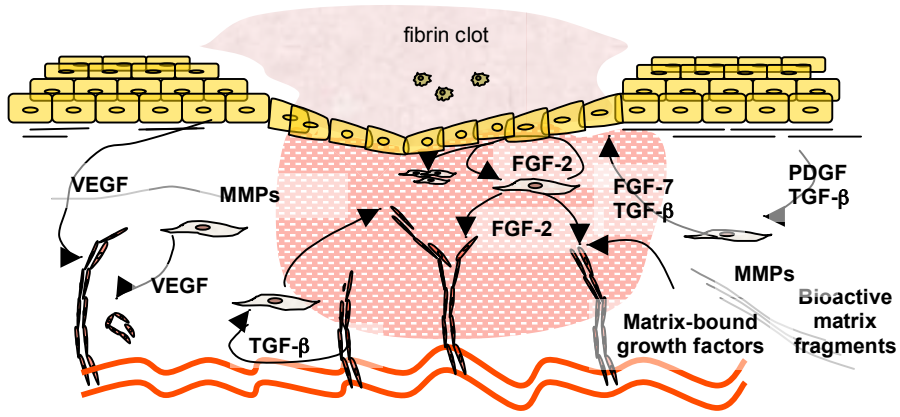

Figure 1.3. Granulation tissue formation.

Granulation tissue formation (proliferative phase) starts at approximately 3 days post-injury and is characterized by increased levels of keratinocyte and fibroblast proliferation, migration and ECM synthesis in response to autocrine, paracrine and juxtacrine growth factors. Angiogenesis/neovascularization also occur during this phase. Newly formed blood vessels give this tissue granular appearance (granulation tissue).

In fact, key signaling intermediates responsible for wound healing angiogenesis and vasculogenesis may be dysfunctional during diabetes (Gallagher et al., 2007). Indeed, diabetic patients prone to the development of chronic wounds (Liu

and Velazquez, 2008) may exhibit deficiencies in either EPC bone marrow release or peripheral tissue homing and engraftment. Therefore, therapies aimed at correcting EPC-linked deficiencies are currently under investigation for treatment of diabetes-induced chronic wounds (Liu and Velazquez, 2008).

1.2.3. Matrix Remodeling and Scar Formation.

Re-establishment of a normal blood supply provides a favorable microenvironment for epidermal and dermal cell migration and proliferation. In turn, this leads to wound re-epithelization and restoration of epidermal integrity. Fibroblasts proliferate within the wound and synthesize extracellular matrix (ECM) forming granulation tissue perfused with newly formed blood vessels (Figure 1.3). Simultaneously, provisional matrix mainly consisting of collagen III, fibrin, fibronectin and hyaluronic acid is progressively substituted with ECM mainly containing collagen I (Singer and Clark, 1999). Next, wound contraction and matrix remodeling occur (Singer and Clark, 1999) (Figure 1.4). Contraction is mainly achieved by differentiated fibroblasts or myofibroblasts that in response to TGF-β, tissue tension and the presence of certain matrix proteins (e.g. ED-A fibronectin and tenascin C), acquire smooth muscle actin-containing stress fibers. Fibroblast-induced contractile forces are then transmitted to the ECM via cytoskeleton-associated and extracellular matrix receptor-dependent mechano-coupling focal adhesion complexes, i.e. integrin receptors (Hinz, 2007a). Another mechanism leading to wound contraction is fibroblast motility with consequent matrix reorganization (Ehrlich et al., 1999). This dynamic and reciprocal process involves slow cycles of ECM synthesis and degradation both occurring in a

stromal- or fibroblastic cell- dependent manner. Here, matrix-remodeling enzymes, particularly, MMPs play important roles in remodeling the local matrix microenvironment in support of several healing responses, including cellular migration, proliferation and angiogenic induction. Finally, apoptosis of fibroblastic cells occurs leading to the formation of a relatively acellular scar tissue whose tensile strength is comparable with unwounded skin (Figure 1.4).

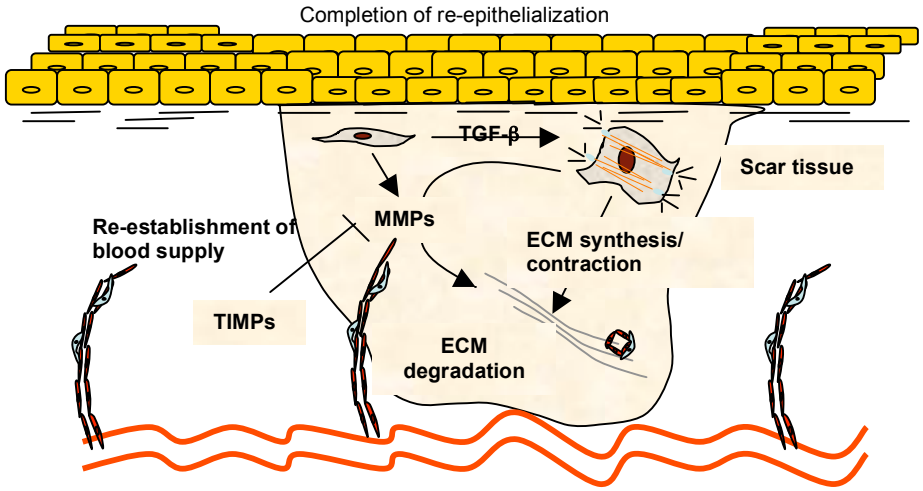

Figure 1.4. Final phase of wound healing: remodeling and scar formation.

At approximately 1-2 weeks post-injury, differentiated fibroblastic cells (myofibroblasts) that present within the granulation tissue begin to remodel extracellular matrix. ECM remodeling followed by apoptosis of resident cells leads to the formation of an acellular scar.

scar formation is widely accepted, the exact triggers of this process during the resolution of wound healing are not well understood (Rai et al., 2005). In

particular, TGF-β, tumor necrosis factor, and surprisingly FGF-2 (that normally is considered as a stimulator of cell proliferation), were reported to increase the number of apoptotic cells during the final phase of healing (Akasaka et al., 2004; Desmouliere et al., 1995). Inability of dermal cells, particularly myofibroblasts to undergo timely apoptosis, has also been linked to wound healing pathologies, e.g. the hypertrophic scar and keloid formation (Seifert and Mrowietz, 2009). Better understanding of the role of apoptosis in these pathologies as well as during normal wound healing may bring about novel approaches for their treatment and/or prevention.

1.3. Chronic Wounds: classification, causes and treatment options.

With the estimated number of elderly persons of 65 years or older in the United States almost doubling (from 35 million to 53 million people) by 2030 (Gosain and DiPietro, 2004), and the estimated risk of developing diabetes for children born in 2000 as high as 35% (Narayan et al., 2003), the anticipated risks of diabetes and age-associated non-healing chronic wounds continues to increase dramatically. In fact, annual chronic wound care costs now exceed one billion US dollars in the United States, alone (Ramsey et al., 1999) and represents ~2% of total EU financial resources (Bitsch et al., 2005) (Table 1.1). Importantly, the majority of the chronic wounds begin as minor traumatic injuries. Penetrating injuries, insect bites or, even, simple scratches of dry skin that would normally heal within a few days/weeks, lead to formation of a non-healing wound in patients with underlying pathologies (Shai and Halevy, 2005).

Chronic wounds can be classified into vascular ulcers (e.g. venous and arterial ulcers), diabetic ulcers, and pressure sores (Table 1.1). Some common features shared by each of these include a prolonged or excessive inflammatory phase (Eming et al., 2007), persistent infections (Edwards and Harding, 2004), formation of drug-resistant microbial biofilms (Wolcott et al., 2008), and the

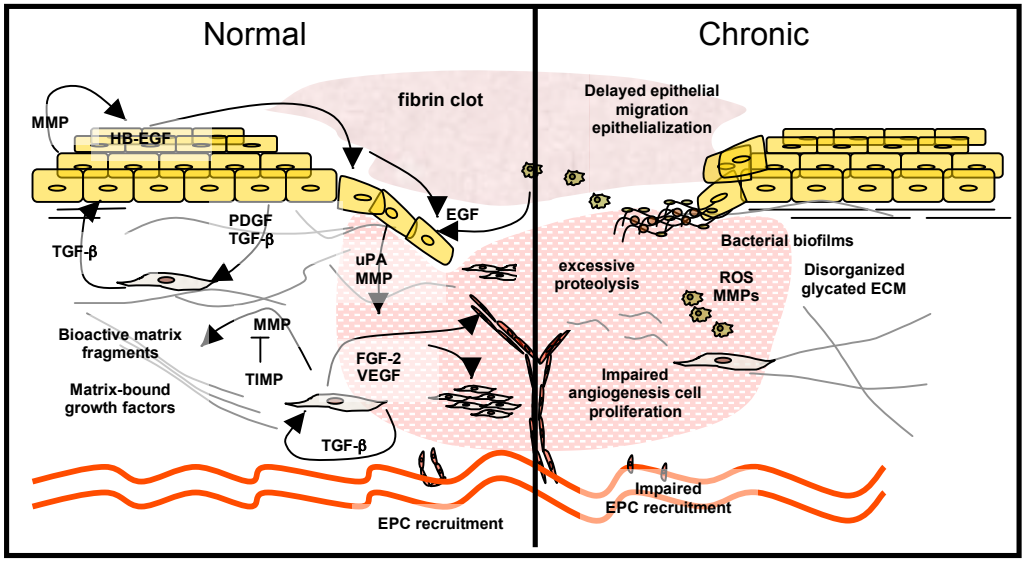

Figure 1.5. Normal vs. chronic wound healing.

Microenvironment within a normal wound bed (left) is characterized by the presence of numerous growth factors, a well-organized ECM and responsive cell populations. Matrix synthesis, here, exceeds its degradation and MMP activity is regulated by the presence of MMP inhibitors (TIMPs). Angiogenesis and neovascularization of normal wounds proceed in a timely manner via well regulated sprouting of existing blood vessels and recruitment of endothelial progenitor cells (EPC), respectively. Finally, unlike their chronic counterparts, acute wounds are generally characterized by low bacterial burden. Chronic wounds (right) have high incidence of bacterial biofilms, leading to persistent inflammation, excessive proteolysis and degradation of critical growth factors, receptors and/or ECM. Cells residing within these wounds are unable to proliferate and/or migrate effectively perhaps due to the absence of functional receptors or appropriate pro-migratory matrix substrates.

In aggregate, these pathophysiologic phenomena result in the failure of these wounds to heal. The underlying pathologies, however, deviate in different type of chronic wounds.

Venous ulcers display profound pathological changes that arise secondary to venous valvular incompetence in the deep and superficial veins. This, in turn, leads to a constant blood backflow resulting in an increase in venous pressure. Pressure-induced changes in blood vessel wall permeability then lead to leakage of fibrin and other plasma components into the perivascular space. Accumulation of fibrin has direct and negative effects on wound healing. It down-regulates collagen synthesis (Pardes et al., 1995), leads to formation of pericapillary fibrin cuffs that create a barrier for normal vessel function and traps blood-derived growth factors (Higley et al., 1995;Walker, 1999). In the 1980s and 1990s, the cuffs were considered as continuous obstructions preventing free blood-dermis oxygen exchange (Walker, 1999). Recently, however, using confocal microscopy it has been demonstrated that fibrin deposits surrounding dermal veins are patch-like and discontinuous (Kobrin et al., 2008). This finding questions the barrier role of fibrin cuffs and suggests the presence of other yet unknown factors contributing to low oxygen tension found in venous ulcers and surrounding tissues. Identification of these factors may reveal novel targets for therapeutic interventions and treatment of venous ulcers.

Arterial ulcers are less common than chronic venous wounds. They occur due to arterial insufficiency caused by atherosclerosis or embolism that can lead to narrowing of arterial lumen and ischemia, which prevents timely healing of

minor traumatic injuries (Bonham, 2003). Unlike venous ulcers, which generally arise between the knee and the ankle, arterial leg wounds may present at any spot distal to arterial perfusion such as a tip of a toe. It is estimated that arterial ulcers affect 100,000 Americans annually (Sieggreen and Kline, 2004). Unlike venous ulcers that often can be improved with therapeutic compression, chronic wounds linked to arterial insufficiency can only be treated successfully after the restoration of arterial function via revascularization (Bonham, 2003). Current options for limb revascularization are rather limited and include reconstructive surgery (angioplasty) or pharmaceutical interventions. Since failure of revascularization procedures almost inevitably leads to limb amputation in arterial ulcer sufferers, novel techniques allowing for restoration of blood supply to the wound bed, including stem cell therapies are now being investigated (Grey et al., 2006).

Pressure ulcers arise due to prolonged unrelieved pressure and shearing force applied to skin and the underlying muscle tissue leading to a decrease in oxygen tension, ischemia-reperfusion injury and tissue necrosis. Pressure ulcers are common in patients with compromised mobility and decreased sensory perception (Defloor, 1999), and are exacerbated in individuals suffering from arterial and venous insufficiencies described above.

Complications of aging and diabetes can lead to and exacerbate vascular pathologies related to both arterial and venous insufficiencies, and worsen pressure ulcers. Other abnormalities leading to development of chronic wounds

Table 1.1. Major types of chronic wounds.

Wound type	Pathology	Number of affected patients	Cost of treatment	Total annual cost
Venous ulcers	Venous insufficiency, thrombosis, varicosis	400,000-600,000	$5,000-10,000	$1.9-$2.5 billion (Etufugh, Phillips, 2007)
Arterial ulcers	Macroangiopathy, Atherosclerosis, arterial insufficiency	100,000 (Sieggreen and Kline, 2004)	$9000-16000	
Diabetic ulcers	Neuropathy, microangiopathy, hyperglycemia	2 million http://www.fetnet.com/statistics.php	$6000/patient	$150 million (Reiber, Diabetes Care 1992)
Pressure sores/ decubitus ulcers	Immobility, excessive pressure	1.3 to 3 million	up to $70 000 (Reddy et al., 2006)	$3.5 to $7.0 billion annually (Salcido et al., 2007)

in diabetic patients (also called diabetic ulcers) include neuropathy, often linked to vascular impairment, deficiencies in muscle metabolism and a number of microvascular pathologies often caused by hyperglycemia (Falanga, 2005). Macroscopic pathologies seen in chronic, particularly diabetic wounds often are linked to cellular phenotypic abnormalities, including low mitogenic/ motogenic potential and inability to respond to environmental cues. Better understanding of these cellular changes and their correction will lead to development of better treatment options for diabetic wound sufferers.

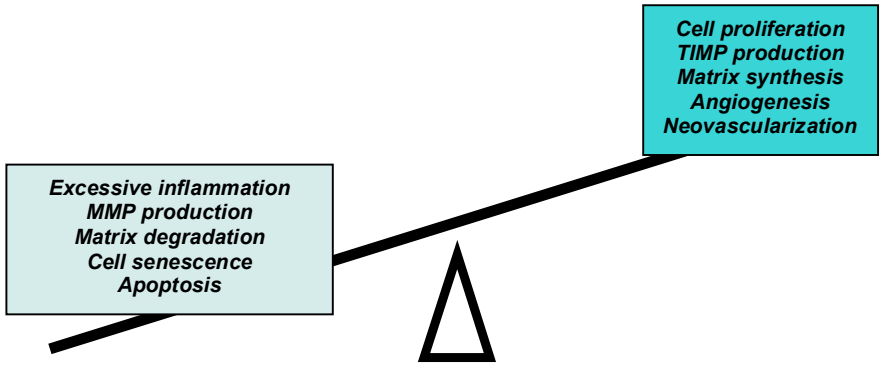

Figure 1.6. Physiologic imbalance: A key feature of chronic wounds.

Inflammation, MMP production, matrix degradation and cell senescence/apoptosis are all elevated in chronic wounds. These processes can not be overcome because of insufficient levels of cell proliferation, ECM synthesis, production of MMP inhibitors (TIMPs) and impaired angiogenesis/neovascularization. This imbalance leads to inability of chronic wounds to heal.

Although all of the wounds described above may have different origins, each wound is characterized by a chronically inflamed wound bed and a failure to heal (Figure 1.6). Excessive recruitment of inflammatory cells to the wound bed often triggered by infection and cell extravasation is facilitated by disproportionate expression of vascular cell adhesion molecule-1, interstitial cell adhesion molecule-1 by resident endothelial cells. Inflammatory cells accumulated inside the chronic wound, produce various ROS that damage structural elements of the extracellular matrix, cell membranes, and lead to premature cell senescence (Ben-Porath and Weinberg, 2005). In addition to these direct negative effects, ROS together with pro-inflammatory cytokines induce production of serine proteinases and MMPs that degrade and inactivate components of the extracellular matrix and growth factors necessary for normal cell function (Eming et al., 2007). Inactivation of proteinase inhibitors by proteolytic degradation augments this process. Therefore, although the production of growth factors is often increased in chronic compared to acute wounds, their quantity and bioavailability is significantly decreased (Lauer et al., 2000;Mast and Schultz, 1996).

Unlike acute wounds, which generally heal without significant interventions, all types of chronic wounds represent major challenges for patients and caregivers. It is now understood that the inability of the chronic wound to heal is caused by both cellular and molecular abnormalities occurring within the wound bed (Figure 1.7). However, proper diagnosis of wound etiology, selection of effective treatment and prevention of wound re-occurrence remain a problem

for chronic wound sufferers and healthcare provides (Bonham, 2003). Below we will describe the most recent advances in the field of wound healing, including the role of tissue microenvironment in normal and pathological wound healing and the opportunities for use of exogenous growth factors for treatment of acute and chronic wounds.

1.3.1. Phenotypic abnormalities in chronic wound cells.

Epidermal and dermis-derived cells residing in chronic wounds have several phenotypic abnormalities. These include lower density of growth factor receptors and lowered mitogenic potential preventing them from responding properly to environmental cues. For instance, fibroblasts, isolated from patients with chronic diabetic, non-diabetic wounds or patients with venous insufficiency, have lower mitogenic response to PDGF-AB, IGF, bFGF and EGF applied separately or in combination. These findings are likely due to a decrease in receptor density (Loot et al., 2002;Seidman et al., 2003;Vasquez et al., 2004). Furthermore, fibroblasts isolated from leptin receptor-deficient diabetic mice as well as derived from patients with chronic venous insufficiency have reduced motogenic potential, compared to normal fibroblasts (Lerman et al., 2003;Raffetto et al., 2001). These cellular abnormalities impede the formation of granulation tissue and extracellular matrix deposition leading to formation of non-healing wounds.

Keratinocytes derived from chronic ulcers have also been reported to possess a “chronic wound-associated” phenotype (Usui et al., 2008). Overexpressing the proliferation marker Ki67, these cells upregulate expression

of several cell cycle associated genes such as CDC2 and cyclin B1 suggesting a hyperproliferative status (Stojadinovic et al., 2008). However, these chronic wound-derived keratinocytes exhibit impaired migratory potential. The mechanisms of this impairment are not completely understood, but have been linked to decreased production of laminin-332 (laminin-5) – an important substrate for injury-induced keratinocyte migration (Usui et al., 2008). Additionally, these cells possess an increased activation of β-catenin/c-myc pathway (Stojadinovic et al., 2005) and do not express markers of differentiation, particularly keratin 10 and 2. Finally, several genes encoding a variety of growth factors are down- or up- regulated, e.g. VEGF, epiregulin and TGF-β2 expression are decreased, whereas PDGF and platelet-derived endothelial growth factor encoding genes are upregulated (Stojadinovic et al., 2008). Decreased growth

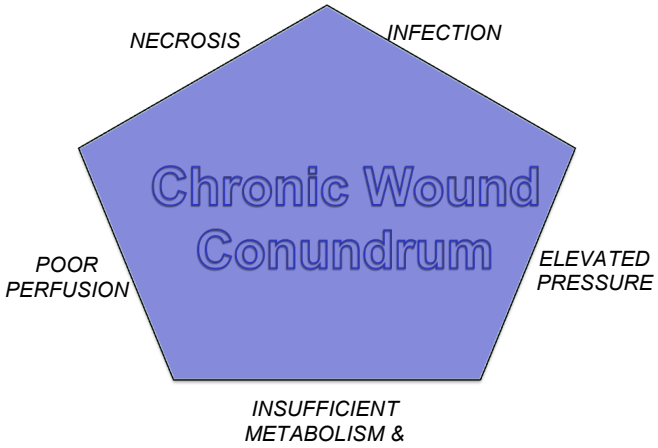

Figure 1.7. Chronic wound conundrum.

Diagrammatic representation of those physiologic functions that are perturbed or dis-equilibrated during chronic wound healing.

factor production directly confirms the impaired state of the keratinocytes residing within a chronic wound and inability to fully participate in repair processes while upregulation of key growth factor genes enable a sustained proliferative capacity suggesting that this could be an 'entry point' for therapeutic intervention. Motogenic stimuli together with activators of keratinocyte differentiation such as recently described hyperforin (Muller et al., 2008) may be able to induce phenotypic changes and transform the chronic wound keratinocytes into competent cells necessary for epithelialization. Similarly, modern transduction techniques (Okwueze et al., 2007) could be used to improve growth factor responsiveness of cells residing in chronic wounds by increasing the density of growth factor receptors. These are just a few examples of how our better understanding of cellular pathologies might lead to development of novel therapeutic modalities, which could be used for treatment of chronic wounds and will be discussed in more detail in the subsequent sections.

1.3.2. Perturbations in the extracellular matrix microenvironment that contribute to sustaining wound chronicity.

The microenvironment of the chronic wound bed is heralded by matrix. Information about the differences in chemical composition of the ECM found in chronic and acute wounds is scarce and controversial. It is known, however, that deposition of a number of matrix components is different in chronic as compared to acute wounds. For example, chronic wounds are characterized by prolonged (Loots et al., 1998) or insufficient expression of fibronectin, chondroitin sulfate, and tenascin, which gives rise to impaired cellular proliferation and migration

(Agren et al., 1999). Recently, reduced production of laminin 322 - a basement membrane component that serves as a haptotactic substrate for post-injury keratinocyte motility (Usui et al., 2008) was found to be one of the reasons for impaired re-epithelialization and wound healing. Changes of the ECM, including post-translational modification of key structural components can also negatively influence cellular responses to injury. For instance, matrix glycation is often seen in diabetic patients and is likely to be responsible for or linked to premature cell senescence, apoptosis, inhibition of cell proliferation, migration and angiogenic sprout formation (Kuo et al., 2007). Glycation adds to matrix instability, disrupts matrix assembly and interactions between collagen and its binding partners, including heparan sulfate proteoglycans (Liao et al., 2009;Reigle et al., 2008). High glucose has also been shown to stimulate MMP production by fibroblasts, macrophages and endothelial cells thus contributing to a 'vicious' cycle of matrix degradation detrimental for cell survival and therefore wound healing (Death et al., 2003;Lee et al., 2007). Matrix instability that occurs due to glycation and insufficient intermolecular crosslinking seen under hypoxic conditions (Dalton et al., 2007) and excessive matrix degradation by MMPs are also detrimental to the healing process. Matrix instability prevents normal cell-matrix interactions necessary for cell survival and function, and, ultimately injury repair. Therefore, inhibition of matrix degradation, addition of exogenous matrices and induction of matrix synthesis by resident cells all provide therapeutic opportunities. As an example, collagen-based dressings (Promogran) have been used in clinical trials, successfully decreasing the levels of matrix degrading enzymes and improving

healing (Lobmann et al., 2006). To date, protease inhibitors have not been used to treat chronic wounds clinically. However, synthetic bisphosphonates are under investigation for application in wound care (Rayment et al., 2008). Further research is sorely needed to delineate the therapeutic potential of both protease inhibitors and/or ECM-based preparations for chronic wound care.

1.3.3. Biofilms and the chronic wound bed.

Infection is an extrinsic factor that causes delay of wound healing, contributing to wound chronicity, morbidity and mortality (Bader, 2008). High bacterial counts of $>10^5$ viable bacteria or any number of β-haemolytic streptococci are considered detrimental. Bacterial toxins (as well as live bacteria) induce excessive inflammatory responses (Ovington, 2003), and tissue damage that can lead to abscess, cellulites, osteomyelitis or limb loss (diabetic patients) (Edwards and Harding, 2004). Furthermore, recruited inflammatory cells as well as bacteria produce a number of proteases (including MMPs), which degrade the ECM and growth factors present within the wound bed. Bacteria that colonize chronic wounds (Figure 1.7) often form polymicrobial communities called biofilms (James et al., 2008). These complex structures are composed of microbial cells embedded in secreted polymer matrix, which provides optimal environment for bacterial cell survival, enabling their escape from host immune surveillance/defense and resistance to antibiotic treatment (Martin et al., 2009). Although biofilms are prevalent in chronic wounds (Falanga, 2005;James et al., 2008), and significantly delay re-epithelialization in animal models (Clark F. Schierle et al., 2009), it remains unclear precisely how they delay healing.

Increased bacterial survival and enhanced production of virulence factors are likely explanations. However, it is possible that extracellular biofilm components possess or display a toxic phenotype for host cell functionality and therefore impede healing. Recently, it has been demonstrated that hindering biofilm formation by RNAIII inhibiting peptide (Cirioni et al., 2007) reverses wound healing delays induced by bacterial biofilms (Clark F. Schierle et al., 2009). Better understanding of the precise mechanisms by which bacterial biofilms delay repair processes together with optimizing methods for biofilm detection and prevention may enhance opportunities for transforming chronic wound beds into those that actively heal.

1.3.4. Current options for treatment of chronic wounds.

Successful treatment of a particular chronic wound requires a detailed understanding of the molecular and cellular components present within each wound bed. Currently, chronic (and acute) wounds of different etiologies are treated using a multi step approach based on contemporary knowledge of wound healing and is known by the acronym TIME (Schultz et al., 2003). First, non-viable tissues (T) from within and around a wound are removed using surgical debridement or debriding agents such as bacterial collagenase. Secondly, infection and inflammation (I) are minimized with antibiotics and anti-inflammatory preparations. Next, moisture (M) imbalance is corrected, generally with carefully selected dressings. Finally, epithelialization (E) and granulation tissue formation are promoted by the application of specific therapies, such as growth factors. However, the use of TIME strategy is not always sufficient and

some wounds remain non-responsive to current therapies. Therefore, we should develop refined methods that will enable personalized therapeutics tailored for each patient's non-healing wound to be developed. To this end, a novel wound diagnosis technology called "bar coding" of the wound has been proposed (Tomic-Canic et al., 2008). It employs sampling of chronic wound fluids and/or collection of tissue biopsies that allow for identification of markers of wound chronicity such as growth factors and their receptors, MMPs, members of β-catenin/c-myc pathway and keratinocyte differentiation markers. "Wound bar coding" can be used for both guiding wound debridement and treatment regiments. Necessary levels of dead tissue removal can be determined by the presence of β-catenin/c-myc positive cells that although they can proliferate, cannot migrate or differentiate and therefore have to be removed. Treatment strategies can also be adjusted based on the needs of individual patients or "bar coding" results. For instance, if cells residing within a wound express low levels of growth factors, growth factor receptors and high levels of MMPs as determined by ELISA, wound care practitioners could choose to use growth factor delivery methods or patient-derived 'engineered' cells that would allow for restoring the wound microenvironment favoring a healing phenotype. In this way, each wound could be considered individually and treatment would be carefully 'personalized' or selected on an individual basis.

1.3.5. Wound bed preparation: the role of debridement.

Removal of non-viable tissue or wound debridement is beneficial for wound healing. Methods of debridement employed in clinical practice include surgical,

autolytic, biological and enzymatic (Ayello and Cuddigan, 2004). Surgical, also known as sharp debridement is performed by excision of necrotic tissue using surgical tools; autolytic debridement involves either careful removal of spontaneously separated necrotic tissues or the use of moisture retaining dressings inducing eschar softening followed by its removal; biological debridement uses larvae of the green blowfly species (maggot therapy); during enzymatic debridement naturally occurring matrix degrading enzymes are used (Attinger et al., 2006;Ayello and Cuddigan, 2004;Turkmen et al., 2009). Both surgical and autolytic debridements non-discriminately remove dead and viable tissues, are very laborious and can be painful. While biological debridement is more selective, larvae are hard to store, may be unpleasant for the patients and medical personnel, and therefore not universally used.

Enzymatic debriding agents are also selective toward necrotic tissues, usually stable for several months upon refrigeration (or even at room temperature) and more aesthetically appealing (Ayello and Cuddigan, 2004). Until recently, two enzymatic debriding preparations were clinically used in the United States – papain-based and collagenase-based products.

Papain – a cysteine protease derived from papaya fruit degrades collagen and fibrin – the major components of eschar; as papain can only degrade denatured protein, urea is often added to the enzyme preparations such as Accuzyme to ensure protein denaturation (Ayello and Cuddigan, 2004). While different preparations of papain were clinically used for over one hundred years and are relatively effective in removing necrotic tissues, FDA never approved the

papain-containing products. Moreover, their benefit for wound healing and its effects on the cells inside the wound are questionable, in fact, papain-urea induces inflammatory response within the wound bed (Ayello and Cuddigan, 2004) and decreases proliferation of cells (Riley and Herman, 2005) thus impeding healing process. Recently, due to the safety concerns, the use of these debriding agents have been discontinued (http://www.fda.gov/).

Another promising debriding agent is bacterial collagenase (Clostridiopeptidase A). It is obtained from a gram-positive bacterium Clostridium histolyticum, and is an active ingredient in a number of debriding agents, including Santyl® (Healthpoint), Iruxol® and Novuxol® (Knoll Nordmark Arzneimittel, GmbH 25430 Uetersen, Germany). Clostridial collagenase, unlike its mammalian counterpart (MMP-1), can degrade both native and denatured collagens I, II, III, IV and V (Mandl, 1982). It efficiently clears the wound of necrotic tissues and decreases bacterial burden. More importantly, preparations of bacterial collagenase enhance migration and proliferation of keratinocytes, endothelial cells, and fibroblasts, by releasing both ECM-, and cell-surface bound growth factors and bioactive matrix fragments (Demidova-Rice and Herman, 2009; Herman, 1996; Herman, 1993b; Postlethwaite and Kang, 1976; Postlethwaite et al., 1978; Radice et al., 1999; Riley and Herman, 2005; Shi et al., 2009; Demidova-Rice et al., 2011). Therefore, in addition to clinically relevant wound debridement, treatment of chronic wounds with preparations of bacterial collagenase will likely help to achieve efficient angiogenesis, epithelialization and ultimately efficient healing (Falanga, 2002). Further randomized controlled

studies are necessary in order to unequivocally determine the wound-healing potential of Clostridial collagenase (Ramundo and Gray, 2008).

Another product that is under investigation for use as enzymatic debriding agents is bromelain. Currently bromelain is being tested in a phase III clinical trial and has been granted Orphan Drug Status by FDA/European CPMP. This enzymatic preparation extracted from pineapple stems and/or flowers is marketed as Debridase (Debrase, MediWound Ltd) (http://www.ahead-bs.com/apage/12205.php#Clinical). Normally, it is applied once for relatively short time periods (4h), resulting in thorough debridement. Further, a small clinical study where the enzyme was used to debride deep second and third degree burns, detected no detrimental effects on surrounding healthy tissues and no significant side effects (Rosenberg et al., 2004). This study however, does not provide any insight into the mechanism of action of bromelain or whether it was beneficial for the healing process or graft success.

Although significant progress has been made in our understanding the mechanisms by which enzymatic debriding agents improve healing of chronic wounds, the delivery of debriding enzymes to the wound bed remains somewhat out-of-date. For example, Debridase is supplied in the form of sterile lyophilized powder and has to be mixed immediately before application in a proprietary hydrating gel provided as a 'kit' (Debrase, MediWound Ltd) (http://www.ahead-bs.com/apage/12205.php#Clinical). Due to short application time, secondary dressings are not necessary in this case. Bacterial collagenase, on the other hand, is supplied premixed in a petrolatum or emulsion ointments, has to be

applied repeatedly and requires secondary dressings. While this delivery system in general is considered relatively efficient and safe, it has been reported that contact dermatitis may in some cases develop upon exposure to both the active ingredient (clostridiopeptidase) or the excipients (Foti et al., 2007;Tam and Elston, 2006). To our knowledge, the only study published in peer-reviewed literature describing a different method of collagenase delivery to an in vivo wound was published by a group from the Netherlands. In this report a biodegradable hydrophilic film containing bacterial collagenase was used. While collagenase activity in this delivery system was preserved, the formulation was unstable (at least at room temperature) (Mekkes et al., 1998). Clearly, more work remains to be done to develop an efficient system for delivery of enzymatic debriding agents. Recently, it has been shown that bacterial collagenase (as well as human MMPs) can be bound to collagen or oxidized regenerated cellulose/collagen sponge (Metzmacher et al., 2007). This, together with the notion that components of the matrix degraded by bacterial collagenase have stimulatory effects on cells within the wound bed – epithelial, endothelial, inflammatory cells and fibroblasts - suggest that matrix-based wound dressings may serve to deliver the enzyme into a wound bed.

1.3.6. Infection control.

While proper wound debridement helps to control bacterial growth (Payne et al., 2008), it is not always sufficient and additional antibiotics may be required. Antimicrobial preparations used in chronic wound care include topical

Table 1.2. Enzymatic debriding agents.

Enzyme/source	specificity	trade name(s)	FDA approval status
Papain/ Carica papaya	Denatured proteins proteins containing cysteine residues (including growth factors)	Accuzyme, Allanfil, Allanzyme, Ethezyme, Gladase, Kovia, Panafil, Pap Urea, Ziox	Not approved, manufacturing discontinued as of November 24, 2008
Collagenase/ Clostridium histolyticum	Denatured and native collagen I, II, III, IV and V	Santyl, Iruxol and Novuxol	Approved by FDA/EMEA
Bromelain/ Ananas comosus	Necrotic cutaneous tissue	Debrase	Currently under investigation, Orphan Drug Status granted by FDA/European CPMP

antiseptics, topical antibacterials and systemic antibiotics, all recently reviewed (Howell-Jones et al., 2005;Lipsky, 2008;Martin et al., 2009).

While many preparations described in these reviews can effectively control bacterial growth, they can be toxic for host tissues. Currently, there is no conclusive evidence that one antibiotic or antiseptic is superior to any other achieving efficient elimination of infection and decreasing time to healing. Many

of modern anti-microbial therapies (Edwards and Harding, 2004) can effectively target planktonic bacteria, which may be beneficial for wound healing (Imegwu et al., 1997;Levenson et al., 1983). However, biofilm-producing microorganisms remain a major challenge (Edwards and Harding, 2004). Biofilms are complex structures that are composed of microbial cells embedded in secreted polymer matrix, which provides optimal environment for bacterial cell survival, enabling their escape from host immune surveillance/defense and resistance to antibiotic treatment (Martin et al., 2009). Although biofilms are prevalent in chronic wounds (Falanga, 2005;James et al., 2008), and significantly delay re-epithelialization in animal models (Clark F. Schierle et al., 2009), it remains unclear precisely how they delay healing. Increased bacterial survival and enhanced production of virulence factors are likely explanations, however, it is possible that extracellular biofilm components possess display toxicity to host cells and therefore impede healing. Recently it has been demonstrated that hindering biofilm formation by RNAIII inhibiting peptide (Cirioni et al., 2007) reverses wound healing delays induced by bacterial biofilms (Clark F. Schierle et al., 2009). Better understanding of the precise mechanisms by which bacterial biofilms delay repair processes together with optimizing methods for biofilm detection and prevention may enhance opportunities for transforming chronic wound beds into those that actively heal. In addition, novel experimental techniques, including photodynamic therapy (Di Poto et al., 2009) and silver-containing dressings (Martin et al., 2009) could successfully eliminate planktonic, biofilm-associated and multi drug resistant bacteria.

1.4. Advanced wound healing techniques.

Thorough wound bed preparation can, in some cases, be sufficient to induce proper cellular responses and healing of complicated wounds. Often however, because such wounds may persist, specific therapies may be necessary. Several of them, including growth factor therapy, low level light therapy and extracellular matrix derived fragments are described below.

1.4.1. Exogenous growth factors and their use in wound care.

Growth factors (Table 1.3.) play critical role during normal wound healing (Barrientos et al., 2008;Werner and Grose, 2003). Chronic wounds on the other hand often have insufficient supply of these biologically active molecules. In fact, deficiency of growth factors is one of the causes of wound chronicity. Since the 1980s application of exogenous (recombinant human) growth factors has been considered as a promising wound healing therapy (Robson et al., 1991). Several members of PDGF, FGF and VEGF families have been tested in wound healing studies both humans and animals.

Platelet derived growth factor (PDGF) family.

PDGF is one of the first factors produced in response to injury and induces cellular responses throughout all phases of repair processes (Figure1.2, Table 1.3). It has numerous functions and is released by platelets, macrophages, keratinocytes, fibroblasts and endothelial cells (Table 1.3) (Werner and Grose, 2003 and references therein). Currently, four PDGF ligands are known: PDGF-A

Table 1.3. Role of growth factors in wound healing and their clinical use.

Growth factor	Sources	Target cells	Clinical use
PDGF	Platelets, macrophages, endothelial cells	Neutrophils, macrophages, smooth muscle cells, endothelial cells, fibroblasts	PDGF-BB is FDA approved for treatment of diabetic ulcers
FGF-1	Macrophages, endothelial cells	Endothelial cells, fibroblasts, smooth muscle cells, keratinocytes	In clinical trails for spinal cord injuries, burns (Cheng et al., 2004;Ma et al., 2007b)
FGF-2	Fibroblasts, endothelial cells, inflammatory cells	Endothelial cells, fibroblasts and keratinocytes	In clinical trials chronic wounds (Barrientos et al., 2008)
FGF-7	fibroblasts	Endothelial cells, keratinocytes	FDA approved for treatment of oral mucositis (Beenken and Mohammadi, 2009); in clinical trials for treatment of venous ulcers (Robson et al., 2001)
VEGF (A)	Fibroblasts, keratinocytes, smooth muscle cells, macrophages, platelets	Endothelial cells, keratinocytes	In clinical trials for limb ischemia, coronary ischemia (Isner et al., 1996;Losordo et al., 1998)
TGF-β 1-3	Platelets, macrophages, fibroblasts, keratinocytes	Monocytes, macrophages, neutrophils, keratinocytes, fibroblasts	TGF-β3 is in clinical trials for pressure ulcers (Hirshberg et al., 2001), Avotermin (rh-TGF-β3) in trials for treatment of excessive scarring (Occleston et al., 2008)

and B can form both hetero- and homodimers and are secreted in their active form, while PDGF- C and D are homodimer-forming species and require extracellular activation (Andrae et al., 2008). PDGF family members exert their activity on cells after binding to a complementary family of receptor tyrosine kinases - PDGFR-αα, PDGFR-αβ and PDGF-ββ (Figure 1.8). Ligand binding followed by homo- or hetero- dimerization of PDGFR and their phosphorylation triggers several signaling pathways, including phospholipase Cγ pathway, phosphatidylinositol3-kinase (PI3K), and a number of mitogen-activated protein kinase (MAPK) pathways (Barrientos et al., 2008;Gao et al., 2005). Activation of these pathways by PDGF generally leads to enhanced cellular migration, proliferation, causing increased VEGF and IGF, production. Importantly, enhanced growth factor receptor expression and extracellular matrix (fibronectin, hyaluronic acid) production ensue (Bennett et al., 2003; Werner and Grose, 2003). It should be noted that under certain conditions PDGF-α can have a negative impact on cell motility, while retaining its pro-mitogenic effect (Alvarez et al., 2006; Gao et al., 2005). PDGFR α and β are normally expressed by several cell types at low levels; however, in response to injury and in the presence of exogenous growth factors, such as EGF and PDGF-AB, receptor expression is markedly up-regulated. This upregulation of PDGFR and its phosphorylation appears to be necessary for timely healing, whereas uncontrolled PDGF signaling may play role in hypertrophic scarring (Alvarez et al., 2006; Gope and Gope, 2009; Werner and Grose, 2003).

The levels of PDGF and PDGF receptor expression are low in diabetic and aged mice with delayed responses to injury (Werner and Grose, 2003). Similarly, PDGF levels are depressed within non-healing human ulcers (Pierce et al., 1995), perhaps due to both underproduction an/or excessive protease-mediated degradation. Predictably, the delivery of exogenous PDGF was reasoned to be beneficial for those patients suffering with chronic wounds. As a result, the FDA granted approval of Regranex® (becaplermin) for the treatment of diabetic ulcers (Leahy and Lawrence, 2007).

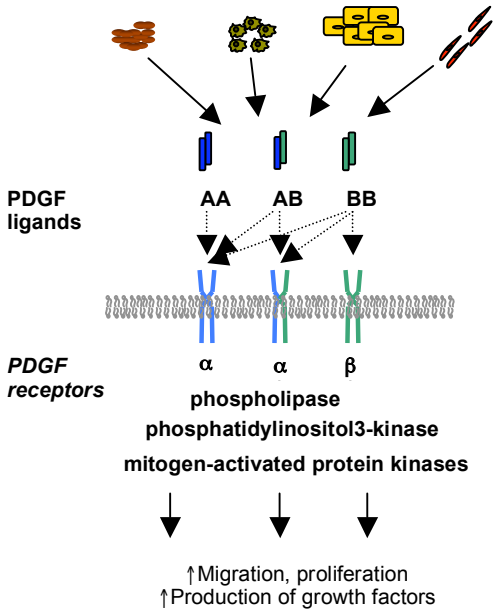

Figure 1.8. Simplified representation of PDGF signaling cascade.

Platelets, macrophages, keratinocytes, endothelial cells produce PDGF ligands – PDGF-AA, PDGF-AB and PDGF-BB during wound healing. The ligands interact with one or several of three types of PDGF receptors: PDGFR-αα, PDGFR-αβ and PDGFR-ββ. The specificity of ligand-receptor interactions is shown with dotted arrows. Receptor-ligand interactions, receptor dimerization and phosphorylation lead to activation of phospholipase Cγ, PI3K and mitogen-activated kinase pathways, which in turn induce increased cellular migration, proliferation, and growth factor production.

Despite this, however, the outcomes of treating diabetic ulcers with this PDGF-containing preparation have been less than convincing or inconclusive. Perhaps non-responsiveness to PDGF treatment, observed in some patients, may be due to low expression levels of PDGF receptors by cells residing within chronic

wounds (Vasquez et al., 2004) or could be caused by rapid degradation of the growth factor by proteolytic enzymes within the chronic wound bed (Falanga, 2005). Also confounding is the fact that epithelial cells within chronic wounds lack PDGF receptors. And, the complexity and persistence of the chronic wound bed suggests that delivery of a single entity as a corrective therapeutic may not be sufficient. A combination and/or patient-specific approach to chronic wound treatment might be required to enable healing and wound closure (Hinchliffe et al., 2008;Tomic-Canic et al., 2008). Therefore, improved outcomes of PDGF and other growth factor-based therapies will undoubtedly come with better understanding of cellular and molecular abnormalities occurring in chronic wounds and/or with development of better drug delivery methods.

Fibroblast growth factor (FGF) family.

Fibroblast growth factor (FGF) family (Figure 1.9) includes 23 members. FGF-1, 2, 7, 10 and 22 are expressed upon dermal injury (Barrientos et al., 2008). The biology of these paracrine growth factors has recently been reviewed (Beenken and Mohammadi, 2009). After their liberation from the ECM, FGF ligands bind and activate FGF receptors (FGFR) in a heparan sulfate proteoglycan (HSPG) dependent manner. Receptor-ligand interaction induces receptor dimerization and trans-phosphorylation leading to activation of downstream signaling including Ras/MAPK and PI3K/Akt pathways (Beenken and Mohammadi, 2009).

FGF-1 and -2, also known as acidic and basic FGF, respectively, are produced by inflammatory cells, vascular endothelial cells, fibroblasts and

keratinocytes. They play roles in re-epithelialization, angiogenesis and granulation tissue formation (Singer and Clark, 1999;Werner and Grose, 2003).

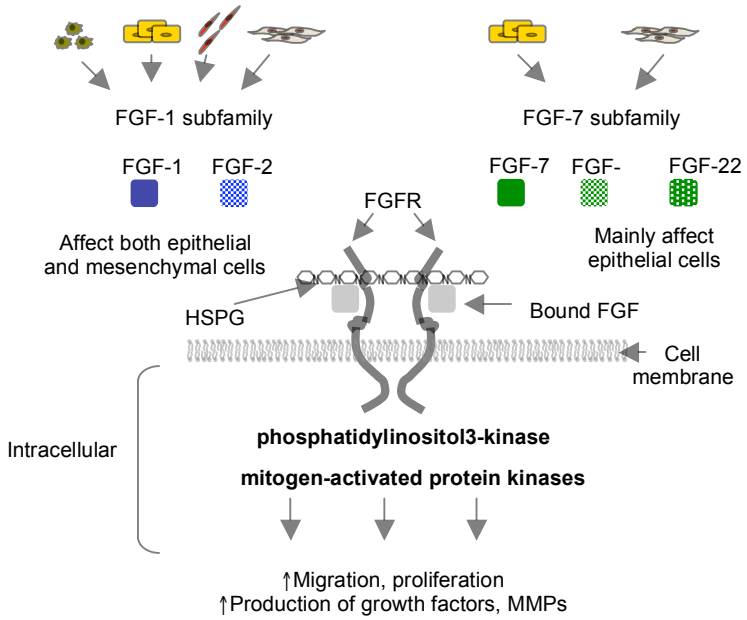

Figure 1.9. FGF signaling and wound healing.

FGF-1 and FGF-2 belong to FGF-1 subfamily and are produced by macrophages, keratinocytes, endothelial cells and fibroblasts to stimulate both epithelial and mesenchymal cells. Members of FGF-7 subfamily (FGF-2, FGF-10 and FGF-22) mainly affect epithelial cells. Interactions between FGF ligands and FGF receptor lead to receptor dimerization and are enhanced by heparan sulfate proteoglycan (HSPG). Receptor-ligand interactions lead to activation of PI3K and mitogen-activated kinase pathways, and induce an increase in cell migration, proliferation, production of growth factors and MMPs.

FGF-2 also stimulates production of ECM and matrix degrading enzymes, thus contributing to matrix synthesis and remodeling which is critical for normal wound healing (Xie et al., 2008). FGF-7, FGF-10 and FGF-22 are expressed by fibroblasts and proliferating keratinocytes (Braun et al., 2004). These factors are mitogenic and motogenic for keratinocytes and induce enzymes important for nucleotide synthesis and production of MMPs (auf demKeller et al., 2004).

In addition to their direct role in wound healing, FGF-7 and FGF-10 stimulate production of TGF-α and other ErbB ligands by dermal keratinocytes thus contributing to epithelialization (auf demKeller et al., 2004). FGF-7 subfamily members also have cytoprotective effects and upregulate ROS-protective enzymes such as peroxiredoxin VI and reduce the levels of inflammatory mediators induced by the injury (Beenken and Mohammadi, 2009; Braun et al., 2004). Finally, FGF-7 has been shown to increase production of VEGF, MMP-9 and urokinase plasminogen activator (uPA) by several tumor types possibly contributing to cancer-induced angiogenesis (Narita et al., 2009; Niu et al., 2007). Future work will be required to reveal whether FGF-7 can indirectly contribute to angiogenesis during normal injury-repair.

It is generally accepted that FGF-FGFR mediated signaling is impaired in chronic wounds (Barrientos et al., 2008). Clinically, both decrease of FGF production and increase in its sequestration by an inhibitory heparan sulfate present in chronic wound fluid has been observed (Cooper et al., 1994; Landau et al., 2001). In animal models of delayed wounds healing (diabetic and aged animals), abnormal expression of FGF-1, 2, 7 and diminished expression of FGF receptors was reported and exogenous FGFs have been successfully used to improve injury-repair (Komi-Kuramochi et al., 2005; Werner et al., 1994). These observations led to development of a number of clinical trials. FGF-1 and 2 have been used for treatment of chronic wounds and burns, with only modest improvements in healing rates (Barrientos et al., 2008; Ma et al., 2007a). FGF-7, which currently is FDA approved for treatment of oral mucositis (Beenken and

Mohammadi, 2009), enhanced repair of venous ulcers in a phase 2A clinical trial (Robson et al., 2001), but failed to increase the percentage of wounds fully healed within the 20 weeks of study (Clinical Trial News. Cathy Thomas Hess, Advances in skin and wound care. December 2003, Volume 16, Issue 7, p 336). These failures have been attributed to insufficient retention of the growth factors within the wound bed, which could be significantly improved using advanced delivery methods such as growth factor-containing biodegradable dressings as described below.

Vascular Endothelial Growth Factor (VEGF) family.

The VEGF family includes six members (Figure 1.10) – placental growth factor (PLGF), VEGF-A, VEGF-B, VEGF-C, VEGF-D and VEGF-E. VEGFs are heparin-binding glycoproteins and exert their functions after binding to several cell-surface tyrosine kinase receptors VEGFR1-3, with VEGFR-1 and VEGFR-2 mainly mediating angiogenesis and VEGFR-3 important for lymphangiogenesis (Ferrara et al., 2003). Novel VEGF receptors known as neuropilins may also be involved in wound healing angiogenesis (Kumar et al., 2009).

While expression of VEGF family members in normal skin is very minor, in response to injury-induced hypoxia their production is markedly up-regulated. In addition to hypoxia, several growth factors, including TGF-β1, FGF-2 and PDGF-BB are important inducers of VEGF (Bao et al., 2008; Bao et al., 2009; Barrientos et al., 2008).

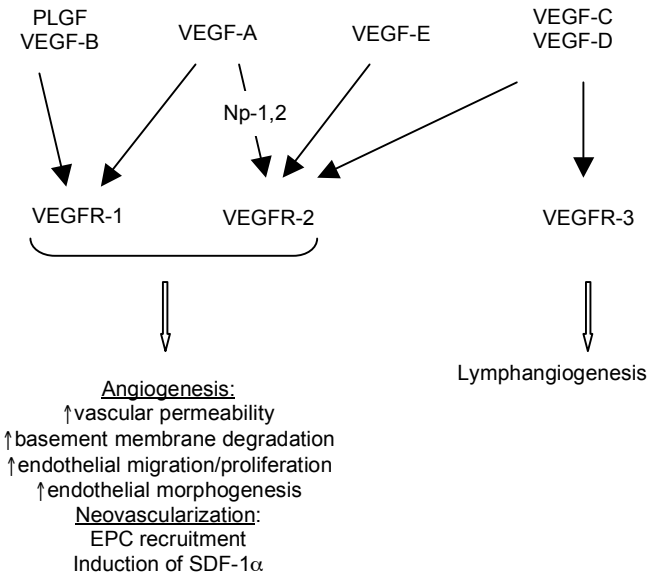

Figure 1.10. VEGF, VEGF receptors and the cellular responses to injury.

Cellular effects of the members of VEGF family are mediated by three VEGF receptors – VEGFR-1, VEGFR-2, VEGFR-3. Activation of VEGFR-1 and VEGFR-2 mainly induce wound healing angiogenesis and neovascularization, while VEGFR-3 is important for lymphangiogenesis. Ligand-receptor interactions and their specificities are shown with arrows. Note, that interaction between VEGF-A and VEGF-R2 is enhanced in the presence of co-receptors neuropilin 1 and 2 (Np-1,2).

During wound healing, platelets, macrophages, fibroblasts, keratinocytes secrete VEGF and it acts in a paracrine manner on endothelial cells inducing and supporting wound angiogenesis (Werner and Grose, 2003). VEGFR-1 and VEGFR-2 activation by VEGF triggers multiple events required for successful angiogenesis during injury repair responses. These include (i) an increase in vascular permeability, (ii) degradation of the basement by uPA and tissue-type plasminogen activators (tPA), MMP-1, MMP-2, (iii) endothelial migration mediated by αvβ3, αvβ5, α1β1 and α2β1 integrin receptors and their ligands

(Senger et al., 1997; Suzuma et al., 1998), and finally (iv) proliferation of vascular cells within the wound bed (Bao et al., 2008). VEGF together with PLGF take part in mobilization of VEGFR-2 expressing EPC to the circulation (Fox et al., 2008). However, the mechanisms of VEGF/PLGF-mediated EPC homing to the wound site remains unknown.

Other effects of VEGF family members include monocyte migration and activation (Barleon et al., 1996), production of MMPs by smooth muscle cells, their migration and proliferation during hypoxia (Grosskreutz et al., 1999; Parenti et al., 2002; sWang and Keiser, 1998), fibroblast proliferation and formation of scars (Wilgus et al., 2008), and keratinocyte motility required for wound re-epithelialization (Bao et al., 2008).

Similar to other growth factors, such as FGF-2, VEGF family members, particularly VEGF-A and B exist in an ECM-bound state (Ikuta et al., 2000;Ishitsuka et al., 2009;Wijelath et al., 2006). VEGF binding to tenascin X both localizes and enhances VEGF stimulatory effects. Interestingly, tenascin X (Ishitsuka et al., 2009) as well as tenascin X-derived fragments (Demidova-Rice et al., 2011) have pro-angiogenic properties, which may prove instrumental as wound healing enhancers (Figure 3.20).

A number of studies performed with chronic wounds of different origin show an increase in VEGF mRNA and decrease in VEGF protein levels due to augmented proteolytic activity observed within the wound bed (Lauer et al., 2000). Additional disruption of VEGF signaling in chronic wounds may come from an increase in soluble VEGFR-1 observed in venous ulcers (Eming et al., 2004).

Importantly, exogenous VEGF has been successfully employed in animal studies (Galiano et al., 2004) and proposed for use in treatment of chronic wounds in humans. Recombinant human VEGF (Telbermin) was well tolerated in clinical Phase I trial in patients with chronic diabetic foot ulcers (Hanft et al., 2008), but failed to improve wound healing in a phase II trials (http://www.gene.com/gene/news/pressreleases/display.do?method=detail&id=10967). The instability of VEGF in protease-rich wound environment could be one of the reasons for its inefficiency. In turn, the use of biologically active and protease-resistant VEGF isoforms could potentially overcome this problem (Mineur et al., 2007). However, it should be recognized that VEGF, which was initially identified as a vascular permeability factor, has been shown to induce uncontrolled growth of non-functional vessels (Senger et al., 1983). Therefore, this growth factor alone may not be sufficient (or appropriate) for the formation of stable blood vessels necessary to successfully repair injury sites or chronic wound beds. Yet, in combination with other enhancers, wound healing might be enabled.

Transforming growth factor-β (TGF-β) family.

The TGF-β superfamily members (Figure 1.11) play multiple regulatory roles in modulating wound healing responses (Singer and Clark, 1999) and scarring (Beanes et al., 2003). While this family includes over 30 mammalian members, (Attisano and Wrana, 2002), so far only TGF-β 1-3, bone morphogenetic proteins (BMP) and activins have been implicated in wound

healing and therefore will be discussed in detail below (Barrientos et al., 2008; McDowall et al., 2008).

TGF-β 1, 2 and 3 – the 'founding members' of the TGF-β family are produced by a variety of cell types including macrophages, platelets, keratinocytes, fibroblasts. With the exception of TGF-β1 produced by platelets in its active form, all TGF-β family members are generated in an inactive precursor form complexed with latent TGF-binding proteins linked to extracellular matrix components. Activation of TGF-β is achieved by MMP-2, 9, thrombospondin-1 and integrin αvβ6 together with membrane type (MT)-MMP (ten Dijke and Arthur, 2007). Typically, active TGF-β binds serine/threonine kinase receptor TβRII, which recruits and phosphorylates a related TβRI. After activation, the receptors trigger canonical SMAD-mediated and non-canonical signaling pathways leading to cytoskeletal rearrangements, induction of cell motility and activation of transcriptional machinery (reviewed in Moustakas and Heldin, 2008).

TGF-β 1, 2 and 3 have overlapping but distinct functions during wound healing. All three are important for recruitment of the inflammatory cells and fibroblasts to the wound bed and facilitation of keratinocyte migration. TGF-β 1 and 2 are prominent inducers of fibroblast-myofibroblast differentiation, extracellular matrix deposition, contraction and scar formation, while TGF-β3 has been shown to inhibit scarring (Barrientos et al., 2008). TGF-β1 effects on cells depend on its concentration: low levels of TGF-β1 stimulate endothelial proliferation and migration, while at high concentrations it enhances matrix production (ten Dijke and Arthur, 2007).

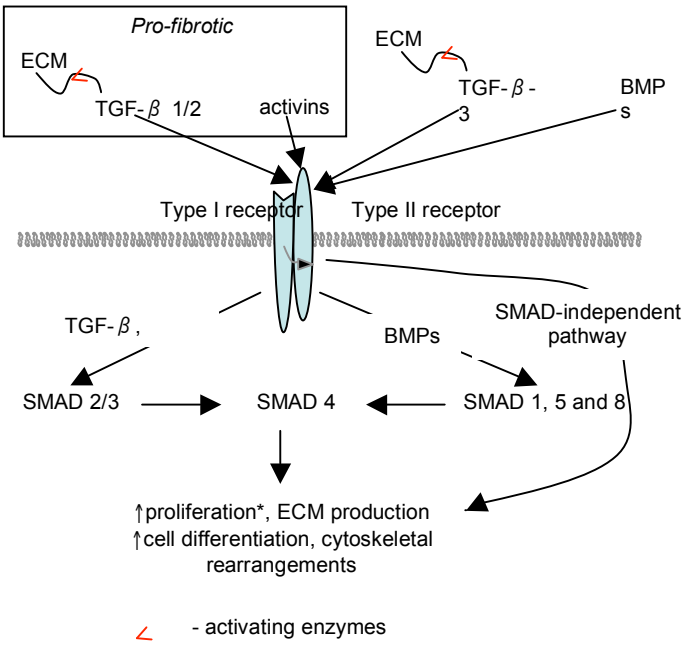

Figure 1.11. Schematic representation of TGF-β - dependent signal transduction.
The members of transforming growth factor-β (TGF-β) family (TGF-β1, 2, 3, bone morphogenetic proteins (BMP) and activins) bind and activate TGF-β receptor type II, which then recruit (curved arrow) and trans-phosphorylate receptor type I. Following injury and during wound healing, ligand-receptor interactions lead to the activation of canonical (SMAD-mediated) or non-canonical pathways, which in turn induce changes in cell proliferation, matrix production, cell differentiation and cytoskeletal rearrangements. The effects of TGF-β on cell proliferation (*) are cell type and growth factor concentration-dependent.

Activin β_A and β_B have been implicated in wound healing. They are expressed by fibroblasts, endothelial cells and keratinocytes and act in a paracrine manner inducing keratinocyte differentiation and leading to an increase in matrix deposition by fibroblasts (McDowall et al., 2008; McLean et al., 2008). Moreover, activins play a prominent role during fibrosis and are involved in formation of

hypertrophic scars and keloids (Mukhopadhyay et al., 2007). Therefore, anti-activin as well as anti-TGF-β 1-2 therapies could be used to treat fibrotic wound healing complications.

BMP-1, 2, 4, 6, 7 have been detected in normal skin where they are involved in the maintenance of the stem cell niche within the hair follicles and regulate matrix assembly (Plikus et al., 2008;ten Dijke and Arthur, 2007). Although BMPs (BMP-6, in particular) seem to be involved in keratinocyte differentiation, their role during wound healing process remains elusive (reviewed by Barrientos et al., 2008).

In chronic wounds, decreased levels of TGF-β ligands have been reported suggesting that addition of exogenous TGF-βs may be beneficial for injury repair (Cowin et al., 2001). However, numerous clinical trials using this growth factor to treat non-healing wounds have failed (Barrientos et al., 2008). This apparent discrepancy can be due to several reasons. First, TGF-β signaling is extremely complex and its effects are cell type and growth factor concentration dependent. Secondly, the TGF-β receptor density on cells residing within chronic wounds is decreased affecting their ability to adequately respond to this growth factor.

The use of TGF-β related proteins as wound healing therapeutics should be approached with great caution as they are implicated in the development of hypertrophic scars and keloids (Beanes et al., 2003). Anti-TGF-β therapies, such as neutralizing antibodies (Shah et al., 1995) are now under investigation for treatment of these debilitating conditions. More work needs to be done to fully reveal the potential of pro- and anti-TGF-β therapies.

Exogenous growth factors in treatment of cutaneous wounds: challenges and opportunities.

Growth factors are critically important for coordinating cell-cell and cell-matrix interactions during normal injury-repair. Exogenous growth factors delivered to non-healing wounds can facilitate cellular responses and lead to timely wound closure (Falanga, 2005). Despite a number of promising studies in animal models showing acceleration of healing upon addition of a variety of growth factors, their clinical use remains limited. Presently, the only growth factor approved for clinical use is rhPDGF-BB (Regranex, Becaplermin). It is used in treatment of chronic and acute wounds (Cohen and Eaglstein, 2001; Hinchliffe et al., 2008), but extremely expensive and often ineffective. Its inefficiency is in part due to rapid degradation of the growth factor in proteolytic wound environment resulting in insufficient concentration of the PDGF in chronic wound bed (Falanga, 2005). The activity of a growth factor within hostile wound environment can be preserved using several methods including addition of protease inhibitors to growth factor-containing formulations or use of recombinant protease resistant growth factors (Lauer et al., 2002; Okumura et al., 1990). However, even prolonged presence of active growth factors within the wound bed may not be sufficient as cells within chronic wounds often have inadequate expression of growth factor receptors. Therefore, despite the introduction of exogenous growth factors and other advanced wound healing therapies, chronic wounds remain a significant problem that affects millions of people worldwide. As such, the development of innovative wound healing modalities is critically important. In this

dissertation we discuss the wound healing potential of Low Level Light and novel ECM-derived peptides.

1.4.2. Low level light therapy: mechanisms and wound healing potential.

History and applications

Low lever light therapy (LLLT), also called “cold laser”, “soft laser”, “laser biostimulation”, “photobiomodulation” or phototherapy (Smith, 2005) employs low doses of coherent light derived from lasers or non-coherent light from lamps and light-emitting diodes (LEDs) to stimulate cellular responses (Hamblin and Demidova, 2006; Huang et al., 2009). The term "laser biostimulation" has first been utilized in 1967 when Endre Mester in Semmelweis University, Budapest, Hungary wanted to test whether laser radiation might cause cancer in mice (Mester et al., 1968). In this study the dorsa of the mice were shaved, the animals were divided into two groups, and one group was exposed to a low powered ruby laser (694-nm). It was demonstrated that the treated mice did not develop cancer, but instead, their hair grew back more quickly than the untreated group. Since then, LLLT has been used experimentally for a several medical applications, including wound healing, inflammation and pain reduction (Chow and Barnsley, 2005; Kiritsi et al., 2010; Minatel et al., 2009a) (Figure 1.12) with the results of over 200 Randomized Controlled Trials published. Furthermore, over thirty light sources have been FDA-cleared for chronic neck and shoulder pain, relief of pain associated with Carpal Tunnel Syndrome. In 2007 the first laser-based device that got FDA-clearance for hair re-growth (www.fda.gov). It should be noted, however, that results of clinical trials have not always been

positive. This is largely due to the complexity of the parameters involved in LLLT such as wavelength of light, total fluence, fluence rate, coherence, pulse structure or continuous wave, and polarization state. These parameters as well as applicable terminology will be discussed below.

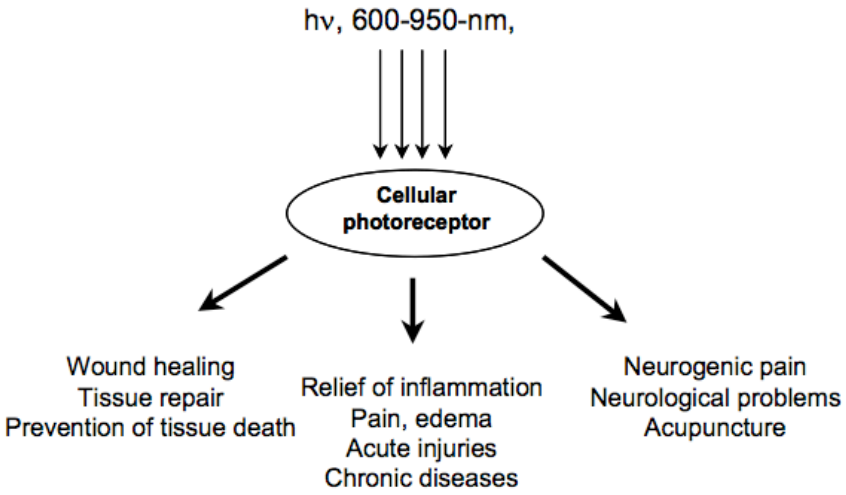

Figure 1.12. Main applications of LLLT.

LLLT parameters.

LLLT parameters are described in the following terms: light wavelength and dose that can be defined by irradiance, energy, energy density and irradiation time.

Light wavelength and activity maxima.

Generally, LLLT employs light sources emitting red, near infrared or infrared light with wavelengths of 600 to 950 nm. This range of wavelengths is chosen based in two considerations.

According to the first law of photobiology, for light to have any effect on a living biological system, the photons must be absorbed by electronic absorption

bands belonging to some molecular photoacceptor (Sutherland, 2002). Many cellular photoacceptors that mediate effects of LLLT, including cytochrome C oxidase, flavins, flavoproteins and porphyrins absorb red and near-infrared light (Karu, 1999). Hence the light of these wavelengths is used in LLLT.

Secondly, in order for light to exert it effect on cells and tissue, it must be able to travel through the tissue far enough to rich its targets. The depth of light penetration depends on its absorption and scattering within the tissues. These parameters, in turn are determined by the light wavelength. Blue and green light with wavelength shorter than 600 nm is mainly absorbed by hemoglobin and melanin, which are abundant within mammalian tissues. Far red and near infrared light (>950 nm) on the other hand are largely absorbed by water. This

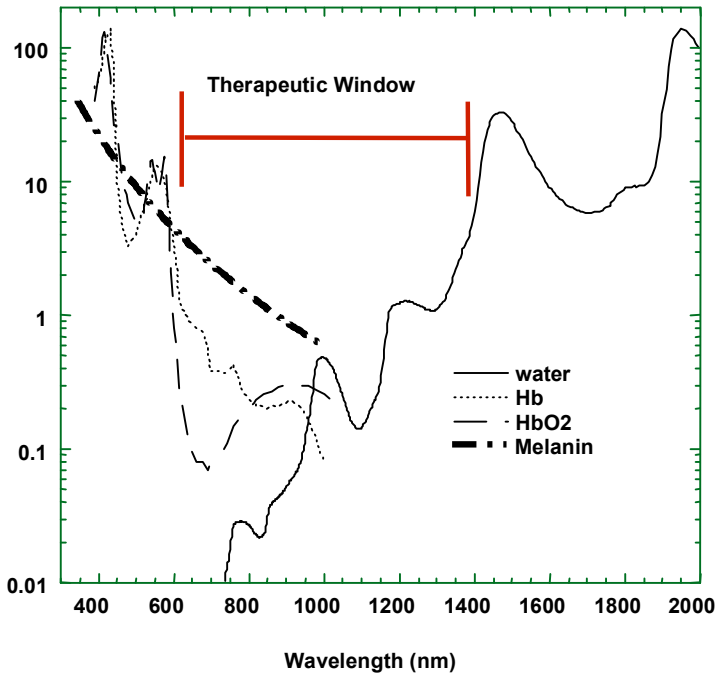

Figure 1.13. Light absorption by biological tissues and therapeutic window.

pattern of light absorption within the tissues creates so called “optical window” or “therapeutic window” where the light penetration depth is maximized (Figure 1.13) (Niemz, 2004).

Within this window there are several activity peaks (Karu and Kolyakov, 2005). Based on effects of monochromatic light on nucleic acids synthesis and rates cell adhesion these peaks have been recorded at 613.5 - 623.5 nm, 667.5 - 683.7 nm, 750.7 - 772.3 nm and 812.5 - 846.0 nm. Peacks of LLLT stimulation for biological responses to light are very similar to absorption spectra obtained for cytochrome c oxidase in different oxidation states. Therefore, this mitochondrial membrane protein has been proposed to be the major photoacceptor mediating the effects of light on mammalian cells (Karu, 1999). Absorption of light by cytochrome c oxidase leads to changes in mitochondrial membrane potential, generation of ROS, alterations in Ca^{2+} flow, cellular nitric oxide levels (Karu, 2008) and consequent induction of cellular responses.

Another parameter that is important for successful application of LLLT is dose of light.

Irradiance, energy, energy density, irradiation time and dose of LLLT.

Irradiance also called power density or intensity (W/cm^2) is calculated according to Equation 1 and represents the power per unit area. The power here is measured at the target tissue.

$$Ir\ (W/cm2) = Power\ (W)/Area\ (cm^2) \qquad \text{Equation 1}$$

Energy depends on amount of laser power applied to a sample and a time of irradiation. It is calculated using Equation 2.

$$\text{Energy (J)} = \text{Power (W)} \times \text{Time (s)} \qquad \text{Equation 2}$$

Energy density (J/cm^2) or fluence takes in the account power, length of irradiation and the area to which the light is applied:

$$\text{Energy density } (J/cm^2) = \text{Energy (J)} / \text{area } (cm^2) \qquad \text{Equation 3}$$

The term “energy density” is commonly used to describe the dose of light. However, it might not be appropriate and misleading: light delivered at high power over the short period of time will have the same energy density as light delivered at lower power over longer period of time but the biological effects will be dramatically different. Therefore, it has been suggested that the dose of LLLT should instead be defined by the length of time of irradiation with light of specific wavelength delivered at particular irradiance. The wavelength and irradiance are considered as “medicine” (Huang et al., 2009).

Cellular effects and mechanisms of LLLT.

LLLT has been shown to stimulate cellular responses both in vitro and in vivo. It increases cellular metabolism, proliferation, migration, and modulates gene expression and protein synthesis (generally accepted that mitochondrial

cytochrome c oxidase is primary photoacceptor of red and near infrared light in living cells (Huang et al., 2009;Karu et al., 2004;Karu, 2008). Exposure of cytochrome c oxidase to red light induces enzyme activation and leads to an increase in proton transfer and ATP generation (Pastore et al., 2000). In turn ATP has been demonstrated to enhance multiple cellular functions. Increase in cellular proliferation in response to increase in ATP is linked to cyclic AMP (cAMP) production and activation of JNK/Ap-1 pathway (Hu et al., 2007). Actin fiber assembly, interactions with actin binding proteins and therefore cell motility are also ATP-dependent as is cell contraction regulated by small GTPases (van Horssen et al., 2009). While increase in cell motility (Hawkins and Abrahamse,

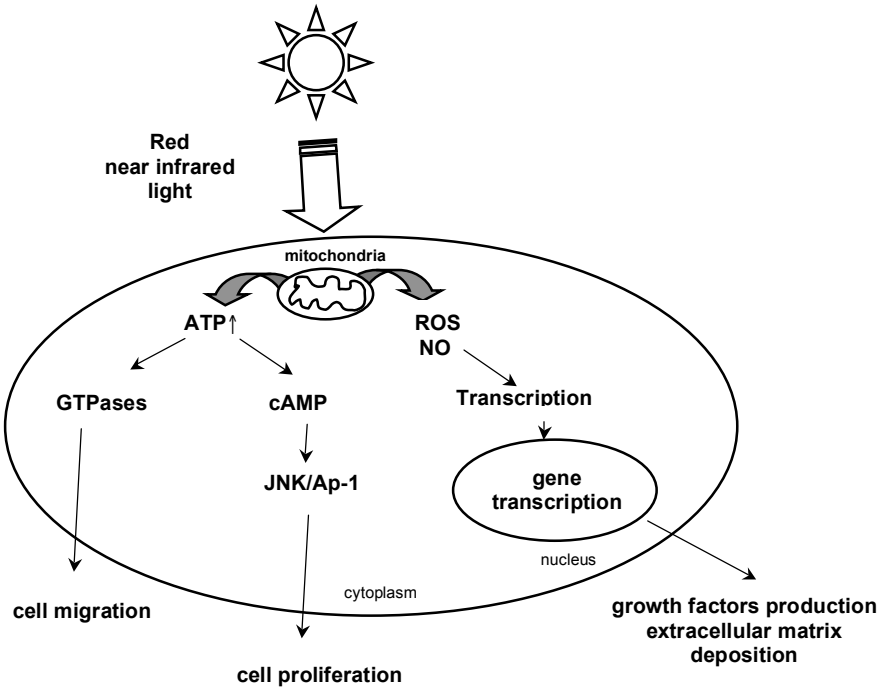

Figure 1.14. Mitochondria-dependent cell signaling pathways activated by LLLT.

2006) and contraction (Demidova-Rice et al., 2007; Medrado et al., 2003) after LLLT are well known phenomena, they have never been directly linked to LLLT-dependent ATP production. Similarly, protein synthesis, which canonly occur in the presence of ATP, has been reported to be enhanced by red light (Vacca et al., 1996). No connection has been made between LLLT-meditated increase in ATP and cellular synthetic activity. Therefore the question remains whether these cellular responses are mediated by ATP or by other light-induced signaling molecules. The latter include nitric oxide (NO) and ROS (superoxide anions $O2^{\bullet -}$) discussed below (Hamblin and Demidova, 2006).

Increase in NO secretion by cells in response to phototherapy is known for over a decade (Karu, 2008; Kipshidze et al., 2000). It is now thought that there are at least three mechanisms by which LLLT-mediated NO production might be augmented. The first involves photodissociation of this molecule from cytochrome c oxidase (Karu et al., 2005). The second mechanism is linked to enhanced expression of nitric oxide synthases (Chen et al., 2008; Kipshidze et al., 2000; Moriyama et al., 2009). The mechanisms of phototherapy-induced NOS expression are not well understood, however the involvement of PI3K/Akt pathway has been suggested (Chen et al., 2008). Finally, upon exposure to near-infrared and blue light, NO can be released from heme-containing proteins distinct from cytochrome c oxidase, NO-hemoglobin and myoglobin (Shiva and Gladwin, 2009; Vladimirov et al., 2000; Zhang et al., 2009). LLLT effects mediated by NO include increase in cell respiration (Karu et al., 2005), protection from cell death (Zhang et al., 2009), vasorelaxation and inhibition of restenosis

(Kipshidze et al., 2000), and modulation of inflammatory responses (Moriyama et al., 2009).

ROS thought to be operating in LLLT include superoxide anions ($O2^{\bullet -}$), hydrogen peroxide (H_2O_2), singlet oxygen ($^1O_2$) and hydroxyl radicals ($^{\cdot}OH$) (Lavi et al., 2010) and references therein). These molecules are mainly generated in mitochondria after activation of complex I and III of respiratory chain. In addition, the ROS are generated in plasma membrane after light absorption by NADPH oxidation system (Lubart et al., 2005). While high doses of ROS are lethal for cell and induce apoptosis (Simon et al., 2000), small amount of these molecules have been demonstrated to activate transcription (Huang et al., 2009) and stimulate cell proliferation possibly via Src-dependent mechanism (Gao and Xing, 2009; Grossman et al., 1998), migration (Yao et al., 2009).

LLLT and its effects on wound healing.

From its beginning in 1960s LLLT has been used for treatment of cutaneous wounds both in human subjects and in animal models (da Silva et al., 2010). Since then considerable progress has been made in our understanding of the mechanisms governing the interactions and effects of red and near infrared light on tissues (Hamblin and Demidova, 2006; Huang et al., 2009; Karu, 2008). Multiple animal and clinical studies have been performed in order to determine whether LLLT can stimulate wound healing (Peplow et al., 2010; Sobanko and Alster, 2008).

Animal models.

Excisional wounds in rodents are the most commonly utilized animal models in these experiments. Using healthy mice several groups demonstrated that red light stimulates wound closure, fibroblast-myofibroblast transition and increase collagen deposition (de Araujo et al., 2007; Prabhu et al., 2010). Similar studies in rats confirm these observations (Reis et al., 2008; Ribeiro et al., 2009; Viegas et al., 2007). Increased collagen synthesis is likely to be linked to an increase in wound tensile strength that is observed in incisional wounds in rats and mice exposed to LLLT (Lyons et al., 1987; Vasilenko et al., 2010).

Effectiveness of phototherapy has also been studied in burn wounds (Erdle et al., 2008; Oliveira et al., 2008). Results of experiments in both mice and rats demonstrate that despite repetitive exposure to LLLT stimulatory effects are only observed at early stages of healing. This is probably due to inability of light to penetrate through a thick scab that often covers burned areas. Therefore, combining LLLT with debriding agents such as bacterial collagenase could improve the outcome of treatment in this model.

Several studies used genetically modified or chemically treated animals characterized by impaired responses to injury in order to determine the healing potential of LLLT for chronic wounds (Chung et al., 2010; Kawalec et al., 2004; Reddy et al., 2001; Reddy, 2003; Yu et al., 1997). Yu an co-authors (Yu et al., 1997) used non-insulin-dependent diabetic mice (C57BL/Ksj/db/db) (Leiter and Chapman, 1994) and demonstrated significant improvement in wound closure rates in animals treated with argon dye laser (630 nm) as compared to untreated controls. Few years later Reddy et. al utilized excisional wounds in

streptozotocin-treated rats to show that treatment with He-Ne laser (632.8 nm) induces an increase in collagen deposition and improve scar tissue stability (Reddy et al., 2001). Similar animal model was used in a follow-up study (Reddy, 2003) employing Ga-As laser (904 nm). Here an enhancement of collagen production was also detected. The comparison of the two light sources performed by the author revealed that stimulatory effects of He-Ne laser are more pronounced (Reddy, 2003). It should be noted however, that this assessment was performed using previously published data obtained using animals of different age. Therefore, the conclusion about superiority of 632.8 nm light over 904 nm light might need re-evaluaion.

In a recent study leptin receptor deficient diabetic mice were used and their responses to LLLT were compared to those observed in normal C57 black mice (Chung et al., 2010). Dorsal cutaneous wounds were created in all the animals and covered with a multi-layer transparent dressing in order to limit wound contraction. The wounds were exposed to 660 nm laser light for 7 consecutive days starting immediately after injury. Analysis of wound closure rates, epithelialization, granulation tissue formation and collagen deposition demonstrated significant improvement of these parameters in diabetic mice treated with 1.6 J/cm^2 of light and to lesser extent in animals receiving 0.36 J/cm^2. Interestingly, non-diabetic mice used in this study did not respond to LLLT (0.36 J/cm^2) (Chung et al., 2010). Similarly, Kawalec and co-workers report that non-diabetic C57 black mice are irresponsive to LLLT with 980 nm laser (Kawalec et al., 2004). The reason for this LLLT resistance is probably two-fold –

firstly, these mice are known to be very good healers, and secondly, the dark pigment present in their tissue might prevent light penetration.

Most studies described above use red, near infrared or infrared light, however, few of them, including a study by Adamskaya and co-authors report that exposure to blue light (470 nm) can also improve wound healing outcome (Adamskaya et al., 2010). Unlike red light that is mainly absorbed by cytochrime C oxidase the blue-light induced effects might be mediated by NO that is released from nitrosyl hemoglobin (Vladimirov et al., 2000). Another possible reason for the effectiveness of this wavelength of light is its bactericidal properties (Guffey and Wilborn, 2006). The efficacy of blue light may however be limited as its tissue penetration is very low.

While majority of animal studies describe positive effects of LLLT on wound healing, there are also several reports showing that exposure to light did not induce any increase in responses to injury (Basford et al., 1986; Cury et al., 2009; Hunter et al., 1984; Lowe et al., 1998; Smith, 2005; Tuner and Hode, 1998). Lowe and co-workers employed X-ray radiation-impaired murine model of excisional wound healing and GaAlAs diode laser (wavelength - 890 nm, energy density - 0.18-1.45 J/cm^2) (Lowe et al., 1998). They did not observe stimulation of wound healing; moreover the highest dose of light induced inhibition of cellular responses. Similar conclusions were reached in a more recent study where two different light sources (lasers at 660 and 780 nm) were used to treat skin flaps in rats (Cury et al., 2009). Unlike the previous study here much higher doses of irradiation (30 or 40 J/cm^2) were used. These studies as well as “positive” reports

described above employ various rodent models of cutaneous wound healing. However, the process of wound healing in rodents differs significantly from that in humans. Porcine wound healing provides more realistic and appropriate model for use in studies aimed at development of clinically relevant treatment modalities. To date, only a few studies employing this animal model and LLLT have been published (Hunter et al., 1984; Smith, 2005). Hunter and others used HeNe laser to treat partial thickness excisional wounds. Laser treatments (irradiance 64 mW/cm^2, energy density 0.96 J/cm^2) were applied daily to half of the wounds created on the dorsal skin of a pig. The authors report no acceleration of the healing process (Hunter et al., 1984). Another paper describes treatment of skin flaps in pigs and rats with HeNe laser (Smith et al., 1992). Here light was applied for 30 s/cm^2 with irradiance of 310 mW/cm^2 (calculated energy density 9.3 J/cm^2) for 4 days pre-operatively, 10 minutes prior to flap elevation and 5 days post-surgery; control wounds were exposed to white light for 30 seconds. Each pig had both control and laser treated wounds. The authors report no improvement in flap survival or decrease in the area of necrosis in laser treated compared to control wounds (Smith et al., 1992).

"Negative" LLLT reports listed above have several typical shortcomings. First, many of them use improper irradiation parameters: inappropriate wavelength, too high or too low power and energy densities. Secondly, some studies employ types of wounds that might not be treatable with LLLT. Specifically, in models like skin flap (Figure 1.15) elevated tissues might hinder light penetration to the wound bed. Finally, the authors often (Hunter et al., 1984;

Smith et al., 1992) do not take in consideration the systemic effects of phototherapy, which could be at play when control and treated wounds are located on the same animal.

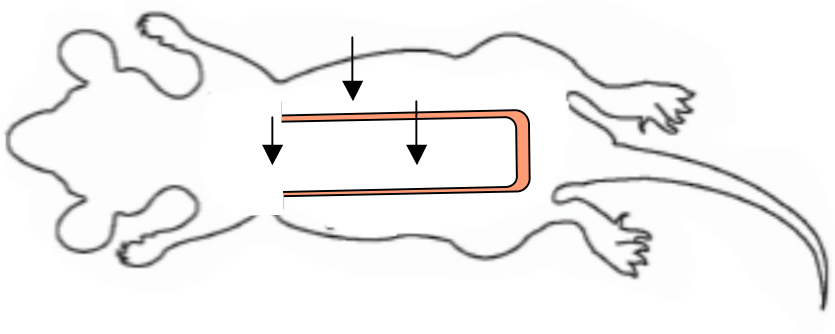

Figure 1.15. Skin flap model of cutaneous wound healing.

Arrows indicate possible site of LLLT application. Exposure of different areas of the wound to LLLT might lead to different outcomes.

Clinical studies.

The use of LLLT for treatment of wounds in human patients is even more controversial with only few randomized controlled trials reporting improvement of healing after phototherapy (Sobanko and Alster, 2008). The reasons for this controversy are similar to those listed above for animal studies: poor study design and poor understanding of complexity of LLLT parameters by healthcare professionals (Tuner and Hode, 1998). Let us compare and contrast two double-blinded randomized controlled clinical trials (RCT) aimed at evaluation of the efficacy of LLLT for management of chronic wounds, but reporting different outcomes (Franek et al., 2002; Minatel et al., 2009). These trials employed red

and/or infrared light of the wavelengths (660, 810 and 890 nm) that have stimulated wound healing in animal models. However, the trial outcomes in clinical settings were dramatically different.

Minatel and co-authors (Minatel et al., 2009) treated 23 ulcers in 14 patients suffering from type II diabetes and mixed arterial/venous insufficiency and/or neuropathy. The ulcers that were present for minimum of 4 weeks before the beginning of the study were randomly assigned to two groups: placebo treated wounds were exposed to sham laser (660 nm, average power less than 1 mW/cm^2). The wounds in experimental group were treated with 660 nm and 890 nm laser light (applied simultaneously), power density 100 mW/ cm^2, fluence 3 J/ cm^2. In both control and experimental groups, the laser probe was held in contact with the wounds, which were covered with transparent film dressing; the entire surface of the wound was exposed to light therefore, the treatment time was longer for larger wounds. Before treatments each ulcer was washed with 0.9% physiological saline and dried; after exposure to light ulcers were dressed with 1% silver sulfadiazine cream, covered with gauze and bandaged. Treatments were performed twice a week for maximum of 90 days or discontinued at the time of wound closure. The effects of LLLT were evaluated starting 15 days after the beginning of the treatment; the rate of granulation tissue formation and wound healing based on the wound size were assessed. The authors report a significant enhancement of wound healing in LLLT treated ulcers compared to those exposed to placebo and conclude that phototherapy is a viable modality that can be used for treatment of chronic leg ulcers.

On the contrary, another double-blind RCT performed in 2002 concludes that phototherapy has not effect on healing of chronic leg ulceration (Franek et al., 2002). Compared to many other LLLT clinical trials this study is well designed. It compares treatment outcomes in three groups of patients: control, placebo and phototherapy treated; each group consists of 21-22 patients all of whom have crural ulcerations. The authors clearly describe treatment conditions, evaluate treatment outcome and analyze the significance the findings using several statistical tests. At first glance LLLT parameters used in this study are very similar to the one reviewed above: the authors use infrared light (810 nm), which has been effectively used in animal studies, delivered at appropriate fluence of 4 J/cm^2. However, there is a major distinction: the power density of light used in these trials. In the first study light was delivered at irradiance of 100 mW/cm^2 (Minatel et al., 2009b), Franek and co-authors on the other hand used light of much higher intensity of 650 mW/cm^2 (Franek et al., 2002). Meanwhile as it has been demonstrated multiple times that light delivered to the tissues at low energy, but high power density can be detrimental for cellular processes (Huang et al., 2009 and references therein). Another difference between the two studies is the duration of LLLT. In the first study the wounds were treated in 30 sessions over 3 months; in the second trial wounds were treated 5 times a week for 4.5 weeks with the total of 22.5 sessions. However experimental evidence from in vitro studies indicates that for LLLT to be effective, it has to be applied with sufficient intervals and that for LLLT to take the effects total treatment duration needs to be sufficient (Houreld and Abrahamse, 2007). Moreover, unlike Minatel

and others, Franek and co-authors used LLLT in combination with compression therapy (CT) and treated control wounds with CT alone. The use of CT in the trial could undermine the effects of LLLT.

The comparison between the two studies reveals that when properly applied LLLT can be considered as viable wound healing modality. However, more double blinded randomized controlled clinical studies are necessary to evaluate its effectiveness for treatment of wounds of different etiology. These studies should take in the account the current knowledge of molecular and cellular bases of LLLT and employ appropriate LLLT parameters (wavelength, power and energy densities), which we delineate below using a standardized animal model of wound healing.

1.4.3. ECM-derived peptides and their wound healing potential.

The role of the ECM components, endogenous ECM remodeling enzymes and wound healing potential of exogenous MMPs were discussed in the previous chapters of this dissertation. Here we will describe the role that ECM-derived peptides play in regulation of cellular functions. Negative regulators of cellular functions especially anti-angiogenic ECM fragments have attracted a lot of attention in recent years and have been thoroughly reviewed (Mundel and Kalluri, 2007; Rhodes and Simons, 2007). Stimulatory fragments are less well known. Meanwhile these biologically active proteinaceous molecules have been demonstrated to enhance cellular responses to injury in vitro and in vivo (Malinda

et al., 2008; Min et al., 2010; Robinet et al., 2005) and therefore can be considered as candidate wound healing therapeutics.

Pro-angiogenic fragments were described from a number of ECM molecules, including laminin, elastin and fibrillin-1. In 1990 several groups worked on isolation of bioactive peptide fragments of laminin alpha1 and beta1 chains (Malinda et al., 1999; Nomizu et al., 1995). Extensive in vitro testing revealed that 13 fragments of both laminin chains stimulate in vitro endothelial morphogenesis on Matrigel, cell sprouting from aortic rings and migration in Boyden chamber assays (Malinda et al., 1999). Further experiments demonstrated that at least two of these peptides can also enhance cellular responces to injury in vivo. In addition to their pro-angiogenic properties the peptides were demonstrated to stimulate keratinocytes and fibroblasts within the wound bed. Application of as low as 5 μg of either peptide improved both epithelialization and granulation tissue formation in excisional wounds in rats (Malinda et al., 2008).

Stimulatory peptides have also been isolated form elastin (Brassart et al., 2001;Kamoun et al., 1995;Robinet et al., 2005;Senior et al., 1980). These peptides are chemotactic for monocytes (Senior et al., 1980) and can stimulate fibroblast proliferation in vitro and activate a number of ECM degrading enzymes, specifically MMP-1 and 3 (Brassart et al., 2001; Kamoun et al., 1995). Activation of the MMPs by elastin derived peptides is linked to their ability to stimulate angiogenesis in vitro and ex vivo (Robinet et al., 2005). Similar properties were

described for fibrillin-1 derived peptide containing GXXPG sequence of amino acids (Booms et al., 2006).

The fragments described above are isolated as a result of structural analysis of the full-length ECM proteins (Malinda et al., 1999) or are derived from the product of mammalian elastase-mediated ECM degradation (Robinet et al., 2005). In this dissertation we describe a novel approach for identification of biologically active ECM fragments using exogenous ECM-remodeling proteases, namely collagenase derived from gram-positive bacteria Clostridium histolyticum. Biologically active peptides derived as a result of ECM degradation by Clostridial collagenase originate from collagen IV, fibrillin-1 and tenascin X and stimulate proliferation of CEC, enhance microvascular remodeling in two-dimensional (2D) model on Matrigel and induce endothelial sprouting in a novel three-dimensional (3D) model of injury repair.

Chapter 2. Low-level light stimulates excisional wound healing in mice.

The data presented in the following chapter of the dissertation have been pubished (Demidova-Rice et al., 2007). The experiments were designed by Michael R. Hamblin, Ira M. Herman and Tatiana N. Demidova-Rice. Elena V. Salomatina and Anna N. Yaroslavsky provided help with light sources. Tatiana. N. Demidova-Rice performed animal surgeries and data collection, immunostaining, imaging and data analysis.

2.1. Introduction.

The first publication about low-level laser therapy (LLLT) (then called laser

biostimulation) appeared almost 40 years ago in Hungary (Mester et al., 1968). Since then large numbers of studies demonstrating positive results of LLLT in cells in vitro, animal models and clinical reports have been published, but the subject remains controversial (Brosseau et al., 2000). Many negative studies have also been published further confounding the issue (Tuner and Hode, 1998). Nevertheless, the use of coherent-light sources (lasers) or noncoherent light sources (light-emitting diodes, LEDs) has become widespread by physical therapists, dentists, and practitioners of sports medicine (Chow and Barnsley, 2005; Sun and Tuner, 2004). In 2002, 510K FDA clearance was issued for an 830-nm diode laser for the treatment of carpal tunnel syndrome. There were several controlled trials reporting significant improvement in pain and some improvement in objective outcome measures (Irvine et al., 2004; Naeser et al., 2002; Weintraub, 1997).

The basic biological mechanism behind the effects of LLLT is thought to be absorption of red and near infrared light by chromophores contained in the protein components of the respiratory chain located in mitochondria, in particular cytochrome c oxidase (Karu et al., 2004; Karu and Kolyakov, 2005). It is thought that this absorption of energy may cause photodissociation of inhibitory nitric oxide from cytochrome c oxidase leading to increased enzyme activity (Wong-Riley et al., 2005), increased electron transport (Pastore et al., 1994) and increased production of ATP (Karu et al., 1995). Moreover, low level light was shown to stimulate the expression of multiple genes related to cellular migration, proliferation, and modulate the production of growth factors and cytokines (Zhang

et al., 2003).

The complexity of the parameters involved in LLLT such as wavelength, total fluence, fluence rate, coherence, pulse structure or continuous wave, and polarization state has meant that a number of negative studies of LLLT as well as many positive studies have been published (Posten et al., 2005). However one important point that has been demonstrated by multiple studies in cell culture (Skinner et al., 1996), animal models (Lyons et al., 1987), and in clinical studies is the concept of a biphasic dose response with the total delivered light energy density (fluence). The reason why the technique is termed **low**-level is that there exists an optimal dose of light for any particular application, and doses lower than this optimum value, or more significantly, larger than the optimum value will have a diminished therapeutic outcome, or for high doses of light a negative outcome may result. While the studies exploring the effects of different power and energy densities on the outcome of the treatment are common, the studies of the wavelength dependency, especially in *in vivo* models are less widespread.

In this report, we describe the effects of LLLT with various optical parameters, including the wavelength, on the outcome of the treatment in a standardized model of full-thickness excisional wound healing in mice. A single exposure of the wound to light thirty minutes after wounding led to increased wound healing especially in the early time points 1-5 days post-injury. The likely mechanism involved in simulation of wound healing by LLLT is enhancement of wound contraction by the dermal cells (fibroblasts and myofibroblasts) at the wound edge.

2.2. Material and Methods.

Animal model of excisional wound healing.

All animal experiments were approved by the Subcommittee on Research Animal Care of Massachusetts General Hospital and were in accordance with NIH guidelines. Mice were housed 5 per cage and given access to food and water ad libitum. Male BALB/c, C57/BL6/1J and SKH1 hairless mice were obtained form Charles River Laboratories (Wilmington, MA). Animals 6-9 weeks of age were used. The backs of BALB/c and C57BL/6 mice were depilated by use of Nair cream (Carter-Wallace, New York, NY) 15-24h before wounding. The mice were anesthetized by an intraperitoneal injection of a ketamine-xylazine cocktail (90 mg/kg ketamine and 10 mg/kg xylazine) before wounding procedures and during treatments. Dorsal full thickness excisional wounds were made with sterile scissors and forceps, the wound was left uncovered during the whole period of experiments, i.e. until fully healed. To insure comparable wound size in all the mice, a 10x13 mm template was used. Single illuminations were performed 30 minutes after wounding; the area illuminated included the wound bed and intact skin at all four wound edges (approximately 5 mm). In total, 55 mice were used.

Light sources, dosimetry and treatment.

Three light sources were used in this study. A non-coherent light source with interchangeable thirty-nm band pass filters (LumaCare, London, UK) was used to deliver 635 ± 15 nm light in order to generate light dose response curves). Fluences delivered were 1, 2, 10 and 50 J/cm^2. Fluence rates used were 80-100

mW/cm^2. Helium-Neon (632.8 nm) laser (Melles Griot, Carlsbad, CA) was used as a source of monochromatic coherent light. Two fluences 1 and 2 J/cm^2 were used. Fluence rates of 2 mW/cm^2 and 1 mW/cm^2 were used to deliver 1 and 2 J/cm^2 of light respectively. Coupled to a monochromator xenon arc lamp (Spectra Physics, Mountain View, CA) was used to produce 670 ± 15, 720 ± 15 and 820 ± 15 nm light. To create a homogeneous light spot with a diameter of 3 cm the light was delivered using a ring light guide (Edmund Optics GmbH, Karlsruhe, Germany). Fluence of 1 J/cm^2 was employed. Fluence rates were 0.59, 0.79 and 0.86 mW/cm^2 for 670 ± 15, 720 ± 15 and 820 ± 15 nm respectively. Power readings of Helium-Neon laser and LumaCare lamp were measured with the Lasermate power meter (Coherent, Inc, Santa Clara, CA). A power meter (Ophir Optronics, Inc, Wilmington, MA) was used for the xenon arc lamp.

Each experimental group contained five to 10 mice. Fifteen mice were used as control; these animals were anesthetized and wounded in as described above, but were not illuminated 30 min after wounding.

Animal follow-up.

General health of the animals was monitored daily. Adverse effects of wounding were not observed. Width and length of the wounds were measured with digital caliper (Control Company, Friendswood, TX) daily and the areas of the wounds were calculated. Wound images were acquired every other day using a digital camera. For all follow-up procedures mice were anaesthetized with isoflurane solution (Baxter, Deerfield, IL). Mice were sacrificed by CO_2 inhalation either 24h

after wounding/treatment in order to obtain skin samples or after complete wound closure.

Immunohistochemistry.

Identification of myofibroblasts was performed in skin samples taken after 24h from two BALB/c mice treated with 820±15 nm light and two control BALB/c mice. Wounds together with underlying muscle layers were excised and fixed in 4% formalin, embedded in paraffin and cut into 5 μm thick sections. Sections were rehydrated, subjected to the antigen retrieval procedure using Retrievagen A solution (BD Biosciences, San Jose, CA) according to manufacturer instructions and rinsed with distilled water following by incubation in phosphate buffered saline (PBS) /0.1% Triton X-100 for 5 min. In order to minimize non-specific binding, sections were treated with Mouse-on-Mouse blocking solution (Vector Labs, Burlingame, CA) for 1h according to manufacturer instructions. Primary antibodies were mouse anti-SMA (Biogenex, San Ramon, CA) used at 1:200 dilution and pre-diluted rabbit polyclonal anti-CD-31 (Abcam, Cambridge, MA). The incubation with primary antibodies was performed for 1h at room temperature. Sections then were washed and co-incubated with fluorescently labeled anti-mouse Alexa 488, anti-rabbit 546 secondary antibodies (Molecular Devices, Sunnyvale, CA) both at 1:250 dilution and 16.2 μM Hoechst 33342 (Molecular Probes, Invitrogen, Carlsbad, CA) for 1h at room temperature. After triple wash in PBS, stained sections were mounted with Fluorosave (CN Biosciences, San Diego, CA). Visualization of the slides was performed with

Axiovert 200M microscope (Carl Zeiss MicroImaging, Thornwood, NY) using 10X and 40X objective lenses.

Data analysis and statistics.

The numbers representing the percent of original wound size were used for healing curve generation using KaleidaGraph program (Synergy Software, Reading, PA). The data between the experimental points were approximated using cubic spline interpolation technique. The areas under the curves were calculated by trapezoidal rule numerical integration. The number of the experimental points determined the number of the nodes employed for the numerical integration. The integrals were used for comparing the effects of different treatment regimens (wavelength, dose of light). Differences in the areas under the curve between control and treatment were used to evaluate the effects of treatment. Microcal Origin 6.1 software (Northampton, MA) was used for area under the curve calculations. All the data are presented as mean ± SEM. Statistical significance was analyzed by one-way ANOVA. The value of $P < 0.05$ was considered significant.

2.3. Results

Low-level light stimulates wound healing in BALB/c mice.

It has been shown previously that low level red light induces acceleration of wound healing in experimental animals and patients (Lyons et al., 1987). Therefore, for initial experiments 2 J/cm^2 of 635 nm non-coherent light was used on full thickness dorsal wounds in BALB/c mice. Treatment was performed 30

min after wounding as described in Material and Methods. Control mice received wound alone. Healing curves generated for control mice demonstrated an initial increase in wound size from day one to day 4 post-wounding. At day 5 control wounds were the same size as the original size on day 0. From day 6 onwards control wounds exhibited a gradual decrease in wound size until accomplishment of total healing at day 17 (Figure 2.1). In marked contrast, the initial wound expansion seen in control mice was absent in mice treated with 2 J/cm^2 of 635-nm light from a non- coherent light source 30 minutes after wounding. Instead of expanding the wound started to contract immediately after illumination and 1 day later the mean wound area was highly significantly ($P < 0.001$) smaller than the mean wound area of the control wounds. This significant difference between control and illuminated wounds was maintained until day 9. Interestingly, at 10 days post-wounding the difference between control and treated wounds became non-significant and the wounds in both groups healed at approximately same rate until both groups achieved complete healing.

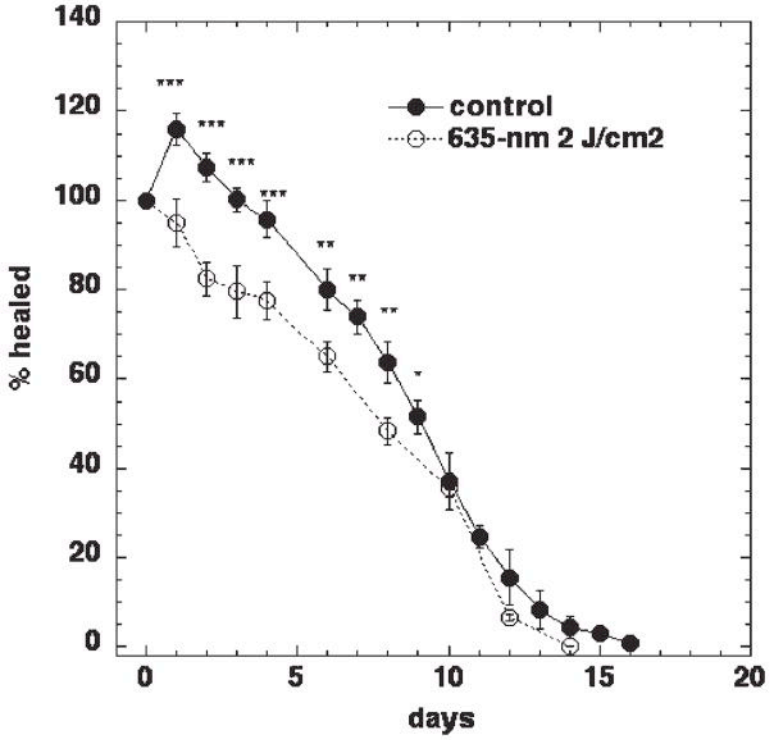

Figure 2.1. The effect of 635 nm light on excisional wound healing in BALB/c mice.

Excisional wounds were created in BALB/c mice and subjected to a single exposure to 2 J/cm^2 of 635-nm light from a filtered lamp delivered 30 minutes after wounding. The wound areas were measured daily. Data points are means of at least ten mice and bars are SEM. Significance was determined by one-way ANOVA and *** = $P < 0.001$; ** = $P < 0.01$; * = $P < 0.05$.

Biphasic dose response between fluence and wound healing.

In order to establish the effect of varying the total energy density delivered on the stimulation of wound healing, in other words to construct a dose-response curve, we used different fluences of light from a 635 nm non-coherent light source. Fluence rates at which light was delivered varied between 80 and 100 mW/cm^2 and the fluences were 1, 2, 10 and 50 J/cm^2. Despite a small variation in fluence

rates between different fluences, the comparison between the groups was performed.

Figure 2.2A shows significant differences between control and illuminated wounds in animals and between different total fluences delivered. As mentioned above, untreated wounds in BALB/c mice tended to expand 1-5 days after wounding. In mice treated with 1 J/cm^2 and in animals treated with 50J/cm^2, this initial wound expansion was also present. Mice that received 50J/cm^2 showed a bigger expansion than that seen in control mice and the wound area did not return to its original size until 7-8 days after wounding. There was very little difference between the 1 J/cm^2 group and no illumination control wounds. Mice treated with 2 or 10 J/cm^2 demonstrate no increase in wound size the next day after treatment and 2 J/cm^2 appears to be better than 10 J/cm2 (Figure 2.2A). To show the effect of treatment, differences in the areas under the curves were calculated. Positive effects compared to control wounds were found for 1, 2 and 10 J/cm^2, however the maximal positive effect was found at 2 J/cm^2. If 50J/cm^2 was used, the area under the control-healing curve was actually smaller that the area under experimental curve, thus the higher dose of 635 nm light - 50J/cm^2

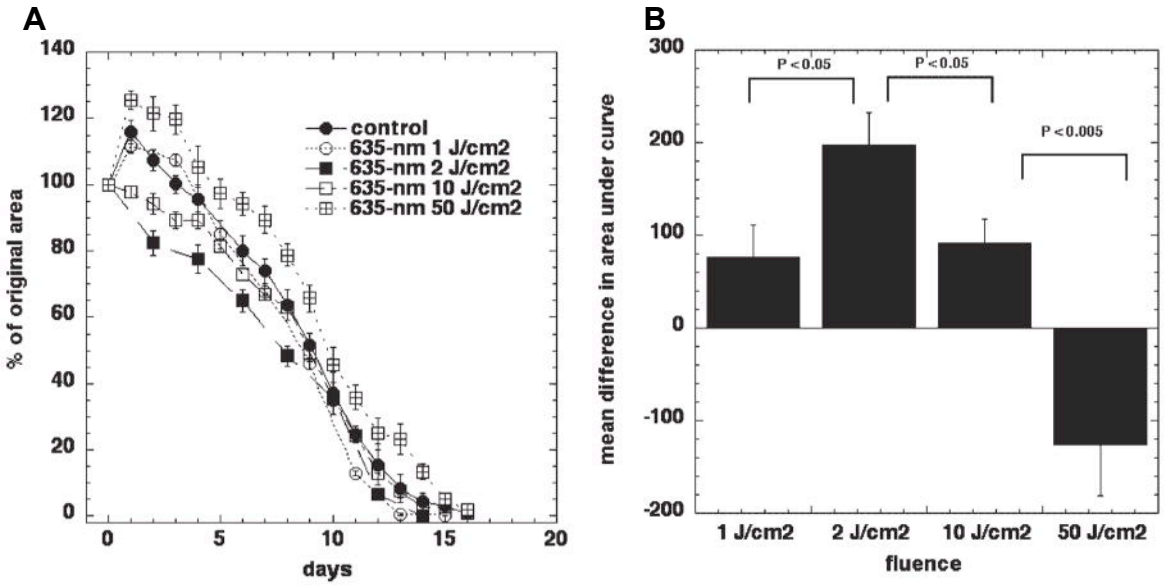

Figure 2.2. Biphasic dose response between fluence and wound healing.

(a). Excisional wound healing in BALB/c mice with no illumination and with a single exposure to 1, 2, 10 or 50 J/cm^2 of 635-nm light from a filtered lamp delivered 30 minutes after wounding. Data points are means of at least ten mice and bars are SEM. (b). The area under each individual mouse healing curve were subtracted from the area under the mean control (no illumination) healing curve and means of these differences in area are shown in Fig 2B with bars = SEM. Statistical significance was analyzed by one-way ANOVA.

had a negative effect on the rate of mouse wound healing. Therefore, in our wound model, a biphasic dose response to 635 nm light from an incoherent light source was demonstrated: 2 J/cm^2 has the largest positive effect, 1 and 10 J/cm^2 improves healing to a lesser extent, while 50 J/cm^2 has a negative effect on wound healing.

820-nm is the most effective wavelength.

We compared four different wavelength ranges of red and near infrared light centered at: 635, 670, 720 and 820 nm delivered from the same non-coherent polychromatic light source to study the tissue response variation with wavelength (Figure 2.3). To minimize the number of variables that could interact with the effects of the light, a standardized wound model, as described above, was used. Irradiation was performed using low fluence rates that were similar for the different wavelength ranges with a fixed fluence of 1 J/cm^2.

The most pronounced stimulation of wound healing by a considerable margin was obtained with 820-nm light. There was no expansion in wound size after wounding and illumination with 820-nm and contraction occurred approximately 3-4 days faster than with the other wavelengths (Figure 2.3A). A noticeable difference between the groups was maintained until day 10 post-wounding. The other wavelengths had lesser effects, with the best one being 635-nm where a significant positive effect was also obtained. It should be noted that the peaks of LLLT activity obtained in this experiment may be different if a different fluence is used. When the biphasic nature of the dose-response curve (Figure 2.2B) is taken into account, this possibility becomes fairly likely.

Wound healing stimulation is mouse strain dependent.

All experimental data presented above were obtained in BALB/c mice. However significant differences in healing rates between mouse strains have been reported in the literature although this is not a well-studied area of research (Li et

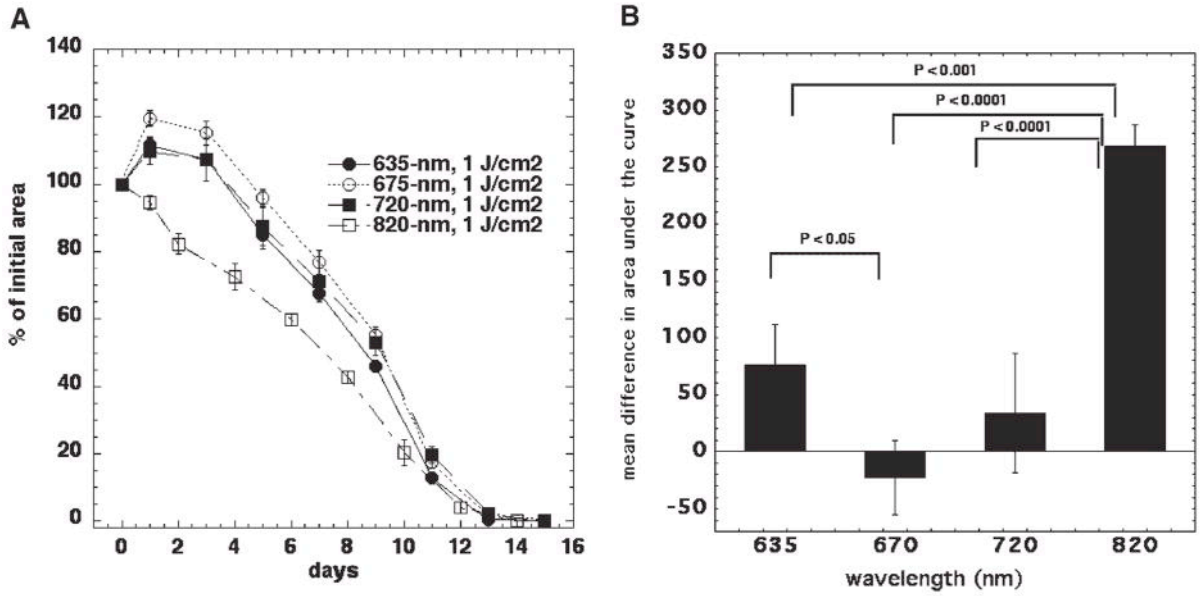

Figure 2.3. **The effect of the wavelength of light on wound healing.**

(a). Excisional wound healing in BALB/c mice with no illumination and with a single exposure to 1 J/cm2 of 635-nm, 675-nm. 720-nm, or 810-nm light from a filtered lamp delivered 30 minutes after wounding. Data points are means of at least ten mice and bars are SEM. (b). The area under each individual mouse healing curve were subtracted from the area under the mean control (no illumination) healing curve and means of these differences in area are shown in Fig 2.3B with bars = SEM.

al., 2001a; Masinde et al., 2006). Therefore we hypothesized that responses to treatment with light may also vary in different strains of mice. To test this hypothesis, we used C57BL/6 black mice and SKH1 hairless mice in addition to the previously studied BALB/c albino mice. Full thickness dorsal excisional wounds were employed. As expected from reports in the literature (Li et al., 2001a; Masinde et al., 2006), in non-illuminated control mice, wounds healed at significantly different rates depending on the mouse strain. In BALB/c and SKH1-hairless mice, wound expansion was seen from day 1 to day 4-5 post wounding. Wounds in C57BL/6 mice did not have any initial expansion and overall healed

significantly faster; complete closure was achieved at day 12 in these mice and day 16-17 in both BALB/c and SKH1 mice (Figs 2.4A and 2.4B). To investigate the effect of LLLT on wound healing in C57BL/6 and SKH1 mice we used 2 J/cm^2 635 nm non-coherent light delivered 30 min after wounding. SKH1 mice behaved in a similar fashion to BALB/c mice in their response to LLLT. It is possible that the response to light was not quite as pronounced in SKH1 compared to BALB/c mice, as there was still a small expansion at day 1 (Figure 2.4A). By contrast, in C57BL/6 mice there was almost no effect of illumination. There was a hint of a smaller wound area at days 1 and 2 post-wounding in the illuminated C57BL/6 mice but this was not significant (Figure 2.4B).

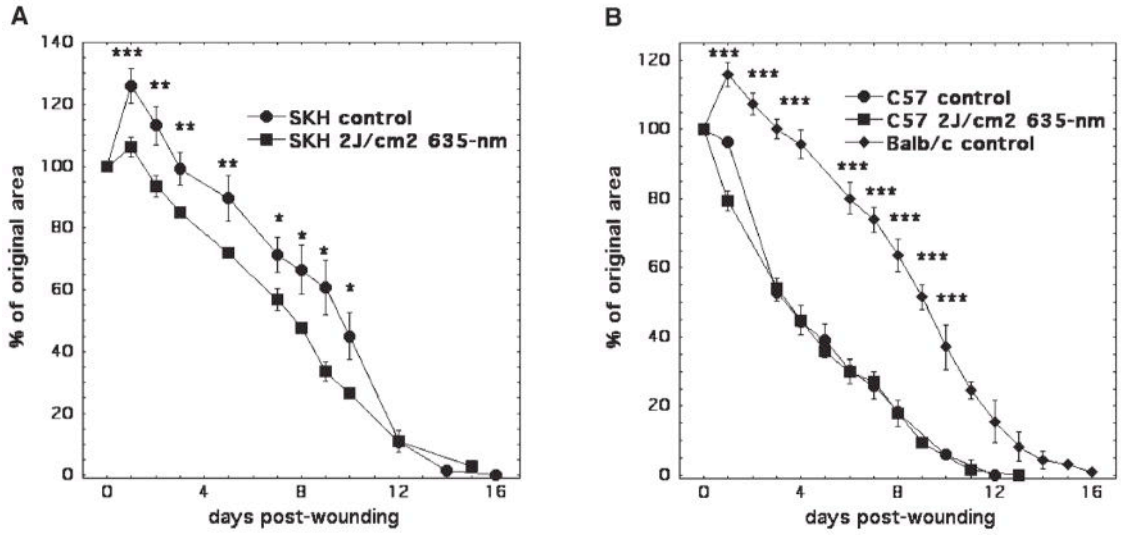

Figure 2.4. **The effects of LLLT on wound healing are mouse strain dependent.** (a). Excisional wound healing in SKH hairless mice with no illumination and with a single exposure to 2 J/cm2 of 635-nm light from a filtered lamp delivered 30 minutes after wounding. (b). Excisional wound healing in C57BL/6 mice and BALB/c with no illumination and C57BL/6 mice with a single exposure to 2 J/cm2 of 635-nm light from a filtered lamp delivered 30 minutes after wounding. Data points are means of at least six mice and bars are SEM. *** = $P < 0.001$; ** = $P < 0.01$; * = $P < 0.05$.

Laser and non-coherent lamp are equivalent.

There is a considerable debate in the literature about the differences between the cellular effects of monochromatic laser light and polychromatic light from non-laser light sources (Flemming et al., 1999; Pontinen et al., 1996). In order to investigate whether the effect of light on wound healing is independent of such properties of light as monochromaticity or coherency, but depends on only wavelength and intensity of light, we compared coherent monochromatic light from He/Ne laser (632.8 nm) and light from a broad band non-coherent light source (635 ± 15 nm). We used the same spot size and the same fluence rate, the differences were in the coherency and monochromaticity of the HeNe laser light which were not present in the filtered broad-band light. BALB/c mice were used in this experiment. Illumination with 2 J/cm^2 was performed 30 min after wounding. Improved wound healing was observed under both experimental conditions (He/Ne laser and 635 ± 15 nm lamp) as compared to controls, however the difference between the light from different sources was not significant (Figure 2.5). There was a hint of an increased effect with HeNe laser at days 1 and 2 after wounding. Therefore we concluded that the wavelength is the main variable that defines the wound healing in response to light. However more research needs to be done using different laser and polychromatic light sources.

Immunohistochemistry demonstrates α-smooth muscle actin-positive cells in wound edge.

Figure 2.6 shows the immunofluorescence staining of tissue sections removed 24h after wounding from non-illuminated and illuminated mice. Nuclei are stained

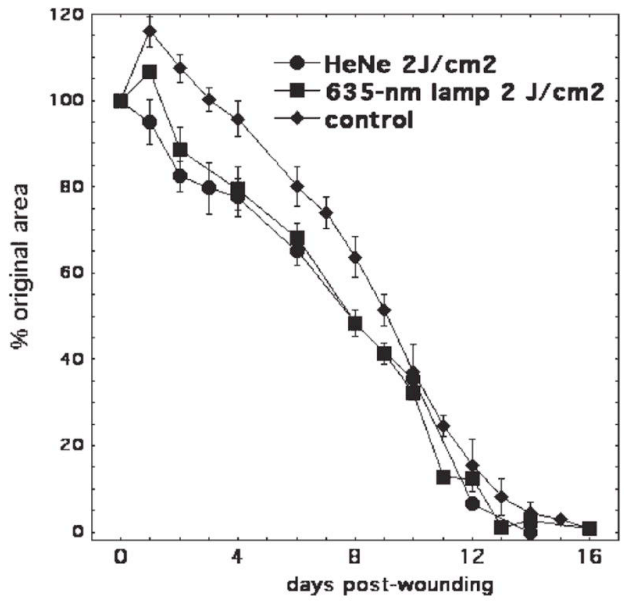

Figure 2.5. **Laser and non-coherent light affect the excisional wound healing in mice.**
Excisional wound healing in BALB/c mice with and without a single exposure to 2 J/cm^2 of 635-nm light from a filtered lamp, or 2 J/cm^2 of 632.8-nm light from a HeNe laser delivered 30 minutes after wounding. Data points are means of at least ten mice and bars are SEM.

in blue, α-smooth muscle actin (SMA) in green and CD31 is stained in red. This triple staining allowed us to distinguish between SMA positive cells that surround small blood-vessels in the dermis from myofibroblastic cells situated in the dermis. SMA-positive cells localized in vicinity to CD31-positive endothelial cells represent smooth muscle cells and/or pericytes restricted to blood vessels; SMA-

positive cells, not co-localized with CD31-positive cells and scattered throughout the dermis are identified as myofibroblasts. The number of green cells (labeled with white arrows) is higher in illuminated wounds.

2.4. Discussion.

There have been numerous reports in the literature over the last thirty years that LLLT with various optical parameters can stimulate wound healing in both small and large animals and also in humans. Even so LLLT for stimulation of wound healing remains controversial, and is not generally accepted as proven by either clinicians or by researchers alike (Kopera et al., 2005; Posten et al., 2005). The reasons for this enduring controversy in both the popular and scientific press is probably due to the high degree of complexity inherent in this technology. A large number of wavelengths of light in the red and near-infrared range of the electromagnetic spectrum have been tested. In addition both the delivered fluence and the fluence rate have been varied quite widely. To further complicate matters there is debate whether the coherent monochromatic light of a laser is better than non-coherent light in a defined wavelength range from a light-emitting diode or a filtered lamp. Furthermore the polarization state, pulse duration and repetition rate are thought by some authors to be important. In addition to the large number of optical parameters that can logically be varied, there remains a large variety of conditions (even within the field of wound healing) that could be treated. A variety of non-healing ulcers occur mainly on the lower extremities that are caused by venous (and arterial) insufficiency, diabetes, prolonged pressure and other comorbid conditions. These chronic wounds are

often proposed as suitable disorders for LLLT. In order for some of these LLLT parameters to be subjected to scientific investigation a reproducible and quantifiable animal model of LLLT effects would be desirable. We believe that an excisional wound-healing model on the mouse back fulfills some of the requirements of such an animal model.

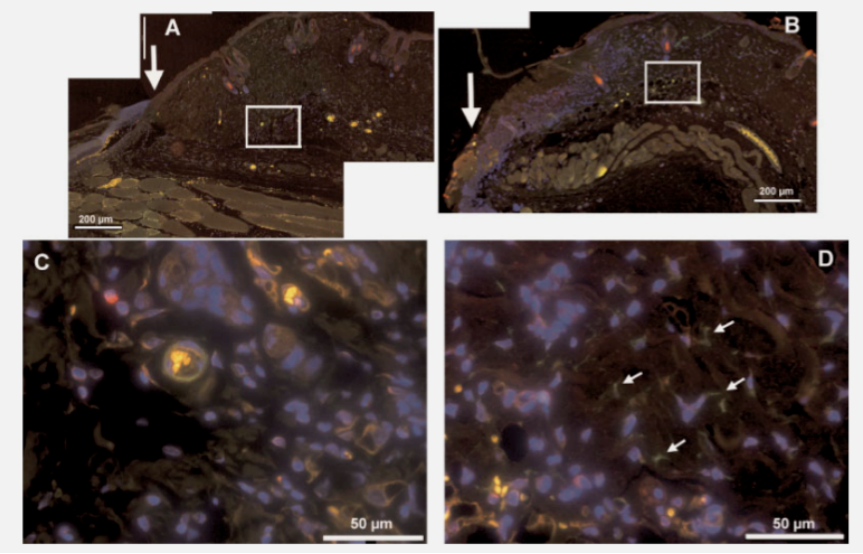

Figure 2.6. The effects of LLLT on mouse dermal fibroblasts in vivo.

Paraffin sections of 1 day old mouse wounds were co-stained with the anti-SMA, anti-CD31 antibodies and nuclear stain. (A) Immunostaining of sections from untreated (a) and treated (b) wounds. Arrows indicate the wound edge. The areas outlined are shown in B. Scale bar 200 μm. (B) High magnification images of wound samples shown in (A). (a). Untreated wound, no SMA-positive myofibroblasts can be seen; the green cells surrounding blood vessel and co-localized with CD31-positive endothelial cells represent smooth muscle cells; (b). Wound treated with 2 J/cm^2 of 820±15 nm light. Individual SMA-positive cells, not co-localized with CD31-positive endothelial cells and representing myofibroblasts, can be seen (arrows). Scale bar 50 μm. Original magnifications: 10x in A, 40x in B. Green – SMA, red – CD31, blue – nuclei.

There have been several previous reports on the use of LLLT in rodent wound healing studies. These reports can be separated into two broad groups depending on whether the animals used were normal, or whether they had been manipulated in some way to depress wound healing. These manipulations employed to impair normal wound healing include diabetes (Byrnes et al., 2004), ionizing radiation (Lowe et al., 1998), treatment with corticosteroids (Pessoa et al., 2004), or malnourishment (Pinheiro et al., 2004). Indeed, it has been asserted that normal healthy rodents may not be a suitable model for studying LLLT effects on wound healing (Karu, 1999). However, our data on healthy animals are useful for establishing treatment parameters that can be used for elucidation of the mechanisms underlying stimulation of wound healing by LLLT in transgenic and knockout mice (Reid et al., 2004) as well as in the models of impaired wound healing.

Our initial experiment in BALB/c mice showed that a single exposure of the excisional wound 30 minutes after wounding to 2 J/cm^2 of 635 $\pm$ 15-nm light delivered at a fluence rate of 80 mW/cm^2 resulted in statistically significantly smaller wounds between 1 and 10 days post-wounding (Figure 2.1). Remarkably, the most noticeable difference between illuminated and control wounds, was observed at 1 day post-wounding. Non-treated wounds showed a noticeable expansion the next day with the mean wound area being almost 20% bigger than it was immediately after wounding. By contrast, the illuminated wounds decreased in size after light delivery and by the next day the mean area was 5% less than it was immediately after wounding. The difference in wound areas

between these two groups of mice at day 1 post-wounding was significantly different ($P < 0.001$), and the difference remained significant although becoming increasingly less pronounced until day 9 post-wounding. On the tenth day after wounding the wounds in the illuminated and control groups of mice had reached the same average area. Using the same light source we were able to carry out an experiment allowing for evaluation of the effects of the dose of light on the healing of mouse wounds. Light was delivered at 1, 2, 10 or 50 J/cm^2 from the same 635-nm light source and at the same fluence rate. At fluences and fluence rates applied, no thermal effects were observed. The comparison of the area under the healing curves generated based on the wound healing rates in control and treated animals, led to a set of four values three of which (1, 2, and 10 J/cm^2) showed positive effects on wound healing and the dose of 50 J/cm^2 gave a negative effect; i.e. illuminated wounds healed slower than controls (Figures 2.2A and 2.2B). This biphasic dose-response (a little light is good but a lot of light is bad) has been reported for studies in LLLT in both cell culture (Pereira et al., 2002) and animal models (Corazza et al., 2007).

The effects of the light wavelength were evaluated by delivering 1 J/cm^2 of light of four different wavelengths (635, 670, 720 and 820-nm) all at +/- 15 nm band passes from a monochromator. Due to the nature of the light source the fluence rate was low, less than 2 mW/cm^2. This therefore meant that we were limited in the size of the total fluence that could be delivered and we therefore chose to deliver only 1 J/cm^2. At this fluence 820-nm had significant positive effect on wound healing and prevented the initial wound expansion observed in

control wounds. There was a small significant effect of 635-nm light, neither of the other wavelengths had any effect. In retrospect, it might have been preferable to deliver a higher fluence as the activity peaks will probably be somewhat different at different absolute fluences. For instance it is possible that although there was no effect of 1 J/cm^2 675-nm light, a positive effect might have been obtained if 5 or 10 J/cm^2 of 675-nm light had been delivered. Equally it is possible that 720-nm (thought to be a non-effective wavelength) would have no effect regardless of the total fluence delivered. The most effective wavelengths correspond to the absorption peaks of the cytochrome C oxidase, that is considered as the main chromophore responsible for cellular effects of LLLT (Wong-Riley et al., 2005). The activation of this enzyme leads to an increase in production of ATP that is required for numerous cellular functions providing both energy and phosphates required for regulation of cellular functions. Moreover, addition of external ATP was shown to stimulate wound healing in an animal model (Chiang et al., 2007). Although no increase in contraction was found in mice treated with external ATP, in vitro observations suggest that ATP increases wound contraction by serving both as an energy source for generation of contractile force and motility, and as a phosphate donor for kinase reactions regulating contraction (Ehrlich et al., 1999; Kreis and Birchmeier, 1980).

Generally, the studies of the effects of LLLT on wound healing are performed in a single strain of mice. Here, in addition to the Balb/c mice, responses to LLLT were tested in SKH1 and C57BL/6 mice. SKH1 is a hairless non-pedigreed immunocompetent mouse on an albino background, while

C57BL/6 is an inbred pigmented strain widely used for transgenic and knock-out models (Kirchner et al., 2003). The differences in healing responses between BALB/c and C57BL/6 mice were described in the model of ear punch (Li et al., 2001b). Similarly, we found large differences in healing of control non-illuminated wounds between the albino mice (BALB/c and SKH1) and the black C57BL/6 mice. The initial expansion in wound size observed in BALB/c mice was also seen in SKH1 hairless mice, but did not occur in C57BL/6 mice. The consequence of this difference in wound expansion was that excisional wounds in C57BL/6 mice healed significantly faster than the same wounds in BALB/c mice for the entire course of the healing process, and reached complete closure 4 days earlier (12 days versus 16 days; Figure 2.4B). The stimulating effect of 2 J/cm2 of 635-nm light was comparable in both mouse strains that exhibited the initial expansion, BALB/c and SKH1 (Figure 2.4A), where the initial expansion was reduced or eliminated. By contrast in C57BL/6 mice that showed no expansion and an overall faster healing process, LLLT had virtually no effect. It appears that wound healing in C57BL/6 is fast and the healing rate is hard to increase, while both BALB/c and SKH1 mice have sub-optimal wound healing that can be stimulated by light. The fact that the C57BL/6 mice did not show the same expansion as the other strains in the absence of light, suggest that the failure of these mice to respond to LLLT is not due to their increased skin pigmentation preferentially absorbing the light and thereby preventing the light reaching its site of action.

There has been considerable debate in the literature concerning the relative merits of laser and non-laser light for LLLT. Because LLLT was originally discovered using light delivered by lasers, for many years it was thought that certain properties of laser light, namely the fact that laser light is coherent and monochromatic, were important or even crucial in the LLLT effects. Since the advent of light-emitting diodes and other non-coherent light sources this assumption has been questioned. Our data compared the effects of 2 J/cm^2 of light delivered at comparable fluence rates originating from a HeNe laser (monochromatic at 632.8-nm and long coherence length) with non-coherent light with a 30-nm band width centered at 635-nm produced by a filtered lamp. Although there might have been a tendency for the HeNe laser to give a slightly better stimulation than light from the lamp, the difference in mean healing curves was non-significant.

Our experimental data suggest that LLLT stimulates mouse wound healing by promoting contraction and/or preventing the expansion of mouse wounds. Wound contraction is thought to be facilitated by SMA expressing myofibroblasts in the dermis surrounding the injured area (Tomasek et al., 2002). There is literature suggesting that LLLT induces the fibroblast-myofibroblast transformation both in vitro and in vivo (Medrado et al., 2003; Pourreau-Schneider et al., 1990; Powell et al., 1999). Therefore, we hypothesized that the illumination delivered at 30-minutes post-wounding affects fibroblasts at the wound edge inducing fibroblast-myofibroblasts transition and, thus, wound contraction. In order to directly test this hypothesis we performed

immunohistochemistry on tissue sections of dermis in removed from mice 24 hours after wounding and light exposure, using anti-SMA, and anti-CD31 specific antibodies. This revealed that there was a significant number of SMA positive cells in tissues surrounding LLLT-treated wounds, but not in non-illuminated control wounds. Unlike SMA-positive cells in untreated wounds, SMA-positive cells in wounds subjected to 820±15 nm light were not co-localized with CD31-positive endothelial cells, suggesting that they were indeed myofibroblasts, rather than pericytes or smooth muscle cells associated with dermal blood vessels. The presence of contractile myofibroblasts at the edge of illuminated wounds could explain the lack of expansion of the wound area observed 1 day post-wounding in BALB/c and SKH1 mice. A recent report (Arany et al., 2007) has shown that LLLT (904-nm laser) both in vivo and in vitro can activate the secreted latent form of transforming growth factor (TGF) β from its inactive state where the polypeptide homodimer is bound to latency associated peptide, into its active unbound state. TGF-β is the most important cytokine involved in the fibroblast-myofibroblast transition and induction of SMA expression (Tamm et al., 1996). The second mechanism by which wound contraction occurs is the locomotion of fibroblasts followed by the reorganization of the extracellular matrix at the edges of the wound (Ehrlich et al., 1999). The hypothesis that LLLT increases the rate of fibroblast migration was not tested in this study, however, it was shown previously that LLLT increases fibroblast motility (Hawkins and Abrahamse, 2006). Therefore, it is possible that LLLT stimulates wound contraction by both promoting fibroblast-myofibroblast differentiation and fibroblast motility.

In summary, this study shows that a single exposure to low levels of red or near infrared light significantly stimulates the wound healing responses in two strains of albino mice, and establish a wavelength and dose dependence of LLLT-mediated wound closure. We demonstrate that exposure of dermal fibroblasts at the wound edge to red light induces their differentiation into contractile myofibroblasts and therefore, accelerates the rates of wound contraction - a necessary step during wound healing. It is know, however, that excessive and uncontrolled contraction can lead to wound healing pathologies called contractures (Hinz, 2007b) that are characterized by a shrinkage of scar, loss of skin elasticity and organ function. Therefore, while LLLT-mediated acceleration wound closure would definitely be beneficial for chronic and acute wound sufferers, our observation of light-induced increase of fibroblast-myofibroblast may indicate that low level light could potentially induce or augment contractures and loss of skin elasticity. This potential adverse effect of light on wound healing can be minimized (or even eradicated) by both optimization of LLLT parameters and by combination of red light therapy with other novel wound healing accelerants such as extracellular matrix-derived peptides described in the following chapter of this dissertation.

Chapter 3. Extracellular matrix-derived peptides promote microvascular morphogenesis and wound healing in vitro and in vivo.

The data presented in the following chapter of the dissertation have been pubished (Demidova-Rice, Geevarghese and Herman, 2011). Ira M. Herman and Tatiana N. Demidova-Rice identified biologically active ECM-derived peptides.

Tatiana N. Demidova-Rice and Anita Geevarghese performed in vitro testing of the peptides.

3.1. Introduction.

Full thickness cutaneous wound healing is a well-organized process that leads to re-establishment of the skin's physical and mechanical integrity. The normal repair process can be divided into several temporally and spatially overlapping phases that include coagulation, inflammation, formation of granulation tissue (proliferative phase), remodeling and scarring (Falanga, 2005). Platelets and inflammatory cells initiate the wound-healing cascade and produce growth factors and cytokines that induce migration and proliferation of epidermal and dermal cells – keratinocytes and fibroblasts. These cells are the key players in the re-epithelization of the wound, formation of granulation tissue and scarring (Falanga, 2005). The function of all cells contributing to wound healing process relies on the presence of an adequate blood supply as a source of nutrients, oxygen and cytokines. Therefore, cellular responses to injury are critically angiogenesis-dependent. In turn, angiogenesis of normal wound healing depends on two major processes: recruitment of the endothelial progenitor cells from the circulation and sprouting of resident endothelial cells from existing adjoining microvascular circuits bordering the wound bed (Liu and Velazquez, 2008). In the latter case, capillary endothelial cells (CEC) become activated in response to injury-induced growth factors such as platelet derived growth factor (PDGF) and vascular endothelial growth factor (VEGF) mainly released by

activated platelets, macrophages and keratinocytes within the wound bed (Beitz et al., 1991; Li et al., 2003). Growth factor mediated stimulation of the endothelium leads to an increase in CEC proliferation and migration. Both of these processes require and depend on the presence of a permissive microenvironment shaped by the ECM. In addition to providing a substrate for CEC migration, native and cleaved ECM molecules bind to and activate endothelial integrin receptors (particularly $\alpha v\beta 3$) that trigger dynamic endothelial responses and sustain angiogenesis (Avraamides et al., 2008).

An important prerequisite for wound healing angiogenesis is basement membrane (BM) degradation. Indeed, BM turnover is regulated by a number of matrix remodeling enzymes - serine proteases and matrix metalloproteinases (MMPs), which include collagenases and gelatinases (Roy et al., 2006) produced by resident endothelial cells. Altogether, BM remodeling helps to coordinate cellular injury responses, including wound healing angiogenesis. Further, ECM degradation allows for efficient cell migration since MMPs liberate matrix-bound growth factors such as basic fibroblast growth factor (bFGF) and VEGF (Bergers et al., 2000; Roy et al., 2006) that enhance the angiogenic cascade and wound healing. Finally, proteolytic matrix degradation gives rise to pro- and anti-angiogenic ECM fragments that regulate endothelial morphogenesis in vitro and angiogenesis in vivo (Bellon et al., 2004; Rhodes and Simons, 2007; Robinet et al., 2005; Xu et al., 2001).

Because of the importance of matrix remodeling for wound healing, it has been suggested that exogenous ECM-remodeling proteases, such as

collagenase derived from gram-positive bacteria *Clostridium histolyticum* may be beneficial for wound healing (Herman, 1993a). Indeed, previous work in our laboratory has demonstrated that this enzyme stimulates epithelial and endothelial response to injury both *in vitro* and in vivo (Herman, 1993a; Riley and Herman, 2005). The question of how bacterial collagenase stimulates wound-healing responses remains. We hypothesize that in addition to the debriding effects, digestion of components of the ECM by the bacterial enzyme leads to the release of bioactive peptides that stimulate wound closure. To test our hypothesis and determine whether matrix remodeling by Clostridial collagenase leads to production of biologically active fragments, we use the well-characterized ECM synthesized by vascular endothelial cells (Healy and Herman, 1992). Results reveal that that there are several unique small peptide fragments of tenascin X, fibrillin-1 and collagen Type IV released during matrix degradation by bacterial, but not human collagenase. These Clostridial collagenase-liberated and capillary endothelial matrix-derived peptides stimulate proliferation of CEC, enhance microvascular remodeling in two-dimensional (2D) model on Matrigel and induce endothelial sprouting in a novel three-dimensional (3D) model of injury repair.

3.2. Materials and Methods.

Cells.

Capillary microvascular cells (CEC) were isolated as described previously (Gitlin and D'Amore, 1983; Healy and Herman, 1992; Murray, 2001). Animal tissues for cell isolation were obtained from an abattoir and therefore, no institutional animal

use committee approval was required or obtained. Briefly, bovine retinal capillary fragments were prepared and plated in DMEM supplemented with bovine calf serum (BCS, Atlanta Biologicals, Inc., Lawrenceville, GA) and antibiotics (Invitrogen, Carlsbad CA). Selection of endothelial cells was performed using selective attachment, media containing 5% human platelet-poor plasma and ultimately, cloning. After isolation, cells were stored in liquid nitrogen and then cultured in DMEM supplemented with 1-5% BCS and antibiotics and used at passages 7-13. These cells were characterized by: (i) labeling with antibodies against Factor VIII (Gitlin and D'Amore, 1983), (ii) ability to bind and internalize di-I-acyl LDL, (iii) fallure to be stained with anti-3G5, a pericyte-specific marker (Helmbold et al., 2001) and (iv) their ability to form capillary-like structures in vitro that bear a resemblance to capillaries formed during angiogenesis in vivo, i.e. endohelial-lined ‘sprouts’ that possess ‘lumenal’ compartments.

Matrix preparation.

The extracellular matrix was prepared as described (Healy and Herman, 1992;Herman and Castellot, 1987). Briefly, CEC at 7-10 days post-confluence were washed 3 times with phosphate buffered saline (PBS) (pH=7.15). Cells were removed with 0.5% sodium deoxycholate buffered with 20 mM Tris-Cl (pH 8.0) containing 15 mM NaCl, 1 mM EGTA (pH 7.0), 1 mM phenylmethyl sulfonyl fluoride. The matrix then was washed with PBS, immediately collected and used for enzymatic degradation and peptide identification.

Enzymatic degradation of the matrices.

Enzymatic matrix degradation was performed as described (Riley and Herman, 2005). Purified Clostridial collagenase was obtained from Advance Biofactures (Lynbrook, NY), dissolved in 1M TRIS-HCl (pH=7) at 1mg/mL and stored at -20C before use for no longer than one week. Immediately before the experiments the enzymes were thawed, diluted in calcium buffered saline at 16U/mL and added to the plates for 1h at 37C. Human MMP-1 (Calbiochem, La Jolla, CA; Cat. # 444208) was activated according to manufacturer instructions, and used for 1h at 37C to perform matrix degradation. Both human and bacterial enzymes were used at the same protein concentration.

Peptide identification and synthesis.

For peptide identification matrices treated with bacterial collagenase or human MMP-1 were prepared as described above and scraped into immunoprecipitation (IP) buffer containing 0.125% bovine serum albumin, 30mM TRIS-Cl (pH=8), 0.1% SDS, 0.5% sodium deoxycholate, 1% NP-40 and supplemented with protease inhibitors (Sigma-Aldrich, St. Louis, MO; Cat. #P8340). Immunoprecipitation was performed using antibody directed either against collagen I (Abcam, Cambridge, MA; Cat. #292) or mixed antibodies against collagens I-V (Abcam, Cambridge, MA; Cat. #ab24117). Protein A Sepharose beads were washed three times in distilled water and resuspended in IP buffer in the presence of protease inhibitors (Sigma-Aldrich, St. Louis, MO; Cat. #P8340). Antibodies were added to resuspended beads at a final concentration of 225 µg/ml and incubated with agitation for 1h at room temperature to allow for bead-antibody interactions.

ECM prepared as described above was digested with either bacterial or human collagenases, scraped in 0.1x IP buffer, lyophilized overnight and reconstituted in 1/10 volume of distilled water. Before addition to antibody-bound beads matrix preparations were pre-cleared by incubation with protein A sepharose (GE Healthcare, Uppsala, Sweden) in the absence of the antibody. Pre-cleared ECM samples were applied onto antibody-bound beads and rotated overnight at 4C in the presence of protease inhibitors to allow for immunoprecipitation. The precipitated complex was washed several times with IP buffer at 4C. Proteins were eluted using boiling SDS sample buffer containing 2% 2-mercaptoethanol (Sigma Aldrich, St. Louis, MO), subjected to gel electrophoresis and stained with Coomassie blue dye for protein detection. Protein bands present bacterial, but not human digests, were excised, washed 2 times in 50% acetonitrile and submitted to Tufts University Core Facility (TUCF) for protein identification. At TUCF the gel bands were degraded further using proteomics-grade trypsin and subjected to liquid chromatography mass spectrometry (Yates et al., 1995). In total over 100 protein fragments were identified, of those 12 containing 10-22 amino acids were selected and submitted to TUCF for synthesis by FastMoc Chemistry (Fields et al., 1991).

Cell proliferation assay.

The unique ECM-derived peptides released by bacterial collagenases were tested for growth-promoting potential toward CEC. CEC were plated at $2x10^3$ cells/well in three 48 well plates in DMEM containing 5% BCS. On the next day, cells in one of the plates were washed with PBS, detached from the substrate

using trypsin and counted using a Coulter Counter model Z-II (Beckman Coulter, Inc, Fullerton, CA) according to the manufacturer's instructions. Cells in the remaining two plates were fed with DMEM/1% BCS with or without the peptides mixed in the media at concentrations ranging from 1-100nM at day 1 and 3 after plating. Cell counts were performed as described above at days 3 and 5 post-plating. Three wells were used per condition and each experiment was repeated at least three times. In this and following assays low serum-containing media were used in order to minimize possible masking effects of serum components on cellular responses to peptide treatment. Under these experimental conditions, no cell detachment or death is observed (Durham and Herman, 2009;Healy and Herman, 1992).

2D in vitro endothelial morphogenesis assay.

In this assay we used growth factor-reduced (GFR) Matrigel (BD Biosciences, Bedford, MA; Cat. #354230). The GFR Matrigel was thawed on ice overnight in the cold room and used immediately. To prevent premature matrix polymerization, all procedures were performed at 4C. Stock (25 mM) solutions of the peptides were prepared in sterile water or 1M TRIS (pH 8.0), added to the GFR Matrigel at a final concentration of 100 nM and mixed thoroughly. Thus prepared peptide-containing GFR Matrigel was placed into the wells of 8-well chamber slides (BD Biosciences, Bedford, MA). Control wells contained GFR Matrigel alone. For positive control we used GFR Matrigel blended with 10 ng/ml (0.6 nM) of pro-angiogenic growth factors bFGF or VEGF (Cross and Claesson-Welsh, 2001). The chamber slides containing GFR Matrigel preparations

containing the peptides, bFGF or 1% BCS then were placed into the tissue culture incubators at 37C for 45-60 minutes to allow for matrix polymerization. After matrix polymerization, CEC at $5x10^4$ cells per well were plated on the surface of polymerized Matrigel in DMEM containing 1% BCS in the presence or absence of the corresponding peptides or FGF-2. Control wells contained DMEM supplemented with 1% BCS. Formation of endothelial sprouts was monitored at 7 and 24 hours post-plating. Visualization of the cells was performed with Axiovert 200M microscope (Carl Zeiss MicroImaging, Thornwood, NY) using 5x or 10x objective lenses. Image analysis and measurement of the length of the structures were performed using ImageJ (available from NIH). Both the length of individual sprouts and total sprout length per field were measured.

3D model of in vitro angiogenesis.

Unlike the 2D model described above, and in an effort aimed at better reflecting the in vivo microenvironment, the 3D construct contains cells that are embedded within a well defined extracellular matrix rather than having the cells being plated upon the matrix surface (Herman and Leung, 2009). The matrix is created by combining GFR Matrigel with rat tail collagen Type I (BD Biosciences, Bedford, MA; Cat # 354236) to the final concentration of collagen 0.7 mg/mL, in the presence of 5 mM NaOH and DMEM supplemented with 1% BCS and placed into the wells of 8 well chamber slides (250 uL/well). After matrix polymerization, $1.5x10^5$ CEC were plated in 250 µL of DMEM supplemented with 1% BCS and Antibiotic-Antimycotic (Invitrogen, Carlsbad, CA). After cell attachment, approximately 1h post-plating, the non-adherent cells and excess media were

carefully removed, then the second layer of Matrigel-collagen mixture was applied and allowed to polymerize for 45-60 minutes at 37C creating 3D structures with CEC “sandwiched” in between two layers of Matrigel-collagen mixture. Circular wounds were made in the middle of each well using a blunt 22 G needle (Tyco Healthcare Group LP, Mansfield MA) attached to a vacuum line inside the tissue culture hood. Immediately after wounding, defects were filled with the Matrigel-collagen mixture blended with the peptides, FGF-2, VEGF or DMEM supplemented with 1% BCS. Wounds were imaged immediately after filling and at days 1, 3, 7 post-wounding using a 5x objective lens. Fifteen to 20 images were taken per wound at each day of observation and merged using Adobe Photoshop CS2 (Adobe, San Jose, CA). The merged images then analyzed manually to estimate the number of angiogenic sprouts formed by cells invading the Matrigel-collagen plugs.

Confocal microscopy of endothelial sprouts formed in 2- and 3D cultures.

Confocal microscopy on living endothelial cell cultures plated in 2- and 3D assays was performed in the following way. Prior to plating, CEC were pre-treated with fluorescent dye, Vybrant DiO. Briefly, CEC were placed in Vybrant DiO labeling solution for 15 min at 37^{o}C according to manufacturers instructions (Molecular Probes, Eugene, OR) washed and plated in 2D or 3D arrays for 7 hours or 3 days, respectively. Live cells bearing Vybrant DiO were observed using a confocal laser-scanning microscopy equipped with an argon laser capable of exciting the dye at 488 nm (LSM-510, Carl Zeiss MicroImaging, Thornwood, NY). Image analysis was then performed using LSM Image

Examiner software (Carl Zeiss MicroImaging, Thornwood, NY).

Animal experiments.

All animal experiments were approved by the Subcommittee on Research Animal Care of Massachusetts General Hospital or Institutional Animal Care and Use Committee at Tufts University and were performed in accordance with NIH guidelines. Two mouse models of impaired wound healing were used. In the first model Balb/c mice were pre-treated with two doses of cyclophosphamide (CY): 150 mg/kg 4 days and 100 mg/kg 1 day before wounding in order to delay wound healing as described previously (Burkatovskaya et al., 2008). In the second model, we used genetically diabetic C57BLKS/J-m Leprdb/+ + mice that luck leptin receptor and therefore are characterized by severe obesity and delayed wound healing (Mudge et al., 2002). In order to evaluate the effects of cyclophosphamide and diabetes on wound healing we used untreated Balb/c mice and C57/BL6/1J mice (5 per group) as controls. These mice received the wounds as described below and were treated with daily application of carboxymethylcellulose (CMC), which was used in this study as a vehicle for peptide application.

The wounds in mice of both strains were created in the following way. The mouse heads were depilated by use of Nair cream (Carter-Wallace, New York, NY) one day before wounding. For wounding procedures and during treatments Balb/c mice were anesthetized by an intraperitoneal injection of a ketamine-xylazine cocktail (90 mg/kg ketamine and 10 mg/kg xylazine); for diabetic mice inhalation anesthesia with Isoflurane was used. Cranial dermal full thickness

excisional wounds were made with sterile 4 mm punch biopsy tool and sterile scissors and forceps. Immediately after injury wounds were covered with transparent film dressing (Tegaderm). A day after injury, the peptides were suspended in 3% CMC in PBS at concentration of 1 mg/mL or 284 μg/mL and injected under the dressings using 25G needle. If the combination of the peptides was used, the final concentration of protein in CMC was 1.284 mg/mL. Control mice were treated with CMC alone. PDGF-containing Regranex gel was used in mice serving as a positive control. All treatments were applied daily and dressings were changed as necessary.

Tissue harvesting and staining.

Collection of animal tissues was performed at 5 or 10 days post-injury. The animals were sacrificed by CO_2 inhalation. The wounds together with underlying tissues and approximately 5 mm of intact dermis surrounding the wound were excised. The wounds then were bisected through the midline. One part of the tissue then was placed in 10% phosphate buffered formalin (Fisher Scientific), fixed for 24h, embedded in paraffin and cut into 5 μm thick sections; the other part was embedded into O.C.T compound (Tissue-Tek) and frozen on dry ice. After freezing the tissues were stored at -80^{o}C and cut into 5 μm thick sections. Paraffin-embedded sections were stained with Hematoxylin and Eosin or Trichrome stain (ThermoScientific). Both stains were used according to manufacturers instructions. Imaging was performed with Zeiss Axiophot microscope (Carl Zeiss MicroImaging, Thornwood, NY) using 5X objective lens.

Frozen sections were subjected to immunohistochemical staining. Briefly, the sections were warmed up the room temperature for 10 min, fixed with DMEM-containing 4% paraformaldehyde and permeabilized with buffered 0.1% TritinX-100 for 90 seconds. After blocking for 2h with 5% goat serum, sections were incubated with rat anti-CD31 antibodies (BD Pharmingen) (1:500) and rabbit anti-HSPG (1:200) overnight at 4^{o}C. Sections then were washed and co-incubated with fluorescently labeled anti-rat Alexa 546, anti-rabbit Alexa 488 secondary antibodies (Molecular Devices, Sunnyvale, CA) both at 1:200 dilution and 16.2 μM Hoechst 33342 (Molecular Probes, Invitrogen, Carlsbad, CA) for 2h at room temperature. After triple wash in PBS, stained sections were mounted with PermaFluor (Lab Vision Corporation, Fremont, CA). Visualization of the slides was performed with Axiovert 200M microscope (Carl Zeiss MicroImaging, Thornwood, NY) using 5X and 10X objective lenses.

Analysis of wound healing and quantification of angiogenic response.

Images of Hematoxylin and Eosin as well as Trichrome-stained sections obtained at low magnification were merged using Adobe Photoshop CS2 (Adobe, San Jose, CA). The merged images were then analyzed by two independent observers blinded to treatment used a histology scale (Table 3.1) to estimate the degrees of wound healing. Levels of epithelialization and granulation tissue formation determined the score.

Table 3.1. Modified histology scale for wound grading.

Score	Criteria
1	No epithelialization, no granulation tissue formed
2	No epithelialization, granulation tissue poorly formed
3	Complete epithelialization, poor granulation tissue formation
4	Complete epithelialization, well-defined granulation tissue

In order to estimate whether the peptides stimulate angiogenesis of wound healing, we used frozen sections stained with anti-CD31 (red) and anti-HSPG (green) antibodies. The areas of antibody co-localization (yellow) representing blood vessels were quantified using ImageJ software (available from NIH).

Data analysis and statistics.

All in vitro experiments were performed at least three times. Counts obtained in cell proliferation assay, in 2D in vitro morphogenesis assay and in a 3D model of wound healing were recorded manually and analyzed using Microsoft Excel (Microsoft, Redmond, WA). Results are presented as mean±SEM. Statistical significance of the findings was analyzed by two-tailed t-test. The value of $p< 0.05$ was considered significant.

In vivo experiments were performed three times using three to five animals per each experimental group, with total number of animals of 9 to 15 per treatment. Wound healing rates determined using wound healing grades were manually recorded using Microsoft Excel (Microsoft, Redmond, WA). Data analysis was performed using one-way ANOVA test, statistical significance of the

findings was then confirmed by Dunnett's and Student-Newman-Keuls tests.

3.3. Results.

Degradation of endothelial ECM by bacterial collagenase gives rise to unique bioactive peptides.

We subjected CEC-derived matrices (Yost and Herman, 1990) to limited digestion using purified bacterial collagenase or human MMP-1 as described in Materials and Methods. Matrix digestion was followed by immunoprecipitation with polyclonal antibodies directed against collagen I or collagens I-V. As can be seen in figure 1, several distinct polypeptides of high (120 kDa), medium (45-50 and 80 kDa) and low (35 kDa) molecular weight were found in matrices degraded by bacterial, but not human collagenase. To reveal the identity of these unique matrix fragments we used liquid chromatography mass spectrometry (Yates et al., 1995). As shown in Table 3.2, immunoprecipitation succeeds in enriching for both collagenous (collagens I and IV) and non-collagenous (tenascin X and fibrillin 1) matrix fragments. Several fragments were synthesized using FastMoc Chemistry at TUCF (Table 3.2). Fragments derived from collagens I and IV include: col1-hyp and col1-leu, derived from the alpha 1 chain of collagen I and col4-1, col4-2 and col4-c originated from non-collagenous domain of Alpha 3 of collagen IV (Table 3.2). Fragments of tenascin X and fibrillin 1 present non-collagenous polypeptides. Ten1, ten3 and ten4 are fragments of EGF-like domain rich regions of tenascin X, ten2 is a fragment of fibronectin III-like domain of tenascin X (Table 3.2). Fibr1, fibr2 and fibr3 are derived from EGF-like

Table 3.2. Structure and function of extracellular matrix-derived pro-angiogenic peptides.

Peptide name	Sequence	Origin	Effects on endothelial cells in vitro	
			Endothelial proliferation	In vitro angiogenesis
Col1-Hyp	GSAGPXGATGFX GAAGR X=hydroxiproline	collagen I alpha 1 chain, aa 704-720	—	—
Col1-Leu	GSAGPLGATGFL GAAGR	collagen I alpha 1 chain, aa 704-720	—	—
Col4-1	MFRKPIPSTVKA	collagen IV alpha 3 chain, NC1 domain, aa 1282-1353	+	+ +
Col4-2	IISRCQVCMKMR P	collagen IV alpha 3 chain, C-terminus, aa 1359-1371	—	+
Col4-C	MFRKPIPSTVKAP PIISRCQVCMKM RP	combination between Col4-1 and col4-2	—	—
Fibr1	DINECELSANL	fibrillin 1, modified EGF-like calcium binding domain 13	—	—

Fibr2	DIDECESSPCINGV	fibrillin 1, EGF-like domain 13, aa 807-846	+	+
Fibr3	DEDECEEGKHDCAE	fibrillin 1, EGF-like calcium-binding domain 39, aa 2247 - 2290,	—	+
Ten1	GVRSCPRGCSQKGRCED	tenascin X, EGF-like domain, aa 306- 322	+	—
Ten2	GEETEVTVEGLEPG	tenascin X, fibronectin III-like domain, combination between aa2425-2430 and aa 3103-3110	—	+ +
Ten3	CVCWPGYTGRD	tenascin X, EGF-like domain rich fragment, aa 360-370	—	—
Ten4	CGTRACPGDC	tenascin X, EGF-like domain rich fragment, aa 490-500	—	+
Comb1	DINECEIGAPAGEETEVTVEGLEPG	combination between fibr1 and ten2	+	+ +

— - no effect; + - peptide induces significant increase in cellular responses; ++ - peptide induce a two-fold increase in cellular responses.

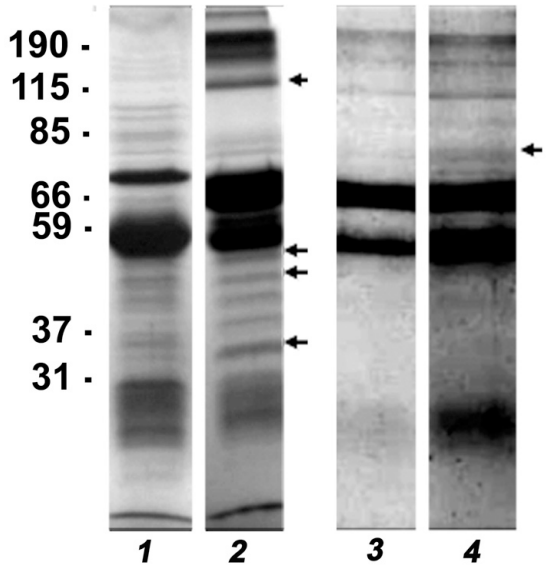

Figure 3.1. Identification of bioactive matrix fragments released by bacterial collagenase from endothelial matrices.

Endothelial matrices synthesized by post-confluent CEC were degraded by either human, or bacterial collagenase and subjected to immunoprecipitation with antibodies directed against collagen I (lanes 1, 2) or collagens type I-V (lanes 3, 4). Arrows indicate unique matrix fragments present in matrices digested by bacterial (lanes 2 and 4), but not human collagenases (lanes 1 and 3).

domains of fibrillin 1. In addition, we have created combinatory peptide (comb1) by combining fragments of EGF-like domains of tenascin X and fibrillin 1. The length of the polypeptides varies between 10 and 25 amino acids (Table 3.2).

Peptides derived from endothelial matrix stimulate endothelial cell proliferation in vitro.

The effects of matrix-derived peptides on endothelial proliferation were evaluated in 5-day assays using CEC plated at low density as described in Materials and Methods. As shown in figure 3.2, four peptides induce a statistically significant

increase in endothelial proliferation. Namely, combinatorial peptide comb1 increases cell growth by 28%; fragments of fibrillin 1 (fibr2), and collagen IV (col4-1) enhance endothelial proliferation by 35%. Strikingly, a fragment of tenascin X (ten1) increases endothelial proliferation rate by 47%. For col4-1, ten2 and comb1 stimulatory effects are present at peptide concentration of 10-100 nM. Fibr2 on the other hand exibits a dose dependent response and is ony active at 100 nM inducing a 35% increase in endothelial proliferation. It is important to emphasize that while proliferation is an essential step during angiogenesis, increase in migration, morphogenesis, sprout and lumen formation by activated endothelial cells are comparably critical for successful formation of a nascent and stabile capillary network. Therefore, we directly tested whether the peptides promote capillary endothelial morphogenesis using 2-D and 3-D in vitro models.

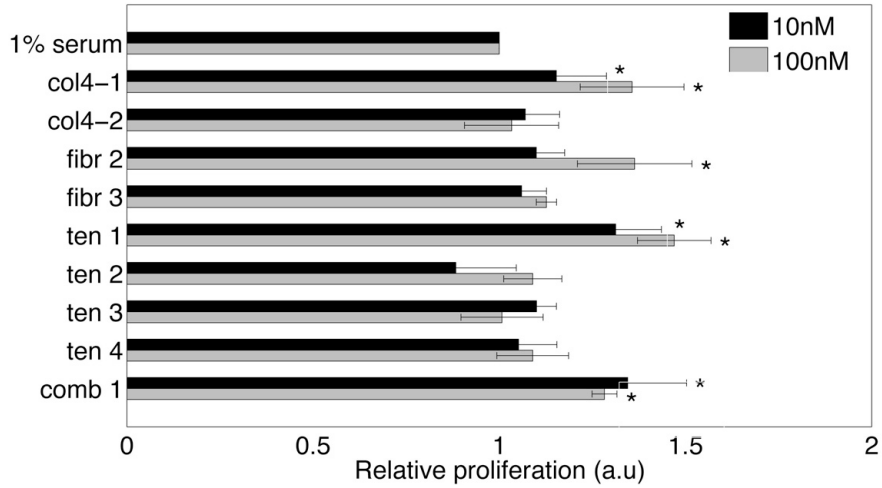

Figure 3.2. Bioactive matrix fragments stimulate endothelial proliferation.

CEC grown in 48 well plates were treated with ECM-derived peptides at 10 or 100 nM at days 1 and 3 post-plating. Cell counting was performed using Coulter Counter at days 1, 3 and 5. Relative proliferation compared to control is shown. Error bars represent standard error of the mean; $*$ - $p<0.05$ compared to serum-stimulated control.

Matrix-derived peptides stimulate microvascular remodeling in vitro: insights from a 2D model.

Next, we examined the ability of the peptides to induce endothelial morphogenesis using a well-established Matrigel-based assay as described in Materials and Methods. The assay enables a quantitative analysis of endothelial morphogenesis as a function of time or experimental condition (Durham and Herman, 2009). Based on previously published observations indicating that endothelial cells plated on Matrigel form lumen-containing structures within 6-12 hours (Kleinman and Martin, 2005), we chose to study peptide effects on microvascular morphogenesis at 7 and 24 hours post-plating. At both time points studied several peptides stimulate CEC morphogenesis and sprout formation in vitro. Phase-contrast images shown in figure 3 demonstrate that two fragments of fibrillin 1 (fibr2 and fibr3) and collagen IV (col4-c) induce a 25-65% improvement in the rate of endothelial morphogenesis and lead to an increase in the number and total length of endothelial structures formed at an early time point (7h) post cell plating. Combinatorial peptide (comb1), a fragment of collagen IV (col4-1) and two fragments of Tenascin X (ten 2 and ten4) induce almost doubling of the total length of sprouts formed on Matrigel within 7h post-plating (Figure 3.3). Peptide effects on angiogenic induction were comparable or superior to FGF-2 and VEGF (Figure 3.3 A-D, Figure 3.5A).

By 24h post-plating the angiogenic sprouts ‘mature’ as they elongate, acquiring a ‘tube-like appearance. By this time the differences in the length of the structures formed by control and treated cells diminish as control cultures acquire

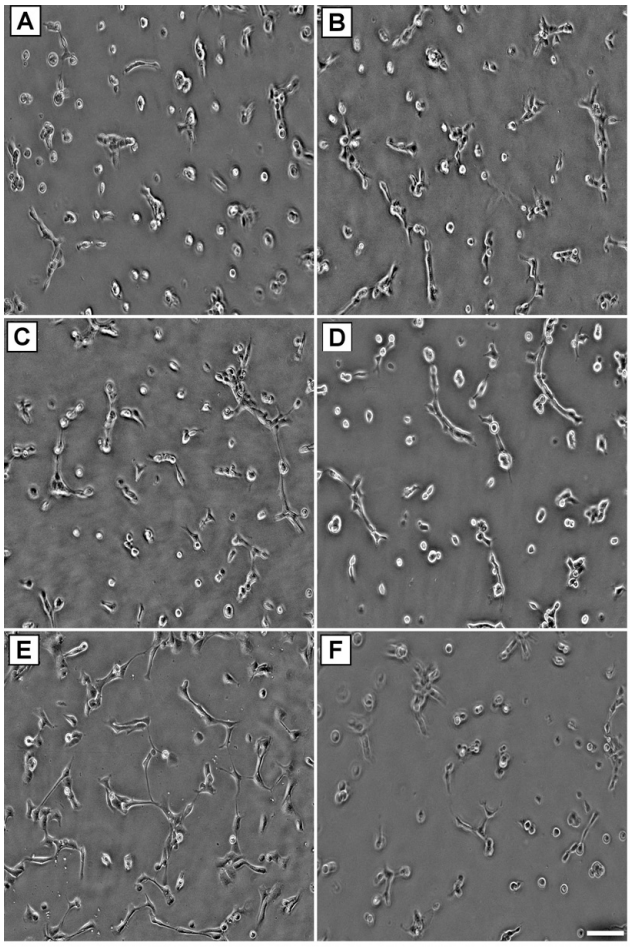

Figure 3.3. Matrix-derived peptides enhance early events during endothelial morphogenesis on Matrigel.

(A-F) Photomicrographs of capillary-like structures formed by CEC cultured on Matrigel for 7h in the absence (A) or presence of 100 nM comb1 (D), ten4 (E) or col4-1 (F). Basic FGF and VEGF are used as positive controls (B and C respectively). Image background was corrected using pseudo flat field function (Image J) and high pass filters (Adobe Photoshop CS2).

the ‘equilibrium’ features observed in peptide-treated endothelial cultures (Figure 3.5B). Nonetheless, tubes formed in the presence of VEGF, FGF-2 (Figure 3.4 B, C, Figure 3.5B) or comb1, ten4 and col4-1 (Figure 3.4 D, E and F respectively and Figure 3.5B) are 34-57% longer than those formed in wells containing Matrigel supplemented with 1% serum, alone (Figure 3.4 A, Figure 3.5B).

Matrix-derived peptides stimulate microvascular remodeling in vitro: insights from a 3D model.

In an effort to learn whether the peptides can be active in a more complex environment and to better approximate their wound healing potential, we tested the most promising peptides in a 3D model of wound healing (25). Three peptides comb1, col4-1 and ten4 that stimulate endothelial proliferation and/or endothelial morphogenesis on Matrigel, were tested as shown schematically in figure 3.6 and as described in Materials and Methods (Herman and Leung, 2009). Imaging of the defects, which are re-filled with Matrigel-collagen immediately after injury, demonstrates that a reliable and reproducible ‘wound’ and associated cellular removal can be achieved. And, addition of the Matrigel-collagen plug post-injury does not disrupt the integrity of the wound edge.

In both large and small wounds (Figure 3.7) visible cellular responses are first seen at 24 hours post-injury. At this time cells begin to establish a plexus and form a microvascular network in the areas proximal to the injury site, which has been re-filled with Matrigel-collagen mixture containing pro-angiogenic peptides, VEGF or bFGF (Figures 3.7 and 3.8). In larger wounds, an ‘angiogenic’

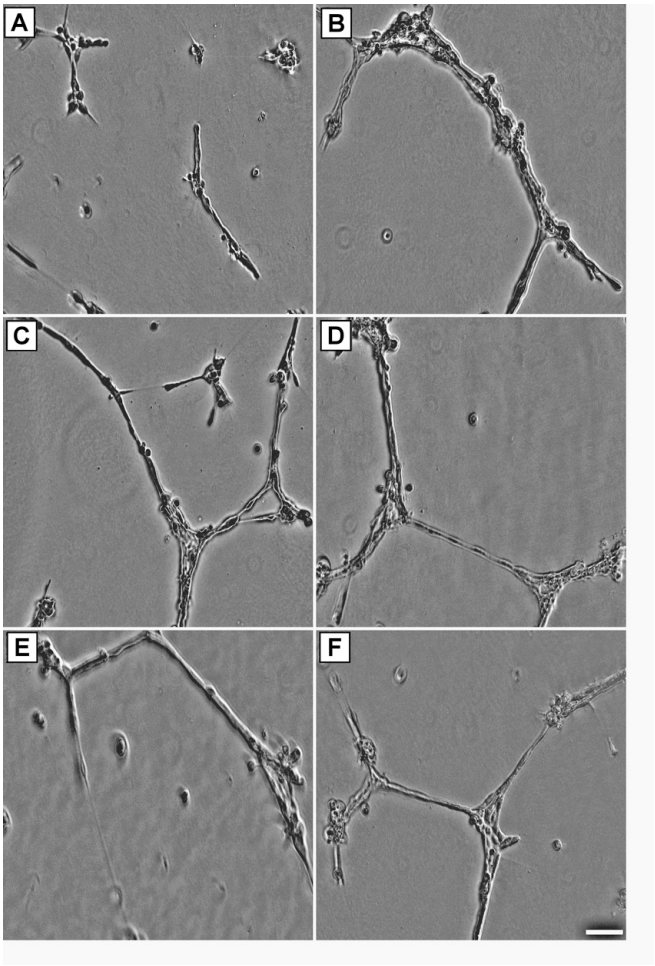

Figure 3.4. Effects of bioactive peptides on endothelial morphogenesis in vitro at 24h post-plating.

(A-F) Photomicrographs of capillary-like structures formed by CEC cultured on Matrigel for 24h in the absence (A) or presence of 100 nM concentration comb1 (D), ten4 (E) or col4-1 (F). Basic FGF and VEGF are used as positive control (B and C respectively). Image background correction was performed as described for figure 3.

network can be seen in proximity to the wounds filled with Matrigel-collagen mixtures supplemented with 1% serum; but, these wounds contain only a few short sprouts. This response to 'injury' is similar to 'wounds' filled with Matrigel-

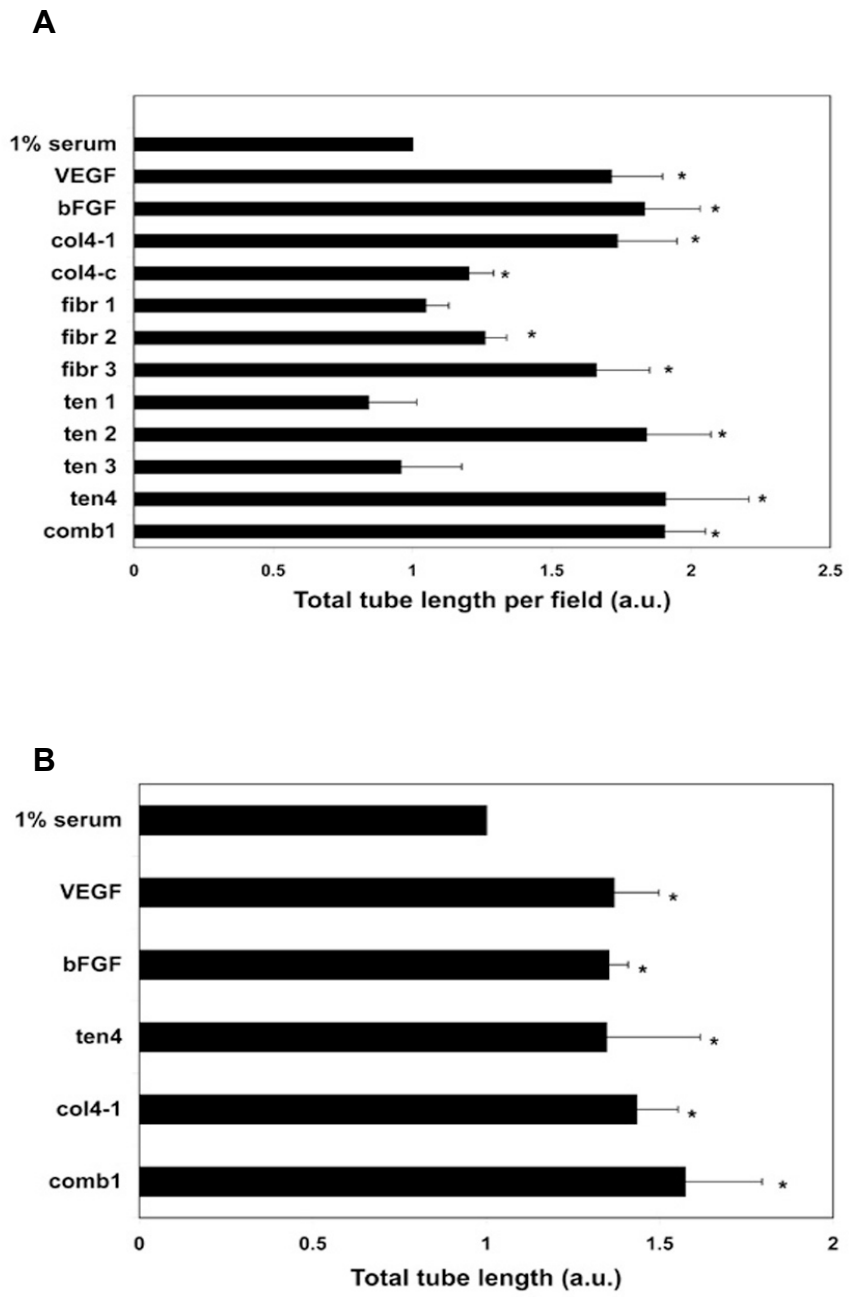

Figure 3.5. Quantitative evaluation of endothelial morphogenesis in a 2D model.

The length of endothelial sprouts was measure as described in Materials and Methods at 7 and 24 hours post-plating. Three fields are evaluated in each of three independent experiments and plotted as relative tube length compared to control. (A) relative sprout length at 7h post-plating, (B) relative sprout length at 24h post-plating. Error bars represent standard errors; ∗ - $p<0.05$ compared to serum-stimulated control.

collagen mixtures containing serum, or those defects that have been filled/ supplemented with the peptides or growth factors (e.g. bFGF). On the other hand, smaller diameter wounds (at 24h post-injury) contain many, many long

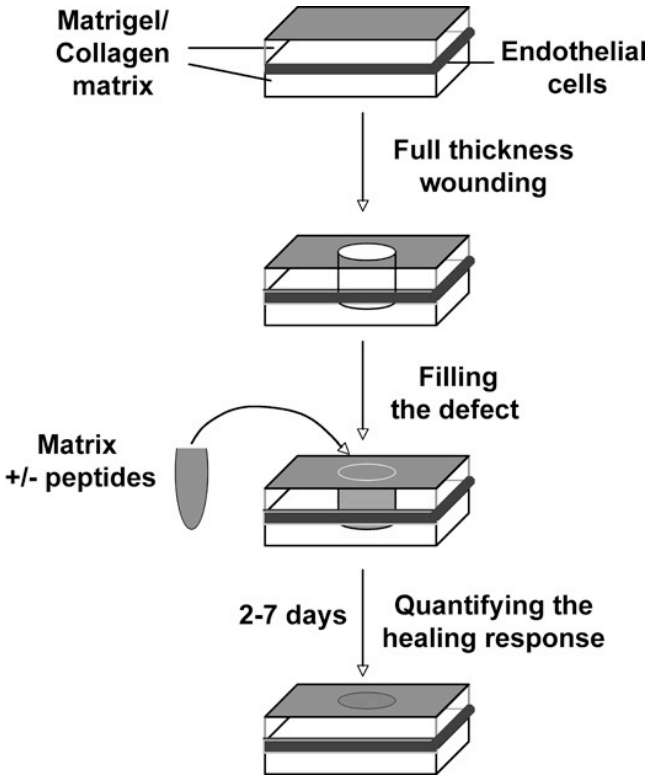

Figure 3.6. Schematic representation of the three-dimensional model of angiogenesis.

The construct consists of two layers of Matrigel-collagen mixture and a layer of endothelial cells sandwiched in between. Full thickness injury is created by aspiration and defect is filled with matrices containing serum, pro-angiogenic growth factors or peptides.

sprouts and an elaborate, post-injury angiogenic network (Figure 3.7). Indeed, CEC within these smaller diameter wounds, and which have been treated with either growth factors or the pro-angiogenic peptides, form significantly more sprouts and more robust angiogenic network when compared to control CEC treated with serum/Matrigel-collagen mixtures, alone (Figures 3.7 and 3.8).

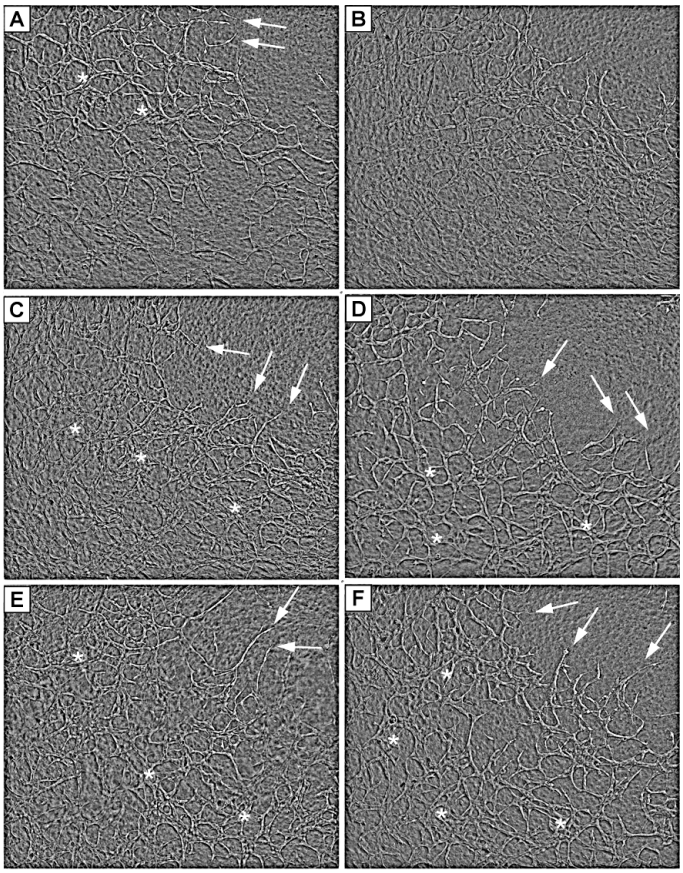

Figure 3.7. ECM-derived peptides stimulate angiogenesis and early responses to injury in a novel 3D model of angiogenesis.

Small full thickness wounds in 3D constructs are filled with the matrices containing 1% serum (A), bFGF (B), VEGF (C), and peptides comb1 (D), ten 4 (E) or col4-1 (F). Images are taken at 1 day post injury. Image background correction was performed as described for figure 3. Arrows indicate endothelial sprouts; asterisks show the areas of dense angiogenic networks formed by the CEC. Scale bar 200 μm.

As the CEC network continues to penetrate the wound defect, e.g. 3 days post-injury, differences between the treatment groups are minimized as cells treated under control conditions begin forming more sprouts, resembling those treated with the peptides or growth factors. In larger wounds at day 3 post-wounding, a robust angiogenic response is seen in wells treated with comb1, ten 4 and bFGF (Figure 3.9), while only small number of structures formed in controls observed at the same timepoint (Figure 3.9). Thus, data derived using the 3D model of injury-repair confirm that the peptides produced by bacterial collagenase degradation of endothelial extracellular matrices, as well as those combinatorial peptides created ex vivo, stimulate a marked endothelial angiogenic response to injury.

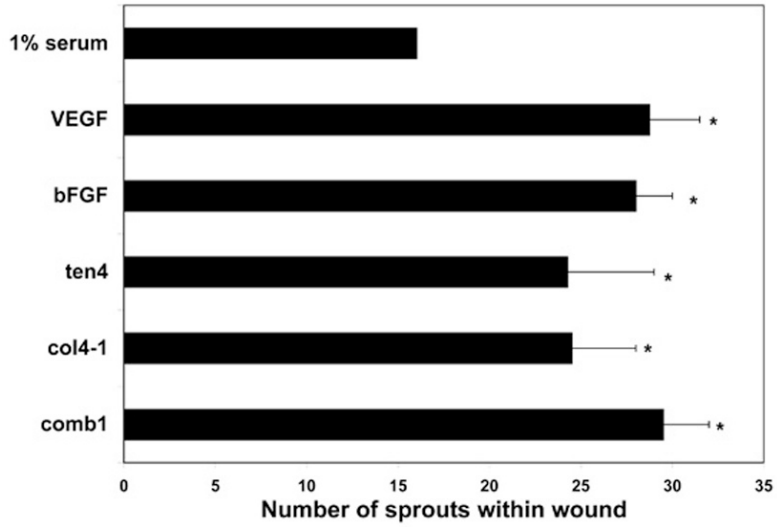

Figure 3.8. Quantitative evaluation of sprout formation by endothelial cells in 3D model of wound healing at day 1 post-wounding.

Cellular structures extended into small wounds by day 1 post-injury are counted manually using merged low power images. The mean number of structures found within wounds in three independent experiments is plotted. Error bars represent standard error of the mean; $*$ - $p<0.05$ compared to serum-stimulated control.

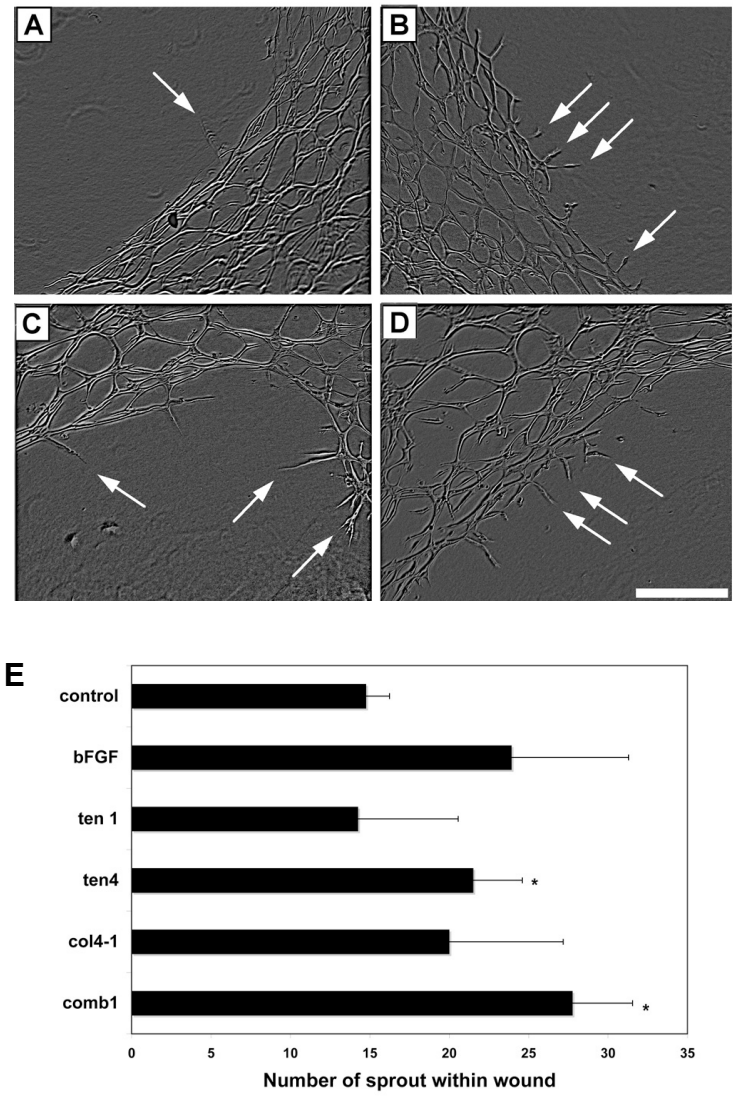

Figure 3.9. Effects of the peptides on endothelial responses to injury in 3D environment: 3 days post wounding.

(A-D) Photomicrographs of large wounds created in 3D matrices containing CEC and treated with 1% BCS (A), 10 ng/mL bFGF (B), 100 nM comb1 (C), and col4-1 (D). Representative images taken at 3 days post-wounding corresponding to each treatment group are shown. The image background correction was performed as described for figure 7. Scale bar 200 um. Arrows indicate angiogenic sprouts formed by the cells. (E) Quantitative evaluation of angiogenic sprouts formed by the CEC in response to peptide treatment. The sprouts were counted manually on the merged low power images of large wounds 3 days post-injury and plotted as the mean+/- standard error. $*$ - $p<0.05$ compared to serum-stimulated control.

Endothelial cells grown in 2- and 3D constructs form lumen-containing structures.

In order to determine whether CEC cultured on or within Matrigel-based substrate form lumen containing structures, we plated fluorescently labeled CEC in 2- or 3D constructs as described in Materials and Methods.

Confocal imaging was performed 7h and 3 days post-plating for cells cultured in 2- and 3D constructs respectively. As shown in Figure 3.10, optical sections in XZ plane (lower panels) through endothelial sprouts formed by CEC plated both on the surface (Figure 3.10, A-C) and embedded within the matrices (Figure 3.10, D-F) reveal the presence of luminal spaces represented by two white lines (fluorescence) separated by a dark space (arrow heads). CEC form lumen-containing structures either in the control conditions (Figure 3.10 A, D), or in the presence of FGF-2 (Figure 3.10 B, E) or comb1 (Figure 3.10 C, F). However, the lumens formed by cells plated in 3D constructs appear to be wider compared to lumens formed by CEC cultured in 2D.

Cyclophosphamide treated and leptin receptor deficient mice have delayed cranial cutaneous wound healing.

Our in vitro experiments demonstrating pro-angiogenic and pro-proliferative effects of ECM-derived peptides, suggest that these bioactive molecules may have wound healing potential in vivo. In order to test this, we used two mouse models of impaired injury repair. In the first model we used Balb/c mice, which were pre-treated with two doses of cyclophosphamide at days 4 and 1 before wounding (Burkatovskaya et al., 2008). The second model

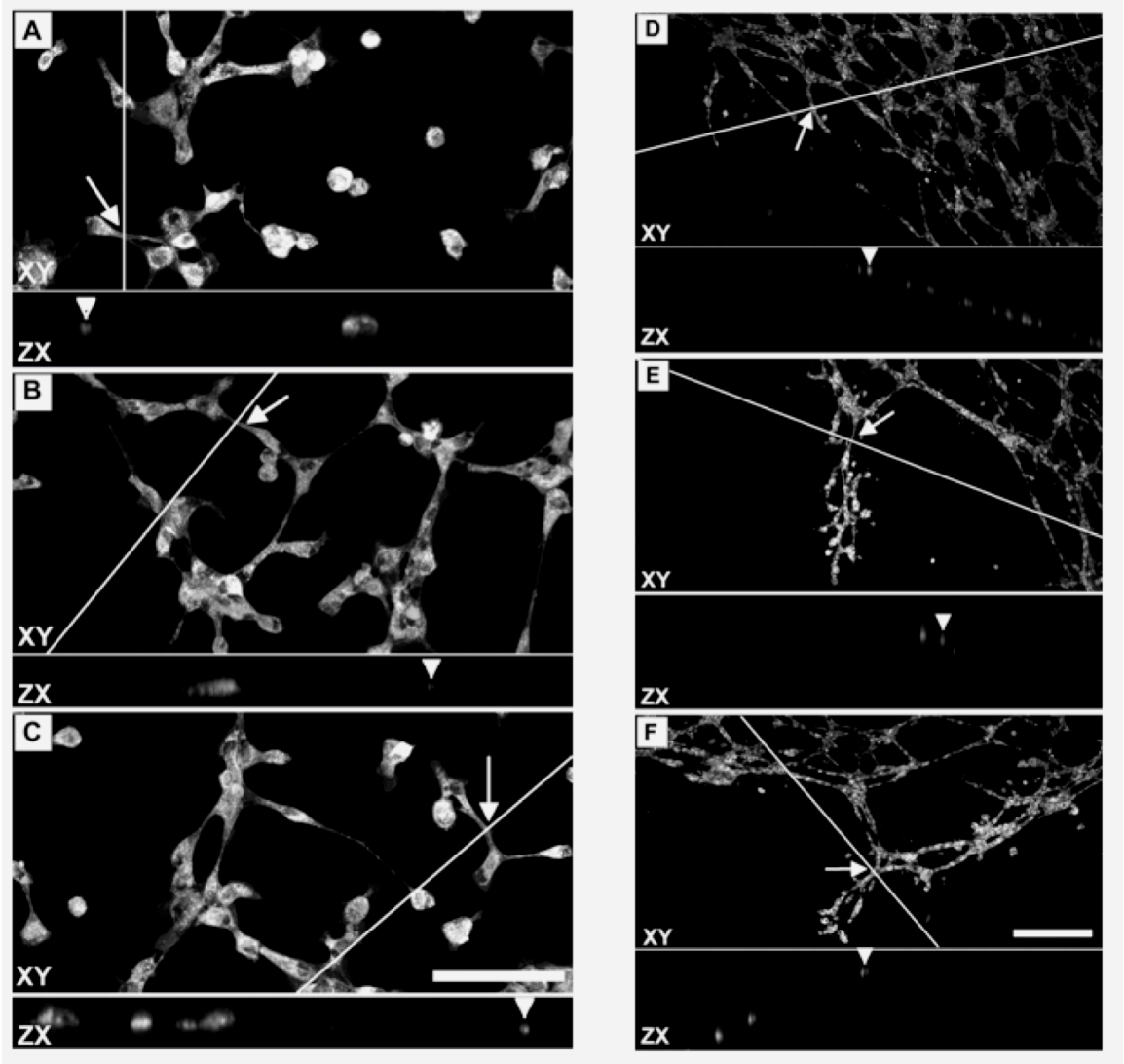

Figure 3.10. Confocal imaging of endothelial morphogenesis and wound healing in 2- and 3-D in vitro models.

(A-C) CEC plated in 2D on the surface of Matrigel in the presence of 1% BCS (A), bFGF (B) or comb1 (C). (D-F) CEC in 3D embedded within collagen/Matrigel blends, wounded and observed 3 days post-injury. (D) – wound filled with collagen-Matrigel blend containing 1% BCS, (E) – wound filled with collagen-Matrigel blend supplemented with bFGF, (F) – wound filled with collagen-Matrigel blend in the presence of 100 nM comb1. Upper panels show images captured in the XY plane while lower panels show optical sections obtained in Z direction (XZ plane) to demonstrate luminal spaces present. Arrowhead denotes the DiO-stained endothelial plasma membrane surrounding 'lumenal' compartment and resembling parallel white lines (fluorescence) separated by a black space. Lines indicate the plane of Z sections. Arrows designate the plane of the XY section from which point an optical section is taken in the XZ direction. Scale bars 100 μm (A-C), 200 μm (D-F).

employs diabetic leptin receptor-deficient mice C57BLKS/J-m Leprdb/+ + (Keswani et al., 2004; Mudge et al., 2002). Impairment of wound healing in both cyclophosphamide treated and genetically diabetic mice has been observed previously (Imegwu et al., 1997;Sharma et al., 2006;Ye et al., 2008), however, all of these studies have used dorsal, but not cranial dermal wounds. Therefore, first we tested whether dermal cranial wound healing will indeed be delayed in cyclophosphamide treated and leptin receptor-deficient animals. In order to estimate the degrees of healing we created/treated the wounds described in Materials and Methods, and used the grading scheme shown in Table 3.1. As revealed in figure 3.11, leptin receptor deficient mice heal their wounds slower than non-diabetic C57/BL6/1J animals. Cyclophosphamide also significantly impairs cranial dermal wound healing (Figure 3.12). Histological evaluation of the degree of wound healing at both 5 and 10 days pos-injury demonstrates that CY indeed delays wound healing in Balb/c mice (Figure 3.12 A and B). Interestingly, this delay was more prominent at the later time point and corresponded to a decrease in the number of blood vessels within the wound beds of CY treated animals compared controls (Figure 3.17).

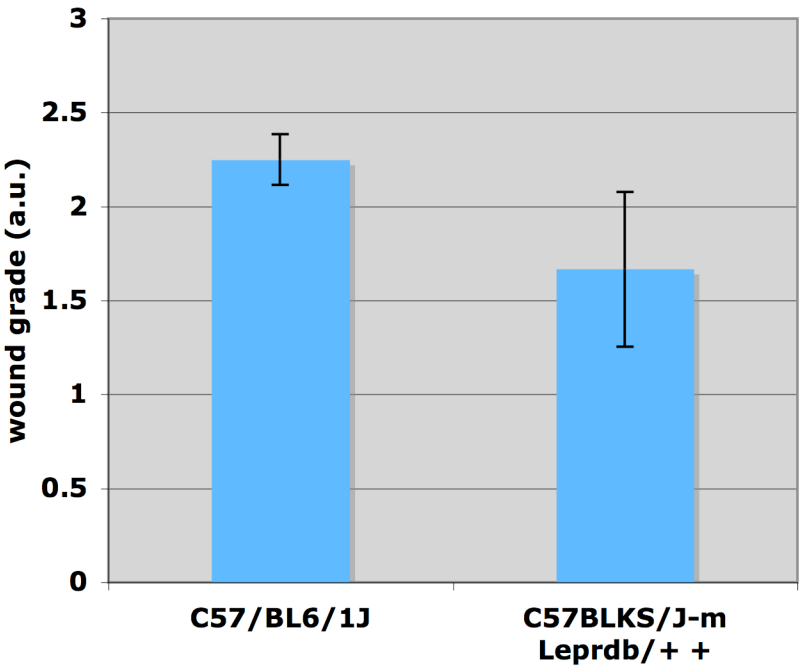

Figure 3.11. Leptin receptor deficient (C57BLKS/J-m Leprdb/++) mice have delayed wound healing as compared normal C57 animals.

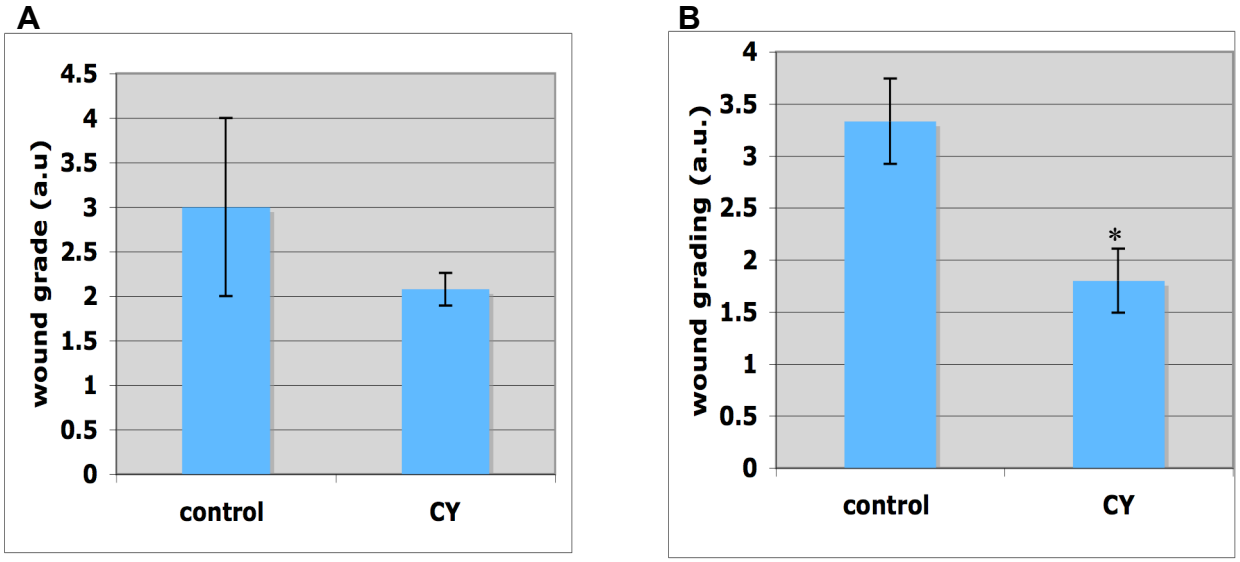

Figure 3.12. CY delays wound healing in Balb/c mice.

The wounds were created as described in Materials and Methods, excised on days 5 (A) or 10 (B) post-injury and stained with HE. Wound grading was performed according to table 3.1. * - $p<0.05$

The peptides stimulate wound healing in CY treated, but not in leptin receptor deficient diabetic mice.

Next we sought to evaluate whether the peptides could reverse the effects of CY and improve impaired wound healing in chemically treated Balb/c or genetically diabetic mice. The effects of the peptides on excisional wound healing were studied in 10 (Figure 3.13, Figure 3.15B) and 5 day assays (Figure 3.15 A). The peptides were suspended in CMC as described above and applied into the wounds daily. CMC or Regranex gels were used as negative and positive controls respectively.

As shown in Figure 3.13, the single peptides as well as their combination improved wound healing in CY-treated Balb/c mice.

Five days after injury the wounds in mice treated with CY alone did not display significant epithelial coverage and had only minor accumulation of granulation tissue. At the same time wounds in peptide treated animals have began to epithelialize and form granulation tissue. As evident from Trichrome stained tissue sections (Figure 3.14), collagen deposition within 5-day old wound beds is minimal in either control or peptide-treated animals. At this time point significant differences were observed between control animals and animals treated with comb1 or a combination of two peptides (Figure 3.15 A).

At a later time point (10 days) the differences between the treatment groups exaggerate. While wounds treated with CMC alone remain largely

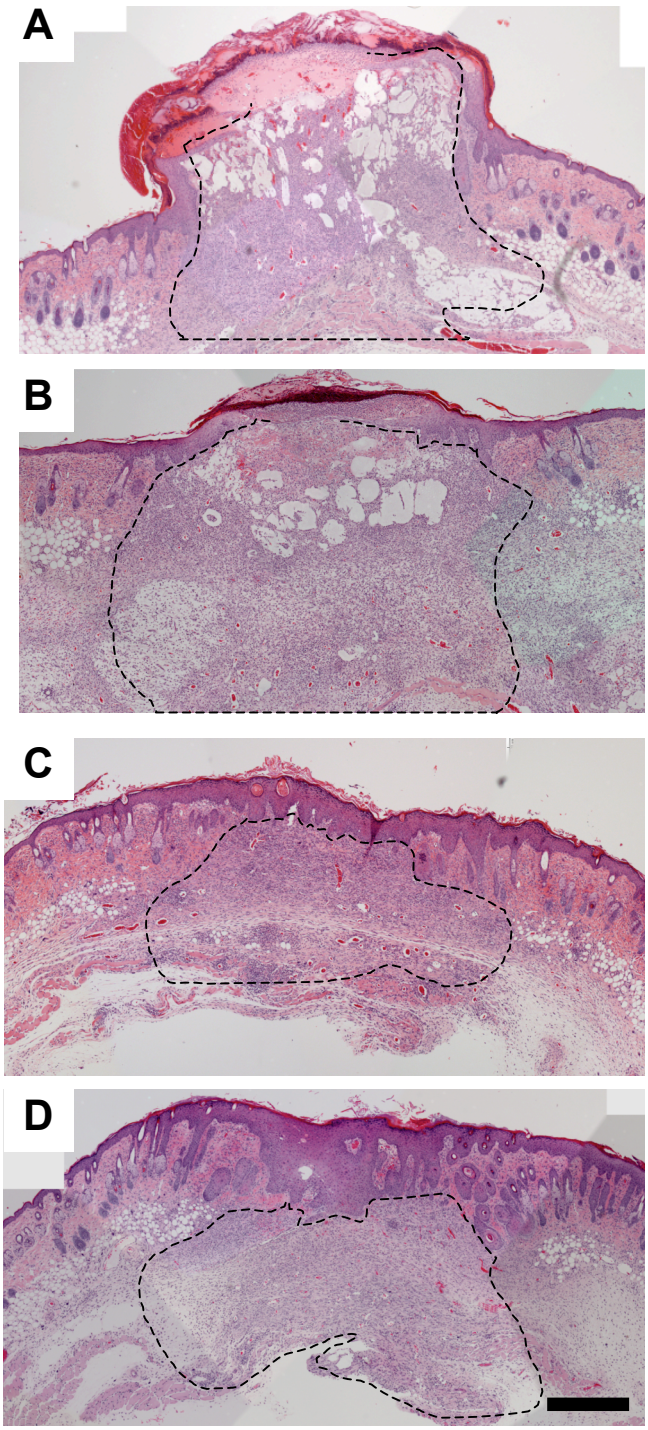

Figure 3.13. The effects of the peptides on excisional wound healing in CY treated Balb/c mice.

Wounds were excised at day 10 post-injury, fixed, sectioned and stained with HE. A – CY only, B – CY + Regranex, C – CY + comb1, D – CY + comb1 + UN3. Dotted line shows wound bed. Scale bar 500 μm.

unepithelialized, wounds treated with the peptides or Regranex are covered with well-defined and stratified epithelium (Figure 3.13 and 3.15 B). Moreover, peptide-treated wounds are characterized by better-defined granulation tissue and significant collagen deposition, especially in wounds treated with UN3 and a combination of UN3 and comb1 (Figure 3.13). Quantitative evaluation of HE stained sections (Figure 3.15 B) confirms that there are significant improvement of healing of wounds treated with the peptides as compared to controls. Interestingly, combination of the peptides (UN3+comb1) (Figure 3.13 and 3.15) further improved the outcome, suggesting the presence of a synergy between the peptides.

The peptides used alone or in combination did not appear to affect wound healing in leptin receptor deficient mice (data not shown). Therefore, we focused our study on the mechanisms by which the peptides stimulate injury repair process in CY treated animals.

Stimulation of wound healing angiogenesis by plasma and ECM-derived peptides.

ECM-derived comb1 significantly improves endothelial proliferation, morphogenesis and responses to injury in vitro (Demidova-Rice et. al., 2011). In addition, our unpublished data suggest that plasma derived UN3 has similar biological activity. Therefore we wanted to determine whether the wound

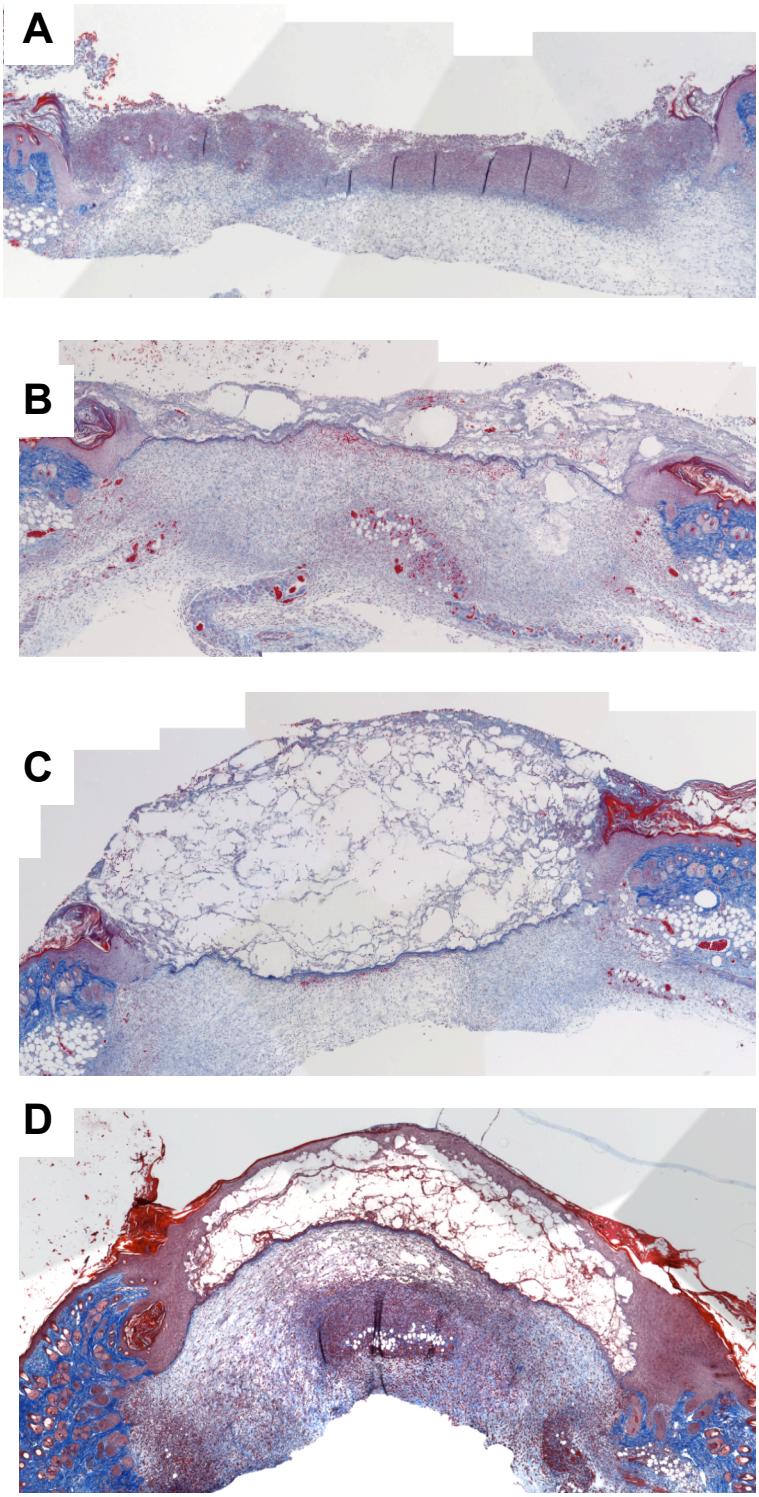

Figure 3.14. ECM-derived peptides stimulate healing of excisional wounds in CY treated Balb/c mice (5 days post-injury).

Wounds were excised at day 5 post-injury, fixed, sectioned and stained with Trichrome. A – CY only, B – CY + Regranex, C – CY + comb1, D – CY + comb1 + UN3.

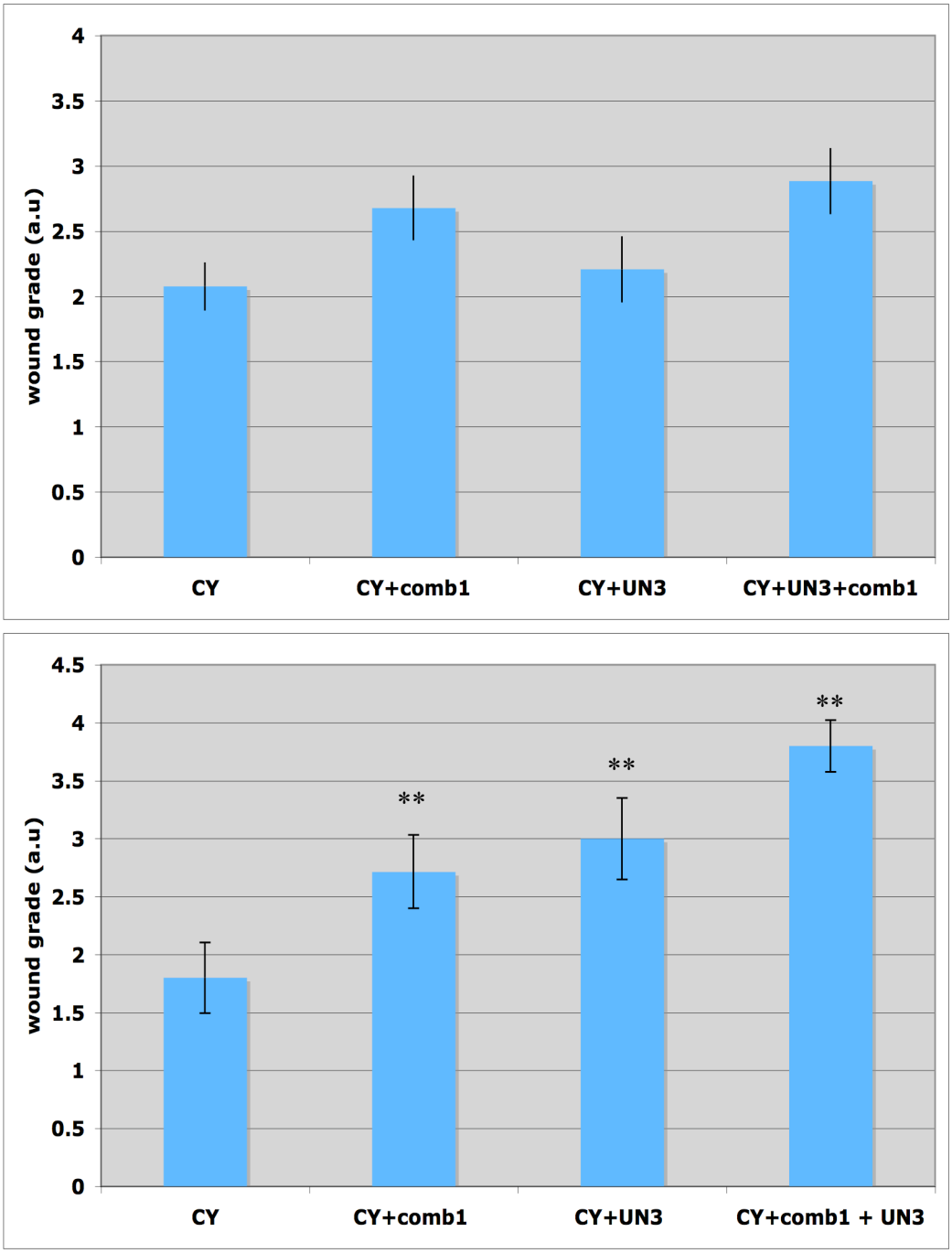

Figure 3.15. Quantitative evaluation of the effect of the peptides on wound healing in CY-treated mice.

Histological sections of wounds excised at day 5 (A) or 10 (B) post-injury were scored, analysed as described in Materials and Methods and plotted as the mean+/- standard error. ** - $p<0.05$.

healing stimulation by the peptides is linked to their pro-angiogenic properties. As described in Materials and Methods, in order to determine blood vessel density we performed immunostaining of frozen wound tissues with anti-CD31 and anti-HSPG antibodies. Analysis of CD31 and HSPG co-localization corresponding to blood vessels demonstrates that combined (comb1+UN3) peptides indeed stimulate wound healing angiogenesis (Figure 3.16). The wounds treated with the peptides have twice as many blood vessels as wounds in animals treated with CY alone (Figure 3.17). Importantly, the peptides reversed negative effects of CY injections on wound angiogenesis: the number of blood vessels within the wounds of CY-injected mice treated with peptides equals to that of control (non-CY-treated) animals (Figure 3.17).

Peptides promote epithelialization and basement membrane formation.

Restoration of epithelial integrity is a critical step during wound healing. We assessed epithelial thickness and a degree of basement membrane formation in both control and peptide treated wounds. As shown in Figure 3.18 wounds treated with UN3 and comb1 combined have significantly increased epithelial thickness at day 10 post-injury compared to CMC and Regranex treated controls, and wounds treated with UN3 or comb1 separately.

Basement membrane formation was assessed using Trichrome stained histological sections of 5 days-old wounds. Results reveal the presence of well-defined basement membrane layer in peptide and Regranex treated but not in CMC treated wounds.

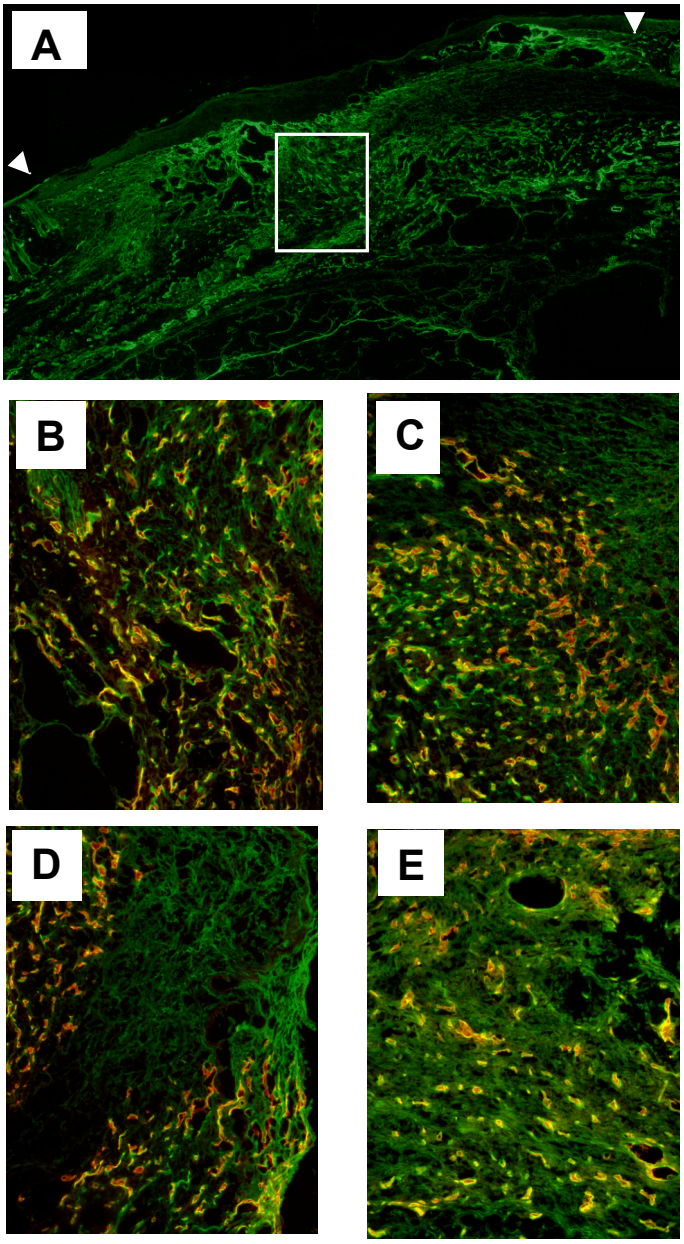

Figure 3.16. Effects of the peptides on wound healing angiogenesis in CY treated Balb/c mice.

Wounds excised at day 10 post-injury were stained with anti-HSPG (green) and anti-CD31 (red) antibodies. Yellow areas represent blood vessels. A – a section of a wound stained with anti-HSPG alone and imaged using 5x objective lens. Arrows indicate the wound edges, white rectangle outlines a central area of the wound where high power images (B-E) were taken. B - control wounds, C, D and E wounds treated with comb1, UN3 and comb1+UN3 respectively.

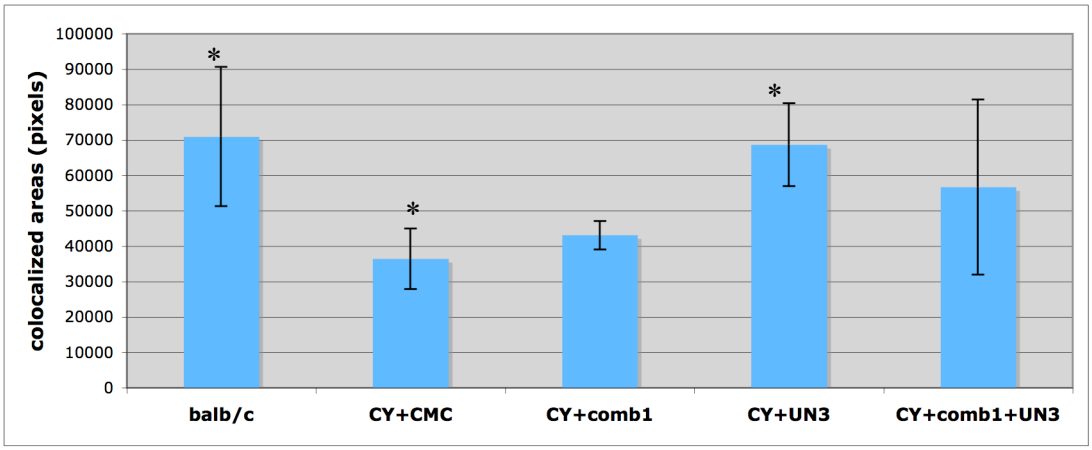

Figure 3.17. Quantitative evaluation of the effects that the peptides have on angiogenesis in CY-treated mice.

The images of 10-day old wounds were taken as described in the legend for Figure 3.17. The areas of colocolization of green (HSPG) and red (CD31) antibodies were quantified using ImageJ and plotted as the mean+/- standard error. The number of wound blood vessels mice treated with CY alone is significantly lower than in control animals or in mice treated with UN3 peptide. * - $p<0.05$

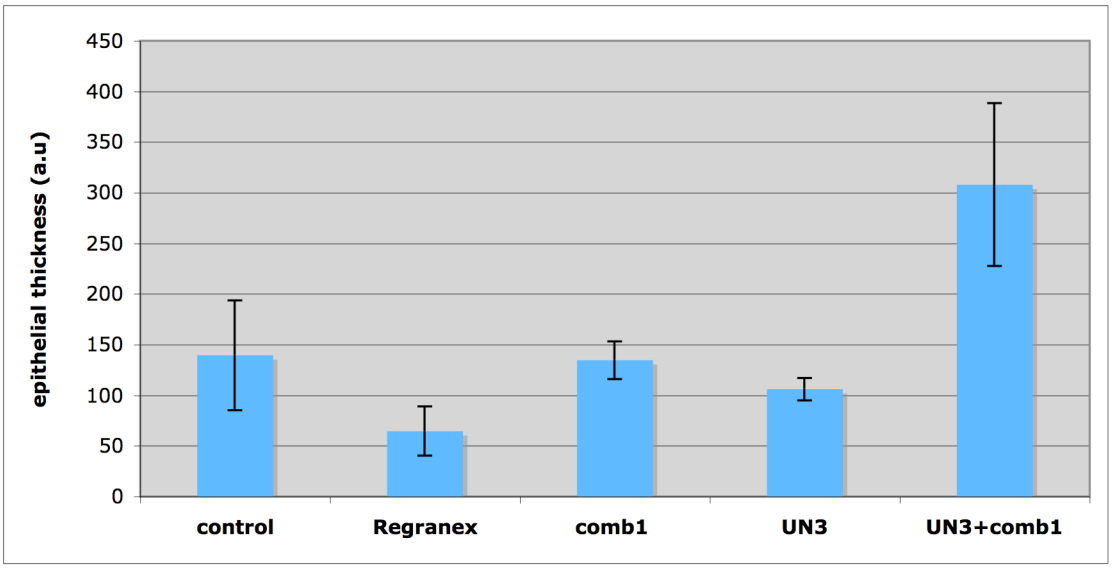

Figure 3.18. Peptides stimulate wound epithelialization in CY treated Balb/c mice.

3.4. Discussion.

Collagenase derived from the gram-positive bacterium Clostridium histolyticum has been used for wound debridement since the 1960s (Ramundo and Gray, 2008). More recently, it has been suggested that in addition to its debriding effects the enzyme has stimulatory effects on resident cells – keratinocytes, fibroblasts and endothelial cells within the wound bed (Herman, 1996; Riley and Herman, 2005). These cells, already exposed to host–derived MMPs, are stimulated further in the presence of an exogenous and highly-purified form of Clostridial collagenase suggesting a direct role in the promotion of wound healing (Riley and Herman, 2005). In this study we demonstrate that low molecular weight collagenous and non-collagenous fragments are liberated from endothelial ECM following degradation with Clostridial collagenase. Importantly, these peptides are bioactive and possess marked pro-angiogenic properties in vitro and stimulate cutaneous wound healing in vivo.

This study was designed to test whether Clostridial, but not human collagenase might yield distinct bioactive fragments that could explain the wound healing activity observed when the bacterial enzyme is added to living cell cultures in vitro or wounds in vivo. To test this hypothesis well defined capillary endothelial derived matrices (Yost and Herman, 1990) were treated with either the human or bacterial collagenases prior to immunoprecipitation of matrix fragments produced by each enzymatic reaction. Results revealed that several fragments are uniquely present in matrices digested with bacterial, but not with the human orthologue (Figure 3.1).

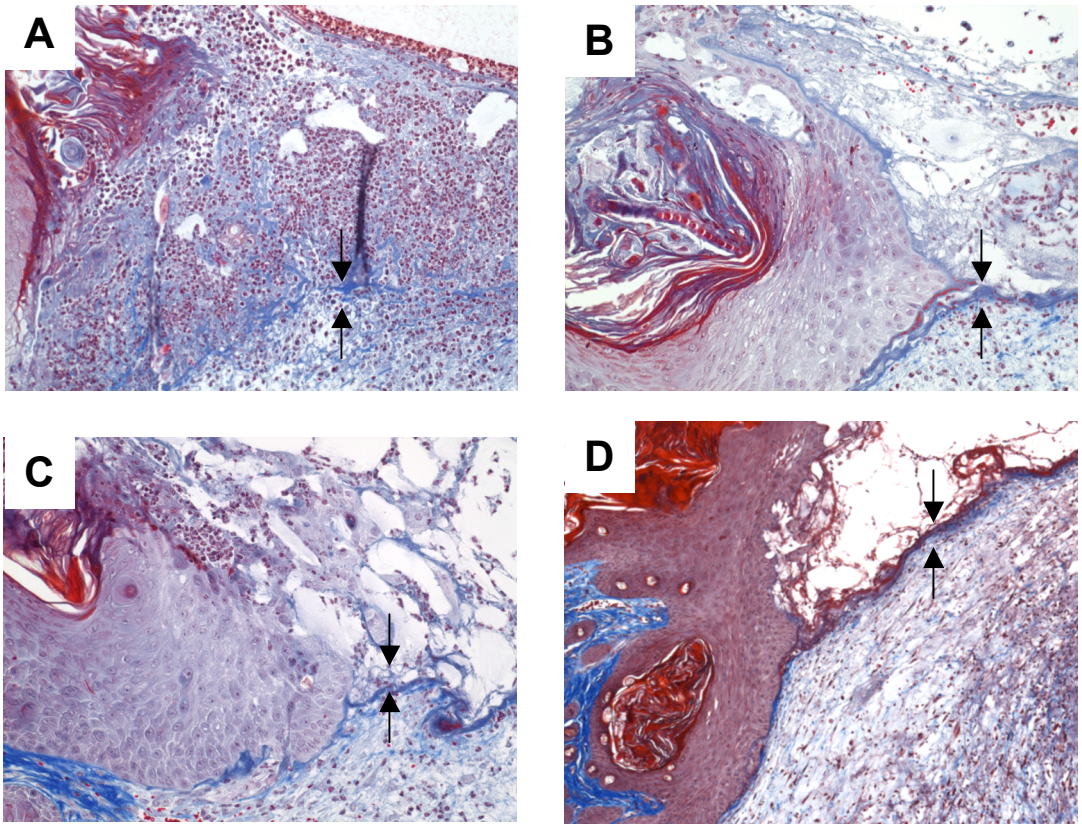

Figure 3.19. Effects of ECM-derived peptides on epithelial basement membrane formation.

The wounds were excised at 5 days post-injury, fixed, sectioned and stained with Trichrome as described in Materials and Methods. A – control wound, B – wound treated with Regranex, C – wound treated with comb1, D – wound treated with comb1+UN3. Arrows indicate forming epithelial basement membrane.

These observable differences in matrix degradation patterns following collagenase digestion reflect what are likely to be the previously reported and differential substrate specificities between the enzymes. Indeed, earlier studies have revealed that mammalian and bacterial enzymes have distinct cleavage sites within the collagen molecule (Bornstein, 1967). The mammalian collagenase cleaves specific Gly-Ile or Gly-Leu bonds of α1 and α2 chains releasing two fragments that represent 1/3 and 2/3 the intact parent collagenous

substrate. Bacterial collagenase on the other hand, attacks the parent collagenous backbone much more frequently, especially at Y-Gly bonds, therein releasing multiple fragments (Bornstein, 1967). Our data validate these earlier reports and lend credence to the notion that the putative wound healing properties embodied in Clostridial collagenase may be linked to its differential substrate specificity and the resultant products of digestion that arise.

Isolation of the specific peptides released by bacterial collagenase revealed the presence of several fragments of collagen: included were fragments of collagen I and collagen IV, both of which have been reported to be produced by endothelial cells (Fouser et al., 1991;Yost and Herman, 1990). Additionally, we observed the presence of non-collagenous components present in the immunoprecipitations performed anti-collagen I IgGs. Of interest and included in this group of non-collagenous components are tenascin X and fibrillin 1. Tenascin X and fibrillin 1 are components of the extracellular matrix that possess multiple domains, including regions that respectively interact with collagen I, III, V, decorin, and fibronectin, elastin and latent transforming growth factor β-binding protein (Ishitsuka et al., 2009; Sabatier et al., 2009). That tenascin X is present within the anti-collagen I IPs is of particular interest since this matrix component has been previously implicated in soft tissue injury and repair in humans (Burch et al., 1997). Moreover, mice deficient in this protein have lower scar breaking strength and abnormalities in the processes of scar maturation suggesting that tenascin X is required for normal wound healing (Egging et al., 2007). That both tenascin X and fibrillin 1 are present in abundance within anti-

collagen immunoprecipitates points to the important roles that collagenous and non-collagenous protein-protein interactions are likely to play in the cellular responses to injury, including the angiogenesis of wound healing. For these reasons, we aimed to test whether any, all or combinations of peptides in this unique Clostridial collagenase-produced peptide 'library' might induce key wound healing responses embodied by purified Clostridial collagenase, i.e. stimulation of cellular proliferation and migration. Further, because of the pivotal role the angiogenesis plays in promoting healing, we tested whether or to what extent each peptide could promote in vitro angiogenesis assays using two- and three-dimensional models.

As shown in Figure 3.1, we have observed that eight of the peptides derived from the matrices degraded by bacterial collagenase have angiogenic potential (Table 3.2). Fragments of EGF-like domains of fibrillin 1 (fibr2 -DIDECESSPCINGV) and tenascin X (ten1 -GVRSCPRGCSQKGRCED) as well as a fragment of non-collagenous domain of collagen IV (col4-1 -MFRKPIPSTVKA) and combinatorial peptide (comb1 -DINECEIGAPAGEETEVTVEGLEPG) induce a significant, up to 47% increase in endothelial proliferation. Pro-angiogenic effects of the peptides in a Matrigel-based assay are even more robust. Seven peptides significantly increase the rate of angiogenesis in this model. Importantly, a fragment of collagen IV (col4-1 -MFRKPIPSTVKA), a fragment of fibronectin-like domain of tenascin X (ten 2 -GEETEVTVEGLEPG), a fragment of EGF-like rich domain (ten 4 -CGTRACPGDC), as well a combinatory peptide (comb1 -

DINECEIGAPAGEETEVTVEGLEPG) induced more angiogenic sprouting than did the FGF-2 positive control (Figure 3.3). While most of the peptides increase either proliferation of endothelial cells or in vitro angiogenesis, two of them, namely comb1 and col4-1, are active in both assays. Interestingly, the effects of the peptides on endothelial morphogenesis in this model are more pronounced at the earlier time point 7h as compared to 24h post-plating. This suggests that in addition to enhancement of the rate of cell-cell interactions, which leads to cellular alignment and tube formation, the peptides also enhance endothelial motility - an early step of angiogenic process.

Our results agree with several earlier reports showing biological activity of matrices degraded by bacterial collagenase. It has been demonstrated that fragments of human eschar degraded by bacterial collagenase stimulate fibroblast proliferation both in vitro and in vivo (Radice et al., 1999). The fragments have not been identified and it is possible that the degraded matrix contains both stimulatory and inhibitory entities. Moreover, it has been reported that several synthetic collagenous di-, tri-peptides and polytripeptides as well as bacterial collagenase degraded collagens, are chemotactic for human fibroblasts monocytes (Postlethwaite and Kang, 1976; Postlethwaite et al., 1978) and neutrophils (Laskin et al., 1986). The effects of these fragments on endothelial cells or angiogenesis have not been reported. However, pro-angiogenic moieties have been isolated from the ECM in the absence of bacterial collagenase (Malinda et al., 2008; Nunes et al., 2008; Robinet et al., 2005). Fragments of laminin α1 and β1 chains can stimulate endothelial cell adhesion, sprouting, tube

formation (Malinda et al., 1999) and wound healing in vivo (Malinda et al., 2008; Min et al., 2010). Fragments of thrombospondin have been shown to interact with cell surface syndecan-4, activate intracellular Akt/PKB pathway and stimulate tube formation on Matrigel (Nunes et al., 2008). Elastin-derived peptides enhanced endothelial migration, tube formation on collagen type I in vitro and in chick chorioallantoic membrane model ex vivo (Robinet et al., 2005). These effects were accompanied by an increase in MT1-MMP production by endothelial cells and attributed to the presence of the GXXPG sequence. Two of our peptides comb1 and ten2 also contain this stretch of amino acids, and both induce angiogenesis in a Matrigel-based assay. However, only a larger combinatorial peptide (comb1), with presumably more complex tertiary structure and two GXXPG domains, also stimulated cellular proliferation. While both ten2 and comb1 can probably stimulate MMP production by cells necessary for endothelial morphogenesis, comb1 is likely to activate other yet undetermined pathways mediating cell proliferation.

Importantly, the chemical structure of other bioactive ECM fragments released by bacterial collagenase and described here is unique and have not been reported by others. The receptors and signaling pathways activated by the peptides remain to be discovered. The receptors may include well-established ECM and growth factor receptors, particularly epidermal factor receptor, that can be activated by proteolytically exposed cryptic sites within matrix molecules (Tran et al., 2005).

Since GxxPG-containing combinatorial peptide (comb1) and a fragment of collagen IV (col4-1) were effective in promoting endothelial proliferation and angiogenesis using Matrigel-based assays, we were interested to learn whether these specific peptides were able to promote wound healing angiogenesis in more realistic 3D model of injury and repair. To these ends, we embedded CEC within the collagen-Matrigel mixtures prior to full thickness injury, and then filled the defect with the matrix containing defined concentrations of the peptides or control pro-angiogenic FGF-2 or VEGF. We have also included pro-proliferative ten 1 and pro-angiogenic ten 4 peptides in the protein library tested in this model in order to reveal whether the peptides active in one or the other assay can stimulate cellular responses in 3D. Results demonstrate that at day 3 post-wounding, the responses seen in the wounds containing comb1 were more pronounced than in wounds supplemented with FGF-2 (Figure 3.9). That comb1 was able to stimulate endothelial responses in a complex 3D environment, as well as in 2D assays, identifies this peptide as potent modulator of angiogenesis. Future experiments will determine whether comb1 has a wound healing potential in vivo.

To our knowledge, this is the first report where this unique 3D model (Herman and Leung, 2009) is used to compare and contrast the compounds with different angiogenic potential. Unlike standard Matrigel-based assays (Kleinman and Martin, 2005) here the cells are embedded within the layers of matrix and, therefore, remain viable for a prolonged time (up to 1 week). Thus, in addition to the identification of promising pro-angiogenic or anti-angiogenic therapeutics,

such 3D constructs can be employed to study the stability of wound healing compounds. In this study we used Matrigel-collagen mixtures in the presence or absence of the peptides to fill the defects created in 3D sandwiches, however, other compounds can be utilized to fill these full-thickness defects and as such the construct may be useful for evaluation of drug delivery systems.

Next we sought to test whether the most biologically active peptides could promote cellular responses to injury in vivo. This was done using mouse models of impaired wound healing - CY treated and leptin receptor-deficient mice (Burkatovskaya et al., 2008; Keswani et al., 2004; Mudge et al., 2002). All mice used in this study were receiving cranial dermal punch biopsies. This type of wound was used in order to minimize the wound contraction, encourage granulation tissue deposition/epithelialization and thus make mouse wound healing more resembling that of tight skinned animals (Chung et al., 2010; Reid et al., 2004). Cranial wounds in both chemically treated and diabetic animals healed slower than in healthy counterparts (Figures 3.11 and 3.12). The peptides especially when used in combination significantly improved wound in CY-treated mice. In these animals, the peptides are more efficient than clinically used Regranex gel. Surprisingly, the healing of dermal cranial wounds in diabetic animals was not accelerated in the presence of the peptides (data not shown). A likely reason for this phenomenon is the dissimilarity of healing impairment mechanisms in C57BLKS/J-m Leprdb/+ + and CY-injected animals. The major reason for delay in responses to injury in diabetic mice is linked to their hyperglycemic status. High blood glucose leads to several abnormalities

including protein glycation (Kuo et al., 2007; Liao et al., 2009; Reigle et al., 2008) that in turn often abrogates protein activity and ability to interact with its binding partners and receptors (Duraisamy et al., 2001). It is possible that in diabetic animals excessive blood glucose has prevented the interaction of the peptides with their putative receptors and therefore peptide-mediated wound healing. This ECM glycation is unlikely to occur in CY-treated mice, which therefore were responsive to treatments. More thorough investigation of the effects that the peptides have on diabetic wound healing is necessary to unequivocally determine their potential for healing of this type of wounds. This might require the use of different wound model (skin flap, incisional wound etc), modifications of peptide concentrations/delivery mode and assessment of different wound healing parameters.

Our in vitro experiments with CEC revealed the pro-angiogenic potential of the peptides. Therefore, we tested whether similar effects could be achieved in vivo. Results reveal that the peptides can stimulate blood vessel formation within the wound bed. Similar pro-angiogenic effects were described for laminin-derived peptides (Malinda et al., 2008). These peptides induced an increase in both number and size of blood vessels at day 4 post-injury. In our experiments the effects on angiogenesis are more pronounced at later time point – 10 days post-wounding (Figure 3.17). To our knowledge, no fragments of tenascin X or fibrillin-1 have been demonstrated to stimulate or inhibit angiogenesis. Several fragments of collagen IV on the other hand are well known for their anti-angiogenic properties (Mundel and Kalluri, 2007). Interestingly, one of collagen

IV fragments (Col4-1) identified in our study, which stimulated endothelial prliferation and migration in vitro, did not enhance wound healing in vivo (data not shown).

Analysis of Trichrome stained sections of mouse wounds excised at day 5 post-injury shows increased epithelialization accompanied by enhanced basement membrane deposition in the presence of the peptides (Figures 3.18 and 3.19). The increase in ECM deposition could be one of the mechanisms by which the peptides stimulate wound healing. Other mechanisms are likely to include activation of ECM receptors, particularly integrins $\alpha v\beta 3$ and $\alpha 5\beta 1$ which were shown to bind to biologically active laminin-derived peptides and induce an increase in migration of both endothelial and epithelial cells (Malinda et al., 2008).

In conclusion, we have shown that degradation of endothelial extracellular matrices with bacterial collagenase releases small bioactive peptide fragments derived from collagenous and non-collagenous substrates, including collagen Type IV, fibrillin-1 and tenascin X. Several of the bioactive peptides derived from these parent matrix macromolecules can stimulate endothelial proliferation and angiogenesis in both 2- and 3D models of wound healing. Moreover, demonstrate that the peptides described here can also stimulate epithelial responses to injury and wound healing in vivo (Figures 3.18 and 3.19). In addition to identification of novel ECM-derived bioactive molecules our work expands the knowledge of the mechanisms underlying stimulatory effects of bacterial collagenase on wound healing. We propose (Figure 3.20) that bacterial

collagenase has multiple direct and indirect positive effects on cellular responses to injury and wound healing: it degrades wound matrix easing dermal and epidermal cell motility, releases ECM and cell surface-bound growth factors. Moreover, it liberates biologically active ECM fragments, which in turn can activate specific, yet unidentified receptors on endothelial and epithelial cells stimulating angiogenesis and epithelialization during wound healing.

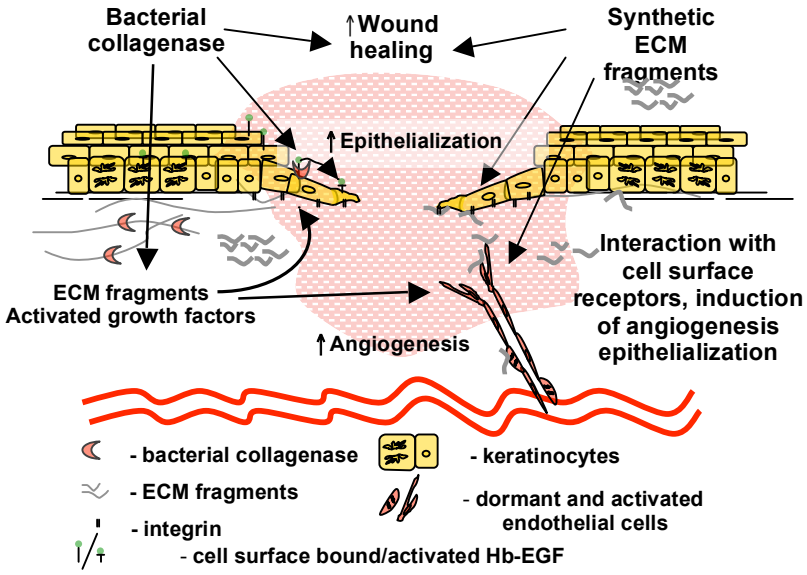

Figure 3.20. Control of wound healing: A role for bacterial collagenase?

Bacterial collagenase clinically used for wound debridement stimulates both endothelial and epithelial responses to injury. Degradation of the ECM in close proximity to the cells the enzyme allows for efficient cell migration. Release of growth factors and liberation of biologically active matrix fragments that can interact with and activate cellular receptors increases motogenic and mitogenic potential of the cells within the wound bed promoting the healing responses. Similarly to naturally occurring ECM fragments released by bacterial collagenase in vivo, synthetic matrix-derived peptides identified and tested our laboratory can enhance cellular responses to injury. Therefore we propose that the peptides could be used in combination or as an alternative to the bacterial products, which foster wound healing in vivo.

Chapter 4. Future research directions.

The studies described in this dissertation demonstrate that LLLT and novel peptides derived from endothelial ECM degraded by bacterial collagenase stimulate cellular responses to injury both in vitro and in vivo. In the first part of the dissertation we have determined the parameters (wavelength, light intensity) that allow for successful stimulation of wound healing responses with low level light. Moreover we revealed that there are significant differences in LLLT responsiveness between different strains of mice and showed that laser and non-coherent light sources are similarly effective. In the second part of the dissertation we have demonstrated that bacterial collagenase liberates biologically active fragments of collagen, tenascin and fibrillin from endothelial extracellular matrices. These fragments as well as a novel combinatorial peptide were tested in both in vitro and in vivo assays and demonstrated profound pro-angiogenic and wound healing activity. Additional studies are needed to reveal molecular mechanisms of activity of both LLLT and ECM-derived peptides.

4.1. Cellular and molecular mechanisms of LLLT.

Experiments described in Chapter 1 of this dissertation reveal that at least in mice exposure of the cells within and on the periphery of the wound bed to 820 nm light induces fibroblast differentiation and wound contraction. It has been demonstrated that LLLT is capable of activation of latent TGF-β1 and 3 (Arany et al., 2007), which in turn are the key regulators of fibroblast differentiation (Hinz, 2007c) and a stimulator of wound contraction. Therefore we hypothesize that LLLT-activated TGF-β family members promote fibroblast-to-myofibroblast

transition. To test this hypothesis several experimental approaches could be used. First, in vitro cultures of murine and/or human fibroblasts can be exposed to 820 nm light and than subjected to immunocytochemical staining with antibodies directed against smooth muscle actin and the key mediators of TGF-β signaling – SMAD2 and 3. An increase in SMAD levels and their translocation to the nucleus after fibroblast exposure to LLLT would indicate involvement of TGF-β in phototherapy induced fibroblast-myofibroblast transition. In order to verify this association, fibroblasts can be exposed to LLLT in the presence of siRNA directed against SMADs 2 and 3, which should diminish fibroblast differentiation. Similar experiments can be performed in vivo. If these experiments are successful, we will test whether LLLT can stimulate contraction of human fibroblasts. We will plate the cells on deformable silicone substrate as described (Kotecki et al., 2010), expose them to LLLT and determine their ability to apply contractile force to the substrate. This would prove that LLLT indeed induces ECM and wound contraction by differentiated fibroblasts.

4.2. ECM-derived peptides and the mechanisms of wound healing stimulation.

Our data reveal that bacterial collagenase-mediated degradation of endothelial ECM liberates biologically active fragments. These peptide stimulate angiogenesis both in vitro and in vivo (Demidova-Rice and Herman, 2009; Demidova-Rice, Geevarghese, and Herman 2011). We hypothesize that pro-angiogenic effects of the peptides are mediated by identifiable cellular receptors activating discrete intracellular pathways (Figure 3.20). The nature of these

receptors and activated signaling cascades remains unknown. In order to identify the receptors mediating the cellular effects of the peptides we will use fluorescein isothiocyanate labeled combinatorial peptide (FITC-comb1). Cell lysates prepared from endothelial cells cultured on Matrigel in the presence or absence of the peptides will be run on SDS-PAGE. Three gels with equal amount of loaded protein will be run simultaneously. One of the gels will be stained with Coomassie or silver stain for protein detection; the proteins from two remaining gels will be transferred to nitrocellulose membrane and probed with FITC-comb1 the presence or absence of its unlabeled counterpart. After incubation with the peptides, membranes will be probed with anti-FITC antibodies and HRP-conjugated secondary antibody. The bands in the Coomassie-stained gel corresponding to those present on the membranes probed with biotinylated peptides, but not on the control membranes will be submitted for mass spectrometry. A cross-linking step will be added before probing with anti-FITC antibody in order to ensure stability of peptide-receptor binding.

Results of our experiments in a mouse model indicate that in addition to their pro-angiogenic properties, the peptides can enhance epithelial responses to injury (Figures 3.18 and 3.19). It remains unknown whether human keratinocytes can also be stimulated in the presence of the ECM fragments. Therefore, we propose to perform in vitro proliferation and migration assays. For proliferation assay the cells will be plated at low density in the presence or absence of the peptides and counted using Coulter counter at 1, 3 and 5 days post-plating. The effects of the peptides on keratinocyte migration will be studied in a scratch

wound assay performed on confluent cells as described (Riley and Herman, 2005).

Our preliminary in vitro data demonstrate that endothelial cells plated on Matrigel in the presence of the peptides produce more laminin compared to cell plated in control conditions (1% BCS). Moreover, analysis of Trichrome-stained mouse tissue sections reveals that the peptide-treated wounds have more prominent epithelial basement membranes (Figure 3.19). Therefore, we think that the peptides might stimulate deposition of the basement membrane proteins particularly laminins. In order to confirm these observations we will perform to sets of experiments. First we will use anti-laminin (laminin 111 and 332) antibodies to stain frozen sections of control and peptide-treated mouse wounds. Next we wil perform qPCR using mRNA extracted from lysates of human endothelial cells or keratinocytes plated in the presence or absence of the peptides and specific laminin (LAMA1, LAMB1, LAMC1, LAMA3, LAMB3, and LAMC2) primers (Akutsu et al., 2005;Kawata et al., 2002). If these experiments will reveal that the peptides can indeed stimulate laminin gene expression and protein deposition we will examine the upstream regulators of laminin production in both endothelial cells and keratinocytes.

In addition we are planning to test the wound healing potential of the peptides in porcine model of wound healing. These experiments will be done using both healthy and diabetic pigs and will allow us to establish whether the peptides can be active in more clinically relevant model of injury repair.

Appendix 1. Identification of cellular receptors mediating the effects of ECM derived peptides.

Introduction.

Our experiments demonstrate that the combinatorial peptide (comb1) derived from endothelial extracellular matrices degraded by bacterial collagenase stimulates cellular responses to injury both in vitro and in vivo. In order to identify the cellular receptors mediating theses responses we have used several approaches including biotin labeled comb1 (b-comb1), which can be visualized using avidin-based detection systems (Wilchek and Bayer, 1990).

Materials and Methods.

B-comb1 synthesis and in vitro angiogenesis assays.

B-comb1 was synthesized at TUCF using FastMoc Chemistry (Fields et al., 1991). Biotin was added to the B-terminus of the peptide via glycine linker as following:

Biotin-GGG-DINECEIGAPAGEETEVTVEGLEPG-OH

In vitro (2D) endothelial morphogenesis assays were performed as described below.

2D in vitro angiogenesis protocol:

Materials:

Matrigel (BD biosciences #354230 – growth factor reduced; #354234

Falcon CultureSlide 8 well glass Chamber slides (BD/Falcon #3-41-8).

Procedure (Demidova-Rice, Geevarghese, and Herman, 2011):

1. Thaw Matrigel at 4C, packed in ice (6h or overnight). Chill the pipette tips. Make sure you have enough Matrigel to use 300 uL/well.
2. Mix the peptides into the Matrigel at 100 nM final peptide concentration.
3. Place Matrigel 300 uL/well into chamber glass slides. Make sure the meniscus contacts all 4 side of the well, leaving somewhat flat surface in the center. This step should be performed at 4C (cold room).
4. Polymerize Matrigel at 37C for 1 h.
5. Add 5x105 cells/well in 500uL DMEM, 1%BCS. Add the peptides (final concentration of the peptides in the media 100 nM).
6. Monitor tube formation (3, 5, 7 and 20h post-plating).

Peptide internalization by CECs.

B-comb1 internalization protocol:

Materials:

Digitonin 0.002% in PBS (stock 2% in DMSO, diluted to 0.002% in PBS)

Dithiobis(succinimidyl) propionate (DSP, Pierce 22585) 0.1mg/mL (stock 10 mg/mL in DMSO, diluted in PBS to final 0.1 mg/mL).

TRIS pH 7.5 (10 mM)

HRP-avidin (Zymed Labs, #43-4423)

Procedure (Healy and Herman, 1992):

1. Plate BREC (35on sterilized glass cover slips in the DMEM supplemented with 5% BCS and antibiotics and allowed to attach for 18h and then transferred to DMEM containing 1% BCS for 2h.
2. The following morning wash cells twice and pre-incubate with DMEM containing 1% BCS 37C (2h). During this time pre-incubate HRP-avidin with biotinylated and control comb1 (30 min at RT). Use ratio 2.2 nM HRP-avidin:100 nM peptide for binding.
3. Move cells into the cold room, let equilibrate, place on ice. Add peptide-HRP-avidin mixture. Incubate for 30 min on ice.
4. Bring to 37C, incubate for 30 minutes.
5. Fix and stain as below.

<u>Fixing and staining of cells:</u>

1. Wash cells 3 times with cold PBS
2. Incubate with 0.1 mg/mL DSP containing 0.002% digitonin for 30 minutes at room temperature.
3. Add 10 mM TRIS to quench the cross-linker, incubate for 15 min.
4. Wash 3 times with PBS.
5. Block with egg white (1 egg white in 100 mL in PBS) for 15 minutes.
6. Block with 5% skim milk for another 20 minutes.
7. Wash with PBS 3x.
8. Incubate with PBS/1% BSA for 15 minutes.
9. Wash with PBS 3x.

10. Incubate with anti-HRP antibody duluted 1:500 in PBS/4% BSA/10% rat serum. Incubate for 1.5h.
11. Wash 3x with PBS/1% BSA.
12. Incubate with Alexa546 anti-rabbit IgG (1:500) for 30 min at room temperature.
13. Wash with PBS 3x, mount, image at 10x.

Identification of potential receptors.

Immunoprecipitation (Welch and Herman, 2002).

Materials:

Crosslinker: 2 mM (3,3´-Dithiobis[sulfosuccinimidylpropionate]) DTSSP (Pierce, 21578)

Quenching buffer: 10mM TRIS-HCl/150 mM NaCl/0.2M glycine

RIPA buffer

Albumine, BSA	0.0625 gram
Tris-HCl, pH 8.0, 1M	1.5 ml
SDS	0.05 gram
Deoxycholate Acid	0.25 gram
NP-40 (Non-ionic detergent)	0.5 ml
	Complete to 50 ml with ddH_2O.

add protease inhibitors 1:100

and 50 nM Calyculin A immediately before use

Protein A Sepharose CL-4B beads (Amersham Biosciences)

Anti-biotin IgG (Novus biologicals, NB120-6643)

Sample buffer: 1M Tris pH 7.0 125mM, SDS 2%, Glycerol, 10%, Bromophenol Blue 1%, Beta Mercaptoethanol 1%.

Procedure:

Cell-peptide interaction and crosslinking (Bennett et al., 2000).

1. Prepare GF-reduced Matrigel films in 4x1/2 of 6 well plates (3 for biot-comb1 +/- x-linking, 3 for control). Place 1mL of liquid Matrigel in the wells, incubate on ice for 4 min, then remove 600 ul of Matrigel (save at -20C for next experiment). Keep the plate in the incubator overnight.
2. Next day, plate BREC at 200k/well in the presence comb1 in order to induce potential receptor(s) or in the absence of comb1 (control). Let attach for 3h (if the tubes are not forming yet, continue incubation of another 2h), gently wash with cold PBS 3x. Transfer to the cold room. In 3 plates add biot-comb1 1uM in 250 uL of DMEM/0.5% BCS (cold), incubate at 4C for 1h to allow for receptor-peptide interaction. Total amount of biotin is 0.9 nmoles.
3. After the incubation, wash all the plates 3x with cold PBS.
4. Add 2 mM DTSSP in PBS. Incubate on ice for 2h according to manufacturers instructions.
5. Wash 3x 5 min with 10mM TRIS-HCl/150 mM NaCl/0.2M glycine to quench DTSSP according to manufacturers instructions.

6. Lyse cells with agitation at RT for 10 min, then use bent needle, spin to clarify. Use 2 mL of RIPA buffer for lysis.

Protein A Sepharose CL-4B beads and anti-biotin IgG interaction (Riley et al., 2003).

1. Weigh out 0.05 g of the beads. Resuspend in 5 mL of dH2O.
2. Spin 3 min at 4C, remove supernatant, repeat.
3. Resuspend in 1 mL of RIPA, split into 4 tubes (250 ul each = 60.5 uL of swollen beads can bind 1 mg IgG).
4. Add 100 ug (0.2 umoles) of IgG into 2 tubes, rotate at 4C for 2h for beads-ab binding (recommended time is 30 min at RT).
5. Meanwhile pre-clear the lysates: add the cell lysates from control cells and cells crosslinked with biot-comb1 into the remaining tubes with the beads. Rotate for 1h at 4C.
6. Spin, use the supernatant in the next step.

Bead-anti-biotin IgG + cell lysates interaction.

1. Take pre-cleared lysates and combine them with the anti-biotin IgG bound beads, rotate at 4C overnight.

Next day:

1. Spin both tubes, wash 3x with RIPA containing protease inhibitors and Calyculin A.
2. Spin again, add 500 uL of buffer containing 30 mM TRIS and 50 mM NaCl, spin remove the supernatant.
3. Boil the beads with 1x sample buffer.

4. Run on 10% polyacrylamide gel.

Cell membrane preparation and western blotting.

Materials:

Buffer for plasma membrane preparations: TRIS-Cl 10mM, EDTA 1 mM, 75 mM NaCl, 2% w/v sucrose. Add protease inhibitors immediately before use.

10-40% sucrose gradient prepared in Centrifuge tubes (Beckman, 344059), 40% on the bottom, 10% on the top

TBS Buffer: Tris pH 7.5 20mM, NaCl 0.9%

TBST Buffer: TBS + 0.05%Tween-20

Activation buffer: MES 1M, NaCl 0.5M

Just before use add 36 mg of dry EDC (Pierce 22980) and 46 mg of dry NHS (Pierce 24500) to 100 mL of activation buffer.

Quenching buffer: 20mM TRIS-Cl pH=8, 0.2 M glycine

Procedure (Riley et al., 2003; Sennoune et al., 2004):

1. Plate BREC in 6 well plates at 250K/well (sparse plating) or 500K/well (dense plating).
2. Wash cells 3x with PBS.
3. Scrape cells into buffer containing 10 mM TRIS-HCl, 1mM EDTA, 75 mM NaCl, pH 7.4, with protease inhibitors containing 2% w/v sucrose. Use 250 uL buffer/well.
4. Spin at 2000 x g for 4 min at 4C to remove nuclei. Apply the supernatant on top of 20-40% w/v sucrose gradient. Spin 200.000 g for 1h at 4C.

5. Collect the membranes from the interphase 20-40 w/v sucrose, dilute in buffer. Spin at 100.000 g for 30 min and store at -80C.
6. Run the fractions on 10% SDS-PAGE. Run simultaneously three gels with equal amount of loaded protein.
7. Transfer overnight to nitrocellulose membrane.
8. Directly after transfer wash the blot 2x15 min with TBS.
9. Block the membrane with 1.5% BSA/5% normal rat serum in TBS for 2h at RT.
10. Wash 3x10 min with TBS/1.5% BSA.
11. Incubate with 0.5% casein in TBS 30 min at RT.
12. Wash 3x10 min with TBS/1.5% BSA.
13. Treat with biotinylated comb1 100 nM or 100 nM biotin in TBS/1.5% BSA 1h at RT.
14. Wash with TBST (TBS + 0.05% Tween) 2h at RT with 2 changes.
15. Crosslink with EDC 2mM/4mM NHS in activation buffer 20 min at RT.
16. Quench with TRIS-Cl pH 8/0.2Mglycine 10 min at RT.
17. Wash with TBST 2x.
18. Incubate with anti-biotin IgG 1:500 ON at 4C.
19. Next day, wash 2x 10 min with TBST.
20. Incubate with 2' ab (anti-goat HRP conjugated 1:25.000)
21. Wash 2x10 min with TBST, followed by 1 wash (5 min) with TBS.
22. Visualize using electrogenerated chemiluminescence.

Identification of changes in cellular proteome induced by comb1.

1. Plate CEC on growth factor reduced Matrigel as described in 2D in vitro angiogenesis protocol. Conditions: Matrigel plus 100 nM comb1, control DMEM 1% BCS, no peptides.
2. At 7h post-plating collect the cells 2X sample buffer.
3. Run on 10% polyacrylamide gel.
4. Stain the gels with Coomassie blue dye for protein detection.
5. Cut out the bands present in the lysates prepared from CECs treated with peptides but not in control lysates, wash 2 times in 50% acetonitrile and submitted to TUCF for protein identification.

Results.

In order to investigate whether biotinylation of the peptide affects its biological activity we used CEC plated on growth factor reduced Matrigel in the presence or absence of the b-comb1 or its unmodified counterpart as described (Demidova-Rice, Geevarghese, and Herman 2011). Results demonstrate that addition of a biotin molecule to the N-terminus of comb1 does not reduce its proangiogenic potential as CEC plated in the presence of either comb1 or b-comb1 form longer tubular structures compared to control cells (Appendix Figure 1).

Next we sought to determine whether the peptide get internalized by the CEC. To this end we exposed CEC to b-comb1, which then was detected using HRP-avidin, and anti-HRP antibodies as described in Materials and Methods. As demonstrated in Appendix Figure 2 HRP-avidin incubated with CEC alone

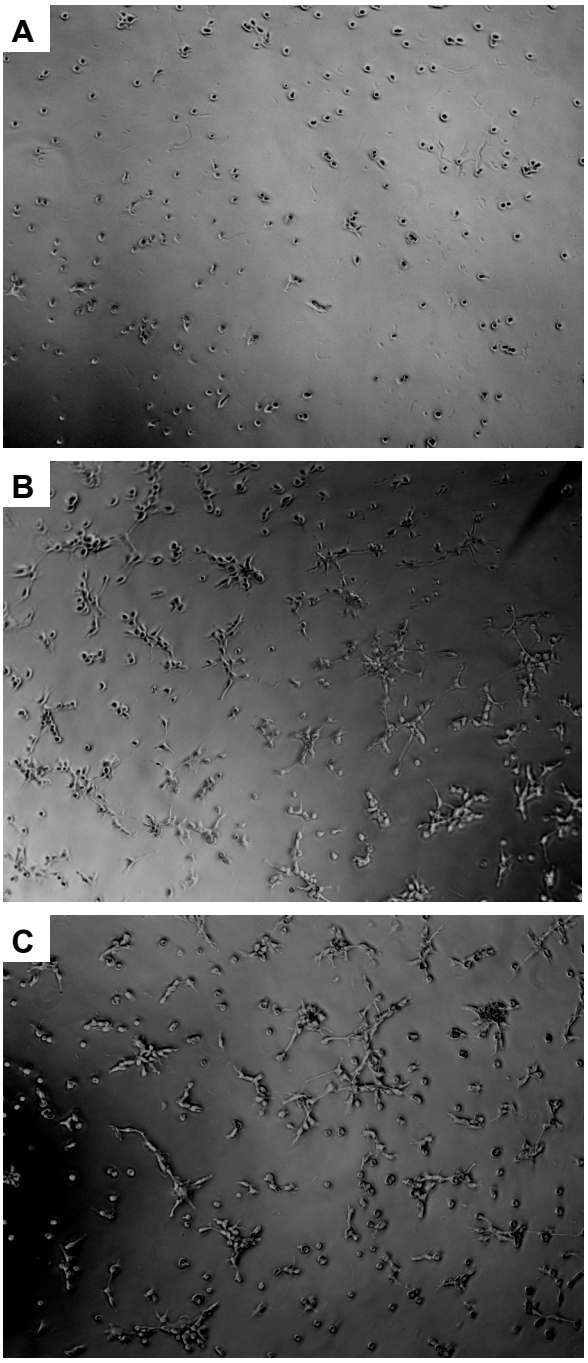

Appendix Figure 1. Biotinylated comb1 stimulates tube formation by CEC plated on GFR-Matrigel.

A – control CEC, B – CEC treated with comb1, C – CEC treated with b-comb1.

(Appendix Figure 2 A) or in the presence of or unlabeled comb1 (Appendix Figure 2 B) remains in the culture media. In contrast, HRP-avidin incubated with b-comb1 and then added to the CEC can be detected inside the cells (Appendix Figure 2 C). This observation indicates that b-comb1 gets internalized by the endothelial cells and suggests the presence of cellular receptors mediating this process as well as the pro-angiogenic effects of the peptide.

In order to identify potential receptors we prepared the cell lysates from CEC plated either on Matrigel or plastic in the presence or absence of b-comb1. The lysates then were subjected to either immunoprecipitation or western blot analysis as described in Materials and Methods. Results of these experiments reveal significant non-specific binding of the antibodies to cellular components, likely due to the presence of endogenous biotin and biotinylated proteins (data not shown). This non-specific binding can be avoided by using fluorescently-labeled comb1.

Next we wanted to identify changes in cellular proteome occurring in response to comb1 treatment. Therefore we prepared cell lysates from CEC grown on Matrigel in the presence or absence of comb1. The proteins were run on SDS-PAGE gel, which then was stained with Coomassie dye. Comparison of the proteins present in lysates from control and comb1-treated cells reveal a high molecular weight band present in the cells treated with the peptide but not in control cells (Appendix Figure 3). Identification of the protein using mass spectrometry reveals that this protein is laminin gamma 1 chain. Similarly, our in vivo data demonstrate that comb1 induces an increase is ECM deposition.

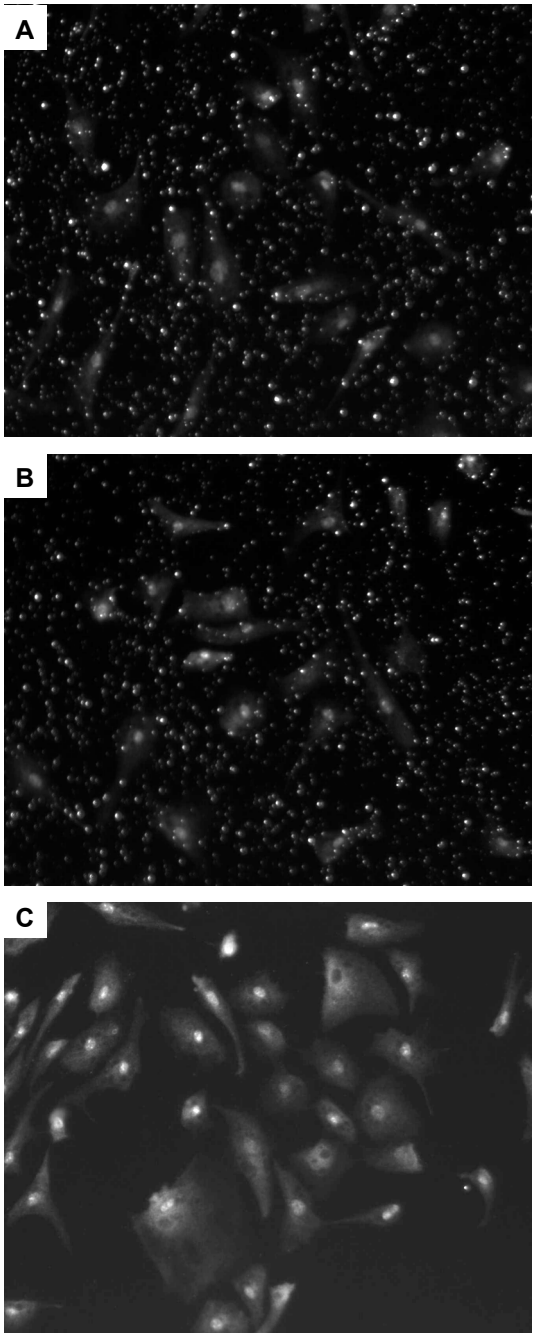

Appendix Figure 2. ECM-derived peptides get internalized by CEC cultured in vitro.

CEC were plated, allowed to attach and incubated with DMEM+1% BCS (A), in the presence of comb1 (B) or in the presence of per-bound HRP-avidin/biotinylated-comb1 (C) for 30 min at room temperature. Cells then were fixed and stained with anti-HRP antibody.

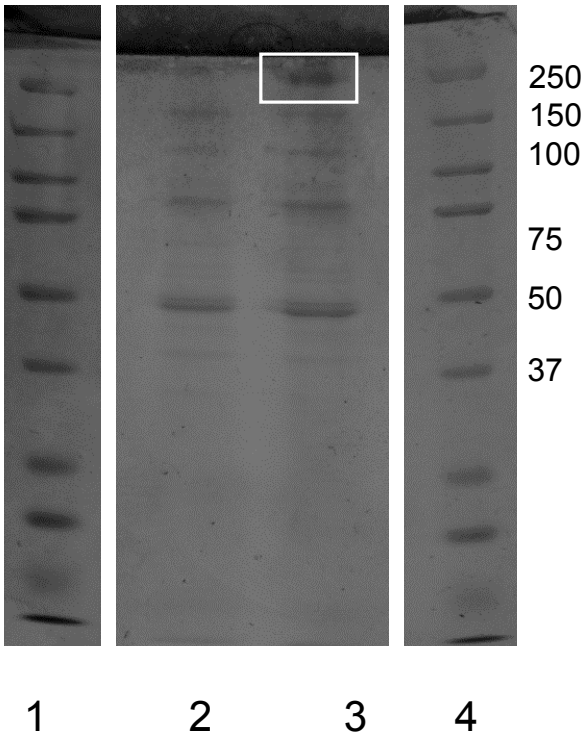

Appendix Figure 3. Changes in cellular proteome induced by comb1 peptide.

Cells were cultured on growth factor reduced Matrigel in the presence or absence of comb1 and cell lysates were collected as described in Materials and Methods. Lanes and 4 – molecular weight markers, 2 – control lysates, 3 – lysates prepared from CEC treated with comb1. While box indicates a high molecular weight band selectively present in treated cells.

Conclusions.

1. Modification of the combinatorial peptide with N-terminal biotin does not decrease pro-angiogenic potential of the peptide.
2. B-comb1 gets internalized into CEC suggesting the presence of cellular receptors mediating the peptide uptake.

3. CEC contain significant amount of endogenous biotin, which did not disallowed identification of comb1 binding partners using b-comb1. In order to avoid the effects of endogenous biotin fluorescently-labeled peptides should be used for future experiments.
4. Comb1 increases production of laminin gamma 1 chain by the CEC in vitro. This observation is in agreement with our in vivo data showing an increase in epithelial basement membrane deposition. Future work will determine molecular mechanisms by which the peptide induces changes in ECM deposition.

References.

Adamskaya, N., Dungel, P., Mittermayr, R., Hartinger, J., Feichtinger, G., Wassermann, K., Redl, H. and van Griensven, M. (2010). Light therapy by blue LED improves wound healing in an excision model in rats. *Injury* **41,** 1038-1042.

Agren, M. S., Steenfos, H. H., Dabelsteen, S., Hansen, J. B. and Dabelsteen, E. (1999). Proliferation and mitogenic response to PDGF-BB of fibroblasts isolated from chronic venous leg ulcers is ulcer-age dependent. *J. Invest. Dermatol.* **112,** 463-469.

Akasaka, Y., Ono, I., Yamashita, T., Jimbow, K. and Ishii, T. (2004). Basic fibroblast growth factor promotes apoptosis and suppresses granulation tissue formation in acute incisional wounds. *J. Pathol.* **203,** 710-720.

Akutsu, N., Amano, S. and Nishiyama, T. (2005). Quantitative analysis of laminin 5 gene expression in human keratinocytes. *Exp. Dermatol.* **14,** 329-335.

Alvarez, R. H., Kantarjian, H. M. and Cortes, J. E. (2006). Biology of platelet-derived growth factor and its involvement in disease. *Mayo Clin. Proc.* **81,** 1241-1257.

Andrae, J., Gallini, R. and Betsholtz, C. (2008). Role of platelet-derived growth factors in physiology and medicine. *Genes Dev.* **22,** 1276-1312.

Arany, P. R., Nayak, R. S., Hallikerimath, S., Limaye, A. M., Kale, A. D. and Kondaiah, P. (2007). Activation of latent TGF-beta1 by low-power laser in vitro correlates with increased TGF-beta1 levels in laser-enhanced oral wound healing. *Wound Repair Regen.* **15,** 866-874.

Asahara, T., Murohara, T., Sullivan, A., Silver, M., van der Zee, R., Li, T., Witzenbichler, B., Schatteman, G. and Isner, J. M. (1997). Isolation of putative progenitor endothelial cells for angiogenesis. *Science* **275,** 964-967.

Attinger, C. E., Janis, J. E., Steinberg, J., Schwartz, J., Al-Attar, A. and Couch, K. (2006). Clinical approach to wounds: Debridement and wound bed preparation including the use of dressings and wound-healing adjuvants. *Plast. Reconstr. Surg.* **117,** 72S-109S.

Attisano, L. and Wrana, J. L. (2002). Signal transduction by the TGF-beta superfamily. *Science* **296,** 1646-1647.

auf demKeller, U., Krampert, M., Kumin, A., Braun, S. and Werner, S. (2004). Keratinocyte growth factor: Effects on keratinocytes and mechanisms of action. *Eur. J. Cell Biol.* **83,** 607-612.

Avraamides, C. J., Garmy-Susini, B. and Varner, J. A. (2008). Integrins in angiogenesis and lymphangiogenesis. *Nat. Rev. Cancer.* **8,** 604-617.

Ayello, E. A. and Cuddigan, J. E. (2004). Debridement: Controlling the necrotic/cellular burden. *Adv. Skin Wound Care* **17,** 66-75; quiz 76-8.

Bader, M. S. (2008). Diabetic foot infection. *Am. Fam. Physician* **78,** 71-79.

Bao, P., Kodra, A., Tomic-Canic, M., Golinko, M. S., Ehrlich, H. P. and Brem, H. (2008). The role of vascular endothelial growth factor in wound healing. *J. Surg. Res.*

Bao, P., Kodra, A., Tomic-Canic, M., Golinko, M. S., Ehrlich, H. P. and Brem, H. (2009). The role of vascular endothelial growth factor in wound healing. *J. Surg. Res.* **153,** 347-358.

Barleon, B., Sozzani, S., Zhou, D., Weich, H., Mantovani, A. and Marme, D. (1996). Migration of human monocytes in response to vascular endothelial growth factor (VEGF) is mediated via the VEGF receptor flt-1. *Blood* **87,** 3336-3343.

Barrientos, S., Stojadinovic, O., Golinko, M. S., Brem, H. and Tomic-Canic, M. (2008). Growth factors and cytokines in wound healing. *Wound Repair Regen.* **16,** 585-601.

Basford, J. R., Hallman, H. O., Sheffield, C. G. and Mackey, G. L. (1986). Comparison of cold-quartz ultraviolet, low-energy laser, and occlusion in wound healing in a swine model. *Arch. Phys. Med. Rehabil.* **67,** 151-154.

Beanes, S. R., Dang, C., Soo, C. and Ting, K. (2003). Skin repair and scar formation: The central role of TGF-beta. *Expert Rev. Mol. Med.* **5,** 1-22.

Beenken, A. and Mohammadi, M. (2009). The FGF family: Biology, pathophysiology and therapy. *Nat. Rev. Drug Discov.* **8,** 235-253.

Beitz, J. G., Kim, I. S., Calabresi, P. and Frackelton, A. R.,Jr. (1991). Human microvascular endothelial cells express receptors for platelet-derived growth factor. *Proc. Natl. Acad. Sci. U. S. A.* **88,** 2021-2025.

Bellon, G., Martiny, L. and Robinet, A. (2004). Matrix metalloproteinases and matrikines in angiogenesis. *Crit. Rev. Oncol. Hematol.* **49,** 203-220.

Bennett, S. P., Griffiths, G. D., Schor, A. M., Leese, G. P. and Schor, S. L. (2003). Growth factors in the treatment of diabetic foot ulcers. *Br. J. Surg.* **90,** 133-146.

Bennett, K. L., Kussmann, M., Bjork, P., Godzwon, M., Mikkelsen, M., Sorensen, P. and Roepstorff, P. (2000). Chemical cross-linking with thiol-cleavable reagents combined with differential mass spectrometric peptide mapping--a novel approach to assess intermolecular protein contacts. *Protein Sci.* **9,** 1503-1518.

Ben-Porath, I. and Weinberg, R. A. (2005). The signals and pathways activating cellular senescence. *The International Journal of Biochemistry & Cell Biology* **37,** 961-976.

Bergers, G., Brekken, R., McMahon, G., Vu, T. H., Itoh, T., Tamaki, K., Tanzawa, K., Thorpe, P., Itohara, S., Werb, Z. et al. (2000). Matrix metalloproteinase-9 triggers the angiogenic switch during carcinogenesis. *Nat. Cell Biol.* **2,** 737-744.

Bitsch, M., Saunte, D. M., Lohmann, M., Holstein, P. E., Jorgensen, B. and Gottrup, F. (2005). Standardised method of surgical treatment of chronic leg ulcers. *Scand. J. Plast. Reconstr. Surg. Hand Surg.* **39,** 162-169.

Bonham, P. A. (2003). Assessment and management of patients with venous, arterial, and diabetic/neuropathic lower extremity wounds. *AACN Clin. Issues* **14,** 442-56; quiz 548-50.

Booms, P., Ney, A., Barthel, F., Moroy, G., Counsell, D., Gille, C., Guo, G., Pregla, R., Mundlos, S., Alix, A. J. et al. (2006). A fibrillin-1-fragment containing the elastin-binding-protein GxxPG consensus sequence upregulates matrix metalloproteinase-1: Biochemical and computational analysis. *J. Mol. Cell. Cardiol.* **40,** 234-246.

Bornstein, P. (1967). Comparative sequence studies of rat skin and tendon collagen. I. evidence for incomplete hydroxylation of individual prolyl residues in the normal proteins. *Biochemistry* **6,** 3082-3093.

Brassart, B., Fuchs, P., Huet, E., Alix, A. J., Wallach, J., Tamburro, A. M., Delacoux, F., Haye, B., Emonard, H., Hornebeck, W. et al. (2001). Conformational dependence of collagenase (matrix metalloproteinase-1) up-regulation by elastin peptides in cultured fibroblasts. *J. Biol. Chem.* **276,** 5222-5227.

Braun, S., auf dem Keller, U., Steiling, H. and Werner, S. (2004). Fibroblast growth factors in epithelial repair and cytoprotection. *Philos. Trans. R. Soc. Lond. B. Biol. Sci.* **359,** 753-757.

Brosseau, L., Welch, V., Wells, G., Tugwell, P., de Bie, R., Gam, A., Harman, K., Shea, B. and Morin, M. (2000). Low level laser therapy for osteoarthritis and rheumatoid arthritis: A metaanalysis. *J. Rheumatol.* **27,** 1961-1969.

Burch, G. H., Gong, Y., Liu, W., Dettman, R. W., Curry, C. J., Smith, L., Miller, W. L. and Bristow, J. (1997). Tenascin-X deficiency is associated with ehlers-danlos syndrome. *Nat. Genet.* **17,** 104-108.

Burkatovskaya, M., Castano, A. P., Demidova-Rice, T. N., Tegos, G. P. and Hamblin, M. R. (2008). Effect of chitosan acetate bandage on wound healing in infected and noninfected wounds in mice. *Wound Repair Regen.* **16,** 425-431.

Byrnes, K. R., Barna, L., Chenault, V. M., Waynant, R. W., Ilev, I. K., Longo, L., Miracco, C., Johnson, B. and Anders, J. J. (2004). Photobiomodulation

improves cutaneous wound healing in an animal model of type II diabetes. *Photomed. Laser Surg.* **22,** 281-290.

Chen, C. H., Hung, H. S. and Hsu, S. H. (2008). Low-energy laser irradiation increases endothelial cell proliferation, migration, and eNOS gene expression possibly via PI3K signal pathway. *Lasers Surg. Med.* **40,** 46-54.

Cheng, H., Liao, K. K., Liao, S. F., Chuang, T. Y. and Shih, Y. H. (2004). Spinal cord repair with acidic fibroblast growth factor as a treatment for a patient with chronic paraplegia. *Spine* **29,** E284-8.

Chiang, B., Essick, E., Ehringer, W., Murphree, S., Hauck, M. A., Li, M. and Chien, S. (2007). Enhancing skin wound healing by direct delivery of intracellular adenosine triphosphate. *Am. J. Surg.* **193,** 213-218.

Chow, R. T. and Barnsley, L. (2005). Systematic review of the literature of low-level laser therapy (LLLT) in the management of neck pain. *Lasers Surg. Med.* **37,** 46-52.

Chung, T. Y., Peplow, P. V. and Baxter, G. D. (2010). Laser photobiomodulation of wound healing in diabetic and non-diabetic mice: Effects in splinted and unsplinted wounds. *Photomed. Laser Surg.* **28,** 251-261.

Cirioni, O., Ghiselli, R., Minardi, D., Orlando, F., Mocchegiani, F., Silvestri, C., Muzzonigro, G., Saba, V., Scalise, G., Balaban, N. et al. (2007). RNAIII-inhibiting peptide affects biofilm formation in a rat model of staphylococcal ureteral stent infection. *Antimicrob. Agents Chemother.* **51,** 4518-4520.

Clark F. Schierle, , Mauricio De la Garza, , Thomas A. Mustoe, and Robert D. Galiano, . (2009). Staphylococcal biofilms impair wound healing by delaying

reepithelialization in a murine cutaneous wound model. *Wound Repair and Regeneration* **17,** 354-359.

Cohen, M. A. and Eaglstein, W. H. (2001). Recombinant human platelet-derived growth factor gel speeds healing of acute full-thickness punch biopsy wounds. *J. Am. Acad. Dermatol.* **45,** 857-862.

Cooper, D. M., Yu, E. Z., Hennessey, P., Ko, F. and Robson, M. C. (1994). Determination of endogenous cytokines in chronic wounds. *Ann. Surg.* **219,** 688-91; discussion 691-2.

Corazza, A. V., Jorge, J., Kurachi, C. and Bagnato, V. S. (2007). Photobiomodulation on the angiogenesis of skin wounds in rats using different light sources. *Photomed. Laser Surg.* **25,** 102-106.

Cowin, A. J., Hatzirodos, N., Holding, C. A., Dunaiski, V., Harries, R. H., Rayner, T. E., Fitridge, R., Cooter, R. D., Schultz, G. S. and Belford, D. A. (2001). Effect of healing on the expression of transforming growth factor beta(s) and their receptors in chronic venous leg ulcers. *J. Invest. Dermatol.* **117,** 1282-1289.

Cross, M. J. and Claesson-Welsh, L. (2001). FGF and VEGF function in angiogenesis: Signalling pathways, biological responses and therapeutic inhibition. *Trends Pharmacol. Sci.* **22,** 201-207.

Cury, V., Bossini, P. S., Fangel, R., Crusca Jde, S., Renno, A. C. and Parizotto, N. A. (2009). The effects of 660 nm and 780 nm laser irradiation on viability of random skin flap in rats. *Photomed. Laser Surg.* **27,** 721-724.

da Silva, J. P., da Silva, M. A., Almeida, A. P., Lombardi Junior, I. and Matos, A. P. (2010). Laser therapy in the tissue repair process: A literature review. *Photomed. Laser Surg.* **28,** 17-21.

Dalton, S. J., Whiting, C. V., Bailey, J. R., Mitchell, D. C. and Tarlton, J. F. (2007). Mechanisms of chronic skin ulceration linking lactate, transforming growth factor-beta, vascular endothelial growth factor, collagen remodeling, collagen stability, and defective angiogenesis. *J. Invest. Dermatol.* **127,** 958-968.

de Araujo, C. E., Ribeiro, M. S., Favaro, R., Zezell, D. M. and Zorn, T. M. (2007). Ultrastructural and autoradiographical analysis show a faster skin repair in he-ne laser-treated wounds. *J. Photochem. Photobiol. B.* **86,** 87-96.

Death, A. K., Fisher, E. J., McGrath, K. C. and Yue, D. K. (2003). High glucose alters matrix metalloproteinase expression in two key vascular cells: Potential impact on atherosclerosis in diabetes. *Atherosclerosis* **168,** 263-269.

Defloor, T. (1999). The risk of pressure sores: A conceptual scheme. *J. Clin. Nurs.* **8,** 206-216.

Demidova-Rice, T. N., Geevarghese, A. and Herman, I. M. (2011). Bioactive peptides derived from vascular endothelial cell extracellular matrices promote microvascular morphogenesis and wound healing in vitro. *Wound Repair Rege*n. **19,** 59-70.

Demidova-Rice, T. N. and Herman, I. M. (2009). Identification and characterization of novel wound-healing peptides derived from extracellular matrices. *Wound Repair and Regeneration. Abstracts of 19th Annual Meeting of the Wound Healing Society SAWC/WHS Joint Meeting* **17,** A22.

Demidova-Rice, T. N., Salomatina, E. V., Yaroslavsky, A. N., Herman, I. M. and Hamblin, M. R. (2007). Low-level light stimulates excisional wound healing in mice. *Lasers Surg. Med.* **39,** 706-715.

Desmouliere, A., Redard, M., Darby, I. and Gabbiani, G. (1995). Apoptosis mediates the decrease in cellularity during the transition between granulation tissue and scar. *Am. J. Pathol.* **146,** 56-66.

Di Poto, A., Sbarra, M. S., Provenza, G., Visai, L. and Speziale, P. (2009). The effect of photodynamic treatment combined with antibiotic action or host defence mechanisms on staphylococcus aureus biofilms. *Biomaterials* **30,** 3158-3166.

Duraisamy, Y., Slevin, M., Smith, N., Bailey, J., Zweit, J., Smith, C., Ahmed, N. and Gaffney, J. (2001). Effect of glycation on basic fibroblast growth factor induced angiogenesis and activation of associated signal transduction pathways in vascular endothelial cells: Possible relevance to wound healing in diabetes. *Angiogenesis* **4,** 277-288.

Durham, J. T. and Herman, I. M. (2009). Inhibition of angiogenesis in vitro: A central role for beta-actin dependent cytoskeletal remodeling. *Microvasc. Res.* **77,** 281-288.

Edwards, R. and Harding, K. G. (2004). Bacteria and wound healing. *Curr. Opin. Infect. Dis.* **17,** 91-96.

Egging, D., van Vlijmen-Willems, I., van Tongeren, T., Schalkwijk, J. and Peeters, A. (2007). Wound healing in tenascin-X deficient mice suggests that tenascin-X is involved in matrix maturation rather than matrix deposition. *Connect. Tissue Res.* **48,** 93-98.

Ehrlich, H. P., Keefer, K. A., Myers, R. L. and Passaniti, A. (1999). Vanadate and the absence of myofibroblasts in wound contraction. *Arch. Surg.* **134,** 494-501.

Eming, S. A., Krieg, T. and Davidson, J. M. (2007). Inflammation in wound repair: Molecular and cellular mechanisms. *J. Invest. Dermatol.* **127,** 514-525.

Eming, S. A., Lauer, G., Cole, M., Jurk, S., Christ, H., Hornig, C., Krieg, T. and Weich, H. A. (2004). Increased levels of the soluble variant of the vascular endothelial growth factor receptor VEGFR-1 are associated with a poor prognosis in wound healing. *J. Invest. Dermatol.* **123,** 799-802.

Erdle, B. J., Brouxhon, S., Kaplan, M., Vanbuskirk, J. and Pentland, A. P. (2008). Effects of continuous-wave (670-nm) red light on wound healing. *Dermatol. Surg.* **34,** 320-325.

Falanga, V. (2002). Wound bed preparation and the role of enzymes: A case for multiple actions of the therapeutic agents. *Wounds*, 47-57.

Falanga, V. (2005). Wound healing and its impairment in the diabetic foot. *Lancet* **366,** 1736-1743.

Ferrara, N., Gerber, H. P. and LeCouter, J. (2003). The biology of VEGF and its receptors. *Nat. Med.* **9,** 669-676.

Fields, C. G., Lloyd, D. H., Macdonald, R. L., Otteson, K. M. and Noble, R. L. (1991). HBTU activation for automated fmoc solid-phase peptide synthesis. *Pept. Res.* **4,** 95-101.

Flemming, K. A., Cullum, N. A. and Nelson, E. A. (1999). A systematic review of laser therapy for venous leg ulcers. *J. Wound Care* **8,** 111-114.

Folkman, J. and Klagsbrun, M. (1987). Angiogenic factors. *Science* **235,** 442-447.

Foti, C., Conserva, A., Casulli, C., Scrimieri, V., Pepe, M. L. and Quaranta, D. (2007). Contact dermatitis with clostridiopeptidase A contained in noruxol ointment. *Contact Dermatitis* **56,** 361-362.

Fouser, L., Iruela-Arispe, L., Bornstein, P. and Sage, E. H. (1991). Transcriptional activity of the alpha 1(I)-collagen promoter is correlated with the formation of capillary-like structures by endothelial cells in vitro. *J. Biol. Chem.* **266,** 18345-18351.

Fox, A., Smythe, J., Fisher, N., Tyler, M. P., McGrouther, D. A., Watt, S. M. and Harris, A. L. (2008). Mobilization of endothelial progenitor cells into the circulation in burned patients. *Br. J. Surg.* **95,** 244-251.

Franek, A., Krol, P. and Kucharzewski, M. (2002). Does low output laser stimulation enhance the healing of crural ulceration? some critical remarks. *Med. Eng. Phys.* **24,** 607-615.

Galiano, R. D., Tepper, O. M., Pelo, C. R., Bhatt, K. A., Callaghan, M., Bastidas, N., Bunting, S., Steinmetz, H. G. and Gurtner, G. C. (2004). Topical vascular endothelial growth factor accelerates diabetic wound healing through increased angiogenesis and by mobilizing and recruiting bone marrow-derived cells. *Am. J. Pathol.* **164,** 1935-1947.

Gallagher, K. A., Liu, Z. J., Xiao, M., Chen, H., Goldstein, L. J., Buerk, D. G., Nedeau, A., Thom, S. R. and Velazquez, O. C. (2007). Diabetic impairments in

NO-mediated endothelial progenitor cell mobilization and homing are reversed by hyperoxia and SDF-1 alpha. *J. Clin. Invest.* **117,** 1249-1259.

Gao, X. and Xing, D. (2009). Molecular mechanisms of cell proliferation induced by low power laser irradiation. *J. Biomed. Sci.* **16,** 4.

Gao, Z., Sasaoka, T., Fujimori, T., Oya, T., Ishii, Y., Sabit, H., Kawaguchi, M., Kurotaki, Y., Naito, M., Wada, T. et al. (2005). Deletion of the PDGFR-{beta} gene affects key fibroblast functions important for wound healing. *J. Biol. Chem.* **280,** 9375-9389.

Gilroy, D. W., Lawrence, T., Perretti, M. and Rossi, A. G. (2004). Inflammatory resolution: New opportunities for drug discovery. *Nat. Rev. Drug Discov.* **3,** 401-416.

Gitlin, J. D. and D'Amore, P. A. (1983). Culture of retinal capillary cells using selective growth media. *Microvasc. Res.* **26,** 74-80.

Gope, M. L. and Gope, R. (2009). Tyrosine phosphorylation of EGF-R and PDGF-R proteins during acute cutaneous wound healing process in mice. *Wound Repair Regen.* **17,** 71-79.

Gosain, A. and DiPietro, L. A. (2004). Aging and wound healing. *World J. Surg.* **28,** 321-326.

Grey, J. E., Harding, K. G. and Enoch, S. (2006). Venous and arterial leg ulcers. *BMJ* **332,** 347-350.

Grosskreutz, C. L., Anand-Apte, B., Duplaa, C., Quinn, T. P., Terman, B. I., Zetter, B. and D'Amore, P. A. (1999). Vascular endothelial growth factor-

induced migration of vascular smooth muscle cells in vitro. *Microvasc. Res.* **58,** 128-136.

Grossman, N., Schneid, N., Reuveni, H., Halevy, S. and Lubart, R. (1998). 780 nm low power diode laser irradiation stimulates proliferation of keratinocyte cultures: Involvement of reactive oxygen species. *Lasers Surg. Med.* **22,** 212-218.

Guffey, J. S. and Wilborn, J. (2006). In vitro bactericidal effects of 405-nm and 470-nm blue light. *Photomed. Laser Surg.* **24,** 684-688.

Hamblin, M. R. and Demidova, T. N. (2006). **Mechanisms of low level light therapy – an introduction.**.

Hanft, J. R., Pollak, R. A., Barbul, A., van Gils, C., Kwon, P. S., Gray, S. M., Lynch, C. J., Semba, C. P. and Breen, T. J. (2008). Phase I trial on the safety of topical rhVEGF on chronic neuropathic diabetic foot ulcers. *J. Wound Care* **17,** 30-2, 34-7.

Harding, K. G., Morris, H. L. and Patel, G. K. (2002). Science, medicine and the future: Healing chronic wounds. *BMJ* **324,** 160-163.

Hawkins, D. and Abrahamse, H. (2006). Effect of multiple exposures of low-level laser therapy on the cellular responses of wounded human skin fibroblasts. *Photomed. Laser Surg.* **24,** 705-714.

Healy, A. M. and Herman, I. M. (1992). Density-dependent accumulation of basic fibroblast growth factor in the subendothelial matrix. *Eur. J. Cell Biol.* **59,** 56-67.

Healy, A. M. and Herman, I. M. (1992). Preparation of fluorescent basic fibroblast growth factor: Localization in living retinal microvascular endothelial cells. *Exp. Eye Res.* **55,** 663-669.

Helmbold, P., Nayak, R. C., Marsch, W. C. and Herman, I. M. (2001). Isolation and in vitro characterization of human dermal microvascular pericytes. *Microvasc. Res.* **61,** 160-165.

Herman, I. M. (1996). Stimulation of human keratinocyte migration and proliferation in vitro: Insights into the cellular responses to injury and wound healing. *Wounds*, 33-42.

Herman, I. M. (1993a). Molecular mechanisms regulating the vascular endothelial cell motile response to injury. *J. Cardiovasc. Pharmacol.* **22 Suppl 4,** S25-36.

Herman, I. M. (1993b). Molecular mechanisms regulating the vascular endothelial cell motile response to injury. *J. Cardiovasc. Pharmacol.* **22 Suppl 4,** S25-36.

Herman, I. M. and Castellot, J. J.,Jr. (1987). Regulation of vascular smooth muscle cell growth by endothelial-synthesized extracellular matrices. *Arteriosclerosis* **7,** 463-469.

Herman, I. M. and Leung, A. (2009). Creation of human skin equivalents for the in vitro study of angiogenesis in wound healing. *Methods Mol. Biol.* **467,** 241-248.

Higley, H. R., Ksander, G. A., Gerhardt, C. O. and Falanga, V. (1995). Extravasation of macromolecules and possible trapping of transforming growth factor-beta in venous ulceration. *Br. J. Dermatol.* **132,** 79-85.

Hinchliffe, R. J., Valk, G. D., Apelqvist, J., Armstrong, D. G., Bakker, K., Game, F. L., Hartemann-Heurtier, A., Londahl, M., Price, P. E., van Houtum, W. H. et al. (2008). A systematic review of the effectiveness of interventions to enhance the healing of chronic ulcers of the foot in diabetes. *Diabetes Metab. Res. Rev.* **24 Suppl 1,** S119-44.

Hinz, B. (2007). Formation and function of the myofibroblast during tissue repair. *J. Invest. Dermatol.* **127,** 526-537.

Hirshberg, J., Coleman, J., Marchant, B. and Rees, R. S. (2001). TGF-beta3 in the treatment of pressure ulcers: A preliminary report. *Adv. Skin Wound Care* **14,** 91-95.

Houreld, N. N. and Abrahamse, H. (2007). Effectiveness of helium-neon laser irradiation on viability and cytotoxicity of diabetic-wounded fibroblast cells. *Photomed. Laser Surg.* **25,** 474-481.

Howell-Jones, R. S., Wilson, M. J., Hill, K. E., Howard, A. J., Price, P. E. and Thomas, D. W. (2005). A review of the microbiology, antibiotic usage and resistance in chronic skin wounds. *J. Antimicrob. Chemother.* **55,** 143-149.

Hu, W. P., Wang, J. J., Yu, C. L., Lan, C. C., Chen, G. S. and Yu, H. S. (2007). Helium-neon laser irradiation stimulates cell proliferation through photostimulatory effects in mitochondria. *J. Invest. Dermatol.* **127,** 2048-2057.

Huang, Y. Y., Chen, A. C., Carroll, J. D. and Hamblin, M. R. (2009). Biphasic dose response in low level light therapy. *Dose Response* **7,** 358-383.

Humar, R., Kiefer, F. N., Berns, H., Resink, T. J. and Battegay, E. J. (2002). Hypoxia enhances vascular cell proliferation and angiogenesis in vitro via rapamycin (mTOR)-dependent signaling. *FASEB J.* **16,** 771-780.

Hunter, J., Leonard, L., Wilson, R., Snider, G. and Dixon, J. (1984). Effects of low energy laser on wound healing in a porcine model. *Lasers Surg. Med.* **3,** 285-290.

Ikuta, T., Ariga, H. and Matsumoto, K. (2000). Extracellular matrix tenascin-X in combination with vascular endothelial growth factor B enhances endothelial cell proliferation. *Genes Cells* **5,** 913-927.

Imegwu, O., Chang, T. H. and Steinberg, J. J. (1997). Staphylococcus aureus peptidoglycan ameliorates cyclophosphamide-induced impairment of wound healing. *Wound Repair Regen.* **5,** 364-372.

Irvine, J., Chong, S. L., Amirjani, N. and Chan, K. M. (2004). Double-blind randomized controlled trial of low-level laser therapy in carpal tunnel syndrome. *Muscle Nerve* **30,** 182-187.

Ishitsuka, T., Ikuta, T., Ariga, H. and Matsumoto, K. (2009). Serum tenascin-X strongly binds to vascular endothelial growth factor. *Biol. Pharm. Bull.* **32,** 1004-1011.

Isner, J. M., Pieczek, A., Schainfeld, R., Blair, R., Haley, L., Asahara, T., Rosenfield, K., Razvi, S., Walsh, K. and Symes, J. F. (1996). Clinical evidence of angiogenesis after arterial gene transfer of phVEGF165 in patient with ischaemic limb. *Lancet* **348,** 370-374.

James, G. A., Swogger, E., Wolcott, R., Pulcini, E., Secor, P., Sestrich, J., Costerton, J. W. and Stewart, P. S. (2008). Biofilms in chronic wounds. *Wound Repair Regen.* **16,** 37-44.

Kamoun, A., Landeau, J. M., Godeau, G., Wallach, J., Duchesnay, A., Pellat, B. and Hornebeck, W. (1995). Growth stimulation of human skin fibroblasts by elastin-derived peptides. *Cell Adhes. Commun.* **3,** 273-281.

Karu, T. (1999). Primary and secondary mechanisms of action of visible to near-IR radiation on cells. *J. Photochem. Photobiol. B.* **49,** 1-17.

Karu, T., Pyatibrat, L. and Kalendo, G. (1995). Irradiation with he-ne laser increases ATP level in cells cultivated in vitro. *J. Photochem. Photobiol. B.* **27,** 219-223.

Karu, T. I. (1999). A suitable model for wound healing: How many times are we to stumble over the same block? *Lasers Surg. Med.* **25,** 283-284.

Karu, T. I. (2008). Mitochondrial signaling in mammalian cells activated by red and near-IR radiation. *Photochem. Photobiol.* **84,** 1091-1099.

Karu, T. I. and Kolyakov, S. F. (2005). Exact action spectra for cellular responses relevant to phototherapy. *Photomed. Laser Surg.* **23,** 355-361.

Karu, T. I., Pyatibrat, L. V. and Afanasyeva, N. I. (2005). Cellular effects of low power laser therapy can be mediated by nitric oxide. *Lasers Surg. Med.* **36,** 307-314.

Karu, T. I., Pyatibrat, L. V. and Kalendo, G. S. (2004). Photobiological modulation of cell attachment via cytochrome c oxidase. *Photochem. Photobiol. Sci.* **3,** 211-216.

Kawalec, J. S., Hetherington, V. J., Pfennigwerth, T. C., Dockery, D. S. and Dolce, M. (2004). Effect of a diode laser on wound healing by using diabetic and nondiabetic mice. *J. Foot Ankle Surg.* **43,** 214-220.

Kawata, Y., Suzuki, H., Higaki, Y., Denisenko, O., Schullery, D., Abrass, C. and Bomsztyk, K. (2002). Bcn-1 element-dependent activation of the laminin gamma 1 chain gene by the cooperative action of transcription factor E3 (TFE3) and smad proteins. *J. Biol. Chem.* **277,** 11375-11384.

Keswani, S. G., Katz, A. B., Lim, F. Y., Zoltick, P., Radu, A., Alaee, D., Herlyn, M. and Crombleholme, T. M. (2004). Adenoviral mediated gene transfer of PDGF-B enhances wound healing in type I and type II diabetic wounds. *Wound Repair Regen.* **12,** 497-504.

Kipshidze, N., Keelan, M. H., Petersen, J. R., Bachutashvili, I., Vossoughi, J., Karanian, J., Ghosh, C., Iversen, P., Roubin, G. S., Leon, M. B. et al. (2000). Photoactivation of vascular iNOS and elevation of cGMP in vivo: Possible mechanism for photovasorelaxation and inhibition of restenosis in an atherosclerotic rabbit models. *Photochem. Photobiol.* **72,** 579-582.

Kirchner, L. M., Meerbaum, S. O., Gruber, B. S., Knoll, A. K., Bulgrin, J., Taylor, R. A. and Schmidt, S. P. (2003). Effects of vascular endothelial growth factor on wound closure rates in the genetically diabetic mouse model. *Wound Repair Regen.* **11,** 127-131.

Kiritsi, O., Tsitas, K., Malliaropoulos, N. and Mikroulis, G. (2010). Ultrasonographic evaluation of plantar fasciitis after low-level laser therapy:

Results of a double-blind, randomized, placebo-controlled trial. *Lasers Med. Sci.* **25,** 275-281.

Kleinman, H. K. and Martin, G. R. (2005). Matrigel: Basement membrane matrix with biological activity. *Seminars in Cancer Biology* **15,** 378-386.

Kobrin, K. L., Thompson, P. J., van de Scheur, M., Kwak, T. H., Kim, S. and Falanga, V. (2008). Evaluation of dermal pericapillary fibrin cuffs in venous ulceration using confocal microscopy. *Wound Repair Regen.* **16,** 503-506.

Komi-Kuramochi, A., Kawano, M., Oda, Y., Asada, M., Suzuki, M., Oki, J. and Imamura, T. (2005). Expression of fibroblast growth factors and their receptors during full-thickness skin wound healing in young and aged mice. *J. Endocrinol.* **186,** 273-289.

Kopera, D., Kokol, R., Berger, C. and Haas, J. (2005). Low level laser: Does it influence wound healing in venous leg ulcers? A randomized, placebo-controlled, double-blind study. *Br. J. Dermatol.* **152,** 1368-1370.

Kotecki, M., Zeiger, A. S., Van Vliet, K. J. and Herman, I. M. (2010). Calpain- and talin-dependent control of microvascular pericyte contractility and cellular stiffness. *Microvasc. Res.*

Kreis, T. E. and Birchmeier, W. (1980). Stress fiber sarcomeres of fibroblasts are contractile. *Cell* **22,** 555-561.

Kumar, I., Staton, C. A., Cross, S. S., Reed, M. W. and Brown, N. J. (2009). Angiogenesis, vascular endothelial growth factor and its receptors in human surgical wounds. *Br. J. Surg.* **96,** 1484-1491.

Kuo, P. C., Kao, C. H. and Chen, J. K. (2007). Glycated type 1 collagen induces endothelial dysfunction in culture. *In Vitro Cell. Dev. Biol. Anim.* **43,** 338-343.

Landau, Z., David, M., Aviezer, D. and Yayon, A. (2001). Heparin-like inhibitory activity to fibroblast growth factor-2 in wound fluids of patients with chronic skin ulcers and its modulation during wound healing. *Wound Repair Regen.* **9,** 323-328.

Laskin, D. L., Kimura, T., Sakakibara, S., Riley, D. J. and Berg, R. A. (1986). Chemotactic activity of collagen-like polypeptides for human peripheral blood neutrophils. *J. Leukoc. Biol.* **39,** 255-266.

Lauer, G., Sollberg, S., Cole, M., Flamme, I., Sturzebecher, J., Mann, K., Krieg, T. and Eming, S. A. (2000). Expression and proteolysis of vascular endothelial growth factor is increased in chronic wounds. *J. Invest. Dermatol.* **115,** 12-18.

Lauer, G., Sollberg, S., Cole, M., Krieg, T. and Eming, S. A. (2002). Generation of a novel proteolysis resistant vascular endothelial growth factor165 variant by a site-directed mutation at the plasmin sensitive cleavage site. *FEBS Lett.* **531,** 309-313.

Lavi, R., Shainberg, A., Shneyvays, V., Hochauser, E., Isaac, A., Zinman, T., Friedmann, H. and Lubart, R. (2010). Detailed analysis of reactive oxygen species induced by visible light in various cell types. *Lasers Surg. Med.* **42,** 473-480.

Leahy, P. J. and Lawrence, W. T. (2007). Biologic enhancement of wound healing. *Clin. Plast. Surg.* **34,** 659-671.

Lee, S. J., Bae, S. S., Kim, K. H., Lee, W. S., Rhim, B. Y., Hong, K. W. and Kim, C. D. (2007). High glucose enhances MMP-2 production in adventitial fibroblasts via Akt1-dependent NF-kappaB pathway. *FEBS Lett.* **581,** 4189-4194.

Leiter, E. H. and Chapman, H. D. (1994). Obesity-induced diabetes (diabesity) in C57BL/KsJ mice produces aberrant trans-regulation of sex steroid sulfotransferase genes. *J. Clin. Invest.* **93,** 2007-2013.

Leone, A. M., Valgimigli, M., Giannico, M. B., Zaccone, V., Perfetti, M., D'Amario, D., Rebuzzi, A. G. and Crea, F. (2009). From bone marrow to the arterial wall: The ongoing tale of endothelial progenitor cells. *Eur. Heart J.* **30,** 890-899.

Lerman, O. Z., Galiano, R. D., Armour, M., Levine, J. P. and Gurtner, G. C. (2003). Cellular dysfunction in the diabetic fibroblast: Impairment in migration, vascular endothelial growth factor production, and response to hypoxia. *Am. J. Pathol.* **162,** 303-312.

Levenson, S. M., Kan-Gruber, D., Gruber, C., Molnar, J. and Seifter, E. (1983). Wound healing accelerated by staphylococcus aureus. *Arch. Surg.* **118,** 310-320.

Li, J., Zhang, Y. P. and Kirsner, R. S. (2003). Angiogenesis in wound repair: Angiogenic growth factors and the extracellular matrix. *Microsc. Res. Tech.* **60,** 107-114.

Li, X., Gu, W., Masinde, G., Hamilton-Ulland, M., Xu, S., Mohan, S. and Baylink, D. J. (2001a). Genetic control of the rate of wound healing in mice. *Heredity* **86,** 668-674.

Li, X., Mohan, S., Gu, W. and Baylink, D. J. (2001b). Analysis of gene expression in the wound repair/regeneration process. *Mamm. Genome* **12,** 52-59.

Liao, H., Zakhaleva, J. and Chen, W. (2009). Cells and tissue interactions with glycated collagen and their relevance to delayed diabetic wound healing. *Biomaterials* **30,** 1689-1696.

Lipsky, B. A. (2008). New developments in diagnosing and treating diabetic foot infections. *Diabetes Metab. Res. Rev.* **24 Suppl 1,** S66-71.

Liu, Z. J. and Velazquez, O. C. (2008). Hyperoxia, endothelial progenitor cell mobilization, and diabetic wound healing. *Antioxid. Redox Signal.* **10,** 1869-1882.

Lobmann, R., Zemlin, C., Motzkau, M., Reschke, K. and Lehnert, H. (2006). Expression of matrix metalloproteinases and growth factors in diabetic foot wounds treated with a protease absorbent dressing. *J. Diabetes Complications.* **20,** 329-335.

Loot, M. A., Kenter, S. B., Au, F. L., van Galen, W. J., Middelkoop, E., Bos, J. D. and Mekkes, J. R. (2002). Fibroblasts derived from chronic diabetic ulcers differ in their response to stimulation with EGF, IGF-I, bFGF and PDGF-AB compared to controls. *Eur. J. Cell Biol.* **81,** 153-160.

Loots, M. A., Lamme, E. N., Zeegelaar, J., Mekkes, J. R., Bos, J. D. and Middelkoop, E. (1998). Differences in cellular infiltrate and extracellular matrix of chronic diabetic and venous ulcers versus acute wounds. *J. Invest. Dermatol.* **111,** 850-857.

Losordo, D. W., Vale, P. R., Symes, J. F., Dunnington, C. H., Esakof, D. D., Maysky, M., Ashare, A. B., Lathi, K. and Isner, J. M. (1998). Gene therapy for myocardial angiogenesis: Initial clinical results with direct myocardial injection of phVEGF165 as sole therapy for myocardial ischemia. *Circulation* **98,** 2800-2804.

Lowe, A. S., Walker, M. D., O'Byrne, M., Baxter, G. D. and Hirst, D. G. (1998). Effect of low intensity monochromatic light therapy (890 nm) on a radiation-impaired, wound-healing model in murine skin. *Lasers Surg. Med.* **23,** 291-298.

Lubart, R., Eichler, M., Lavi, R., Friedman, H. and Shainberg, A. (2005). Low-energy laser irradiation promotes cellular redox activity. *Photomed. Laser Surg.* **23,** 3-9.

Lyons, R. F., Abergel, R. P., White, R. A., Dwyer, R. M., Castel, J. C. and Uitto, J. (1987). Biostimulation of wound healing in vivo by a helium-neon laser. *Ann. Plast. Surg.* **18,** 47-50.

Ma, B., Cheng, D. S., Xia, Z. F., Ben, D. F., Lu, W., Cao, Z. F., Wang, Q., He, J., Chai, J. K., Shen, C. A. et al. (2007a). Randomized, multicenter, double-blind, and placebo-controlled trial using topical recombinant human acidic fibroblast growth factor for deep partial-thickness burns and skin graft donor site. *Wound Repair Regen.* **15,** 795-799.

Ma, B., Cheng, D. S., Xia, Z. F., Ben, D. F., Lu, W., Cao, Z. F., Wang, Q., He, J., Chai, J. K., Shen, C. A. et al. (2007b). Randomized, multicenter, double-blind, and placebo-controlled trial using topical recombinant human acidic fibroblast growth factor for deep partial-thickness burns and skin graft donor site. *Wound Repair Regen.* **15,** 795-799.

Maeng, Y. S., Choi, H. J., Kwon, J. Y., Park, Y. W., Choi, K. S., Min, J. K., Kim, Y. H., Suh, P. G., Kang, K. S., Won, M. H. et al. (2009). Endothelial progenitor cell homing: Prominent role of the IGF2-IGF2R-PLCbeta2 axis. *Blood* **113,** 233-243.

Malinda, K. M., Nomizu, M., Chung, M., Delgado, M., Kuratomi, Y., Yamada, Y., Kleinman, H. K. and Ponce, M. L. (1999). Identification of laminin alpha1 and beta1 chain peptides active for endothelial cell adhesion, tube formation, and aortic sprouting. *FASEB J.* **13,** 53-62.

Malinda, K. M., Wysocki, A. B., Koblinski, J. E., Kleinman, H. K. and Ponce, M. L. (2008). Angiogenic laminin-derived peptides stimulate wound healing. *Int. J. Biochem. Cell Biol.* **40,** 2771-2780.

Mandl, I. (1982). Bacterial collagenases and their clinical applications. *Arzneimittelforschung* **32,** 1381-1384.

Martin, J. M., Zenilman, J. M. and Lazarus, G. S. (2009). Molecular microbiology: New dimensions for cutaneous biology and wound healing. *J. Invest. Dermatol.*

Masinde, G. L., Li, R., Nguyen, B., Yu, H., Srivastava, A. K., Edderkaoui, B., Wergedal, J. E., Baylink, D. J. and Mohan, S. (2006). New quantitative trait loci that regulate wound healing in an intercross progeny from DBA/1J and 129 x 1/SvJ inbred strains of mice. *Funct. Integr. Genomics* **6,** 157-163.

Mast, B. A. and Schultz, G. S. (1996). Interactions of cytokines, growth factors, and proteases in acute and chronic wounds. *Wound Repair Regen.* **4,** 411-420.

McDowall, M., Edwards, N. M., Jahoda, C. A. and Hynd, P. I. (2008). The role of activins and follistatins in skin and hair follicle development and function. *Cytokine Growth Factor Rev.* **19,** 415-426.

McLean, C. A., Cleland, H., Moncrieff, N. J., Barton, R. J., de Kretser, D. M. and Phillips, D. J. (2008). Temporal expression of activin in acute burn wounds--from inflammatory cells to fibroblasts. *Burns* **34,** 50-55.

Medrado, A. R., Pugliese, L. S., Reis, S. R. and Andrade, Z. A. (2003). Influence of low level laser therapy on wound healing and its biological action upon myofibroblasts. *Lasers Surg. Med.* **32,** 239-244.

Mekkes, J. R., Zeegelaar, J. E. and Westerhof, W. (1998). Quantitative and objective evaluation of wound debriding properties of collagenase and fibrinolysin/desoxyribonuclease in a necrotic ulcer animal model. *Arch. Dermatol. Res.* **290,** 152-157.

Mester, E., Ludany, G., Sellyei, M., Szende, B., Gyenes, G. and Tota, G. J. (1968). Studies on the inhibiting and activating effects of laser beams. *Langenbecks Arch. Chir.* **322,** 1022-1027.

Metzmacher, I., Ruth, P., Abel, M. and Friess, W. (2007). In vitro binding of matrix metalloproteinase-2 (MMP-2), MMP-9, and bacterial collagenase on collagenous wound dressings. *Wound Repair Regen.* **15,** 549-555.

Min, S. K., Lee, S. C., Hong, S. D., Chung, C. P., Park, W. H. and Min, B. M. (2010). The effect of a laminin-5-derived peptide coated onto chitin microfibers on re-epithelialization in early-stage wound healing. *Biomaterials* **31,** 4725-4730.

Minatel, D. G., Frade, M. A., Franca, S. C. and Enwemeka, C. S. (2009a). Phototherapy promotes healing of chronic diabetic leg ulcers that failed to respond to other therapies. *Lasers Surg. Med.* **41,** 433-441.

Minatel, D. G., Frade, M. A., Franca, S. C. and Enwemeka, C. S. (2009b). Phototherapy promotes healing of chronic diabetic leg ulcers that failed to respond to other therapies. *Lasers Surg. Med.* **41,** 433-441.

Mineur, P., Colige, A. C., Deroanne, C. F., Dubail, J., Kesteloot, F., Habraken, Y., Noel, A., Voo, S., Waltenberger, J., Lapiere, C. M. et al. (2007). Newly identified biologically active and proteolysis-resistant VEGF-A isoform VEGF111 is induced by genotoxic agents. *J. Cell Biol.* **179,** 1261-1273.

Moriyama, Y., Nguyen, J., Akens, M., Moriyama, E. H. and Lilge, L. (2009). In vivo effects of low level laser therapy on inducible nitric oxide synthase. *Lasers Surg. Med.* **41,** 227-231.

Moustakas, A. and Heldin, C. H. (2008). Dynamic control of TGF-beta signaling and its links to the cytoskeleton. *FEBS Lett.* **582,** 2051-2065.

Mudge, B. P., Harris, C., Gilmont, R. R., Adamson, B. S. and Rees, R. S. (2002). Role of glutathione redox dysfunction in diabetic wounds. *Wound Repair Regen.* **10,** 52-58.

Mukhopadhyay, A., Chan, S. Y., Lim, I. J., Phillips, D. J. and Phan, T. T. (2007). The role of the activin system in keloid pathogenesis. *Am. J. Physiol. Cell. Physiol.* **292,** C1331-8.

Muller, M., Essin, K., Hill, K., Beschmann, H., Rubant, S., Schempp, C. M., Gollasch, M., Boehncke, W. H., Harteneck, C., Muller, W. E. et al. (2008).

Specific TRPC6 channel activation, a novel approach to stimulate keratinocyte differentiation. *J. Biol. Chem.* **283,** 33942-33954.

Mundel, T. M. and Kalluri, R. (2007). Type IV collagen-derived angiogenesis inhibitors. *Microvasc. Res.* **74,** 85-89.

Murray, J. C. (2001). *Angiogenesis Protocols*, pp. 267. Totowa, N.J.: Humana Press.

Naeser, M. A., Hahn, K. A., Lieberman, B. E. and Branco, K. F. (2002). Carpal tunnel syndrome pain treated with low-level laser and microamperes transcutaneous electric nerve stimulation: A controlled study. *Arch. Phys. Med. Rehabil.* **83,** 978-988.

Narayan, K. M. V., Boyle, J. P., Thompson, T. J., Sorensen, S. W. and Williamson, D. F. (2003). Lifetime risk for diabetes mellitus in the united states. *JAMA* **290,** 1884-1890.

Narita, K., Fujii, T., Ishiwata, T., Yamamoto, T., Kawamoto, Y., Kawahara, K., Nakazawa, N. and Naito, Z. (2009). Keratinocyte growth factor induces vascular endothelial growth factor-A expression in colorectal cancer cells. *Int. J. Oncol.* **34,** 355-360.

Niemz, M. H. (2004). *Laser-Tissue Interactions : Fundamentals and Applications*, pp. 305. Berlin ; New York: Springer.

Niu, J., Chang, Z., Peng, B., Xia, Q., Lu, W., Huang, P., Tsao, M. S. and Chiao, P. J. (2007). Keratinocyte growth factor/fibroblast growth factor-7-regulated cell migration and invasion through activation of NF-kappaB transcription factors. *J. Biol. Chem.* **282,** 6001-6011.

Nomizu, M., Kim, W. H., Yamamura, K., Utani, A., Song, S. Y., Otaka, A., Roller, P. P., Kleinman, H. K. and Yamada, Y. (1995). Identification of cell binding sites in the laminin alpha 1 chain carboxyl-terminal globular domain by systematic screening of synthetic peptides. *J. Biol. Chem.* **270,** 20583-20590.

Nunes, S. S., Outeiro-Bernstein, M. A., Juliano, L., Vardiero, F., Nader, H. B., Woods, A., Legrand, C. and Morandi, V. (2008). Syndecan-4 contributes to endothelial tubulogenesis through interactions with two motifs inside the pro-angiogenic N-terminal domain of thrombospondin-1. *J. Cell. Physiol.* **214,** 828-837.

Occleston, N. L., O'Kane, S., Goldspink, N. and Ferguson, M. W. (2008). New therapeutics for the prevention and reduction of scarring. *Drug Discov. Today* **13,** 973-981.

Okumura, K., Kiyohara, Y., Komada, F., Iwakawa, S., Hirai, M. and Fuwa, T. (1990). Improvement in wound healing by epidermal growth factor (EGF) ointment. I. effect of nafamostat, gabexate, or gelatin on stabilization and efficacy of EGF. *Pharm. Res.* **7,** 1289-1293.

Okwueze, M. I., Cardwell, N. L., Pollins, A. C. and Nanney, L. B. (2007). Modulation of porcine wound repair with a transfected ErbB3 gene and relevant EGF-like ligands. *J. Invest. Dermatol.* **127,** 1030-1041.

Oliveira, P. C., Meireles, G. C., dos Santos, N. R., de Carvalho, C. M., de Souza, A. P., dos Santos, J. N. and Pinheiro, A. L. (2008). The use of light photobiomodulation on the treatment of second-degree burns: A histological study of a rodent model. *Photomed. Laser Surg.* **26,** 289-299.

Ovington, L. (2003). Bacterial toxins and wound healing. *Ostomy Wound. Manage.* **49,** 8-12.

Pardes, J. B., Takagi, H., Martin, T. A., Ochoa, M. S. and Falanga, V. (1995). Decreased levels of alpha 1(I) procollagen mRNA in dermal fibroblasts grown on fibrin gels and in response to fibrinopeptide B. *J. Cell. Physiol.* **162,** 9-14.

Parenti, A., Brogelli, L., Filippi, S., Donnini, S. and Ledda, F. (2002). Effect of hypoxia and endothelial loss on vascular smooth muscle cell responsiveness to VEGF-A: Role of flt-1/VEGF-receptor-1. *Cardiovasc. Res.* **55,** 201-212.

Pastore, D., Greco, M. and Passarella, S. (2000). Specific helium-neon laser sensitivity of the purified cytochrome c oxidase. *Int. J. Radiat. Biol.* **76,** 863-870.

Pastore, D., Greco, M., Petragallo, V. A. and Passarella, S. (1994). Increase in <--H+/e- ratio of the cytochrome c oxidase reaction in mitochondria irradiated with helium-neon laser. *Biochem. Mol. Biol. Int.* **34,** 817-826.

Payne, W. G., Salas, R. E., Ko, F., Naidu, D. K., Donate, G., Wright, T. E. and Robson, M. C. (2008). Enzymatic debriding agents are safe in wounds with high bacterial bioburdens and stimulate healing. *Eplasty* **8,** e17.

Peplow, P. V., Chung, T. Y. and Baxter, G. D. (2010). Laser photobiomodulation of proliferation of cells in culture: A review of human and animal studies. *Photomed. Laser Surg.* **28 Suppl 1,** S3-40.

Pereira, A. N., Eduardo Cde, P., Matson, E. and Marques, M. M. (2002). Effect of low-power laser irradiation on cell growth and procollagen synthesis of cultured fibroblasts. *Lasers Surg. Med.* **31,** 263-267.

Pessoa, E. S., Melhado, R. M., Theodoro, L. H. and Garcia, V. G. (2004). A histologic assessment of the influence of low-intensity laser therapy on wound healing in steroid-treated animals. *Photomed. Laser Surg.* **22,** 199-204.

Pierce, G. F., Tarpley, J. E., Tseng, J., Bready, J., Chang, D., Kenney, W. C., Rudolph, R., Robson, M. C., Vande Berg, J. and Reid, P. (1995). Detection of platelet-derived growth factor (PDGF)-AA in actively healing human wounds treated with recombinant PDGF-BB and absence of PDGF in chronic nonhealing wounds. *J. Clin. Invest.* **96,** 1336-1350.

Pinheiro, A. L., Meireles, G. C., de Barros Vieira, A. L., Almeida, D., Carvalho, C. M. and dos Santos, J. N. (2004). Phototherapy improves healing of cutaneous wounds in nourished and undernourished wistar rats. *Braz. Dent. J.* **15 Spec No,** SI21-8.

Plikus, M. V., Mayer, J. A., de la Cruz, D., Baker, R. E., Maini, P. K., Maxson, R. and Chuong, C. M. (2008). Cyclic dermal BMP signalling regulates stem cell activation during hair regeneration. *Nature* **451,** 340-344.

Pontinen, P. J., Aaltokallio, T. and Kolari, P. J. (1996). Comparative effects of exposure to different light sources (he-ne laser, InGaAl diode laser, a specific type of noncoherent LED) on skin blood flow for the head. *Acupunct. Electrother. Res.* **21,** 105-118.

Posten, W., Wrone, D. A., Dover, J. S., Arndt, K. A., Silapunt, S. and Alam, M. (2005). Low-level laser therapy for wound healing: Mechanism and efficacy. *Dermatol. Surg.* **31,** 334-340.

Postlethwaite, A. E. and Kang, A. H. (1976). Collagen-and collagen peptide-induced chemotaxis of human blood monocytes. *J. Exp. Med.* **143,** 1299-1307.

Postlethwaite, A. E., Seyer, J. M. and Kang, A. H. (1978). Chemotactic attraction of human fibroblasts to type I, II, and III collagens and collagen-derived peptides. *Proc. Natl. Acad. Sci. U. S. A.* **75,** 871-875.

Pourreau-Schneider, N., Ahmed, A., Soudry, M., Jacquemier, J., Kopp, F., Franquin, J. C. and Martin, P. M. (1990). Helium-neon laser treatment transforms fibroblasts into myofibroblasts. *Am. J. Pathol.* **137,** 171-178.

Powell, D. W., Mifflin, R. C., Valentich, J. D., Crowe, S. E., Saada, J. I. and West, A. B. (1999). Myofibroblasts. I. paracrine cells important in health and disease. *Am. J. Physiol.* **277,** C1-9.

Prabhu, V., Rao, S. B., Rao, N. B., Aithal, K. B., Kumar, P. and Mahato, K. K. (2010). Development and evaluation of fiber optic probe-based helium-neon low-level laser therapy system for tissue regeneration-an in vivo experimental study. *Photochem. Photobiol.*

Radice, M., Brun, P., Bernardi, D., Fontana, C., Cortivo, R. and Abatangelo, G. (1999). Clostridial collagenase releases bioactive fragments from extracellular matrix molecules. *J. Burn Care Rehabil.* **20,** 282-291.

Raffetto, J. D., Mendez, M. V., Marien, B. J., Byers, H. R., Phillips, T. J., Park, H. Y. and Menzoian, J. O. (2001). Changes in cellular motility and cytoskeletal actin in fibroblasts from patients with chronic venous insufficiency and in neonatal fibroblasts in the presence of chronic wound fluid. *J. Vasc. Surg.* **33,** 1233-1241.

Rai, N. K., Tripathi, K., Sharma, D. and Shukla, V. K. (2005). Apoptosis: A basic physiologic process in wound healing. *Int. J. Low Extrem Wounds* **4,** 138-144.

Ramsey, S. D., Newton, K., Blough, D., McCulloch, D. K., Sandhu, N., Reiber, G. E. and Wagner, E. H. (1999). Incidence, outcomes, and cost of foot ulcers in patients with diabetes. *Diabetes Care* **22,** 382-387.

Ramundo, J. and Gray, M. (2008). Enzymatic wound debridement. *J. Wound Ostomy Continence Nurs.* **35,** 273-280.

Rayment, E. A., Dargaville, T. R., Shooter, G. K., George, G. A. and Upton, Z. (2008). Attenuation of protease activity in chronic wound fluid with bisphosphonate-functionalised hydrogels. *Biomaterials* **29,** 1785-1795.

Reddy, G. K. (2003). Comparison of the photostimulatory effects of visible he-ne and infrared ga-as lasers on healing impaired diabetic rat wounds. *Lasers Surg. Med.* **33,** 344-351.

Reddy, G. K., Stehno-Bittel, L. and Enwemeka, C. S. (2001). Laser photostimulation accelerates wound healing in diabetic rats. *Wound Repair Regen.* **9,** 248-255.

Reddy, M., Gill, S. S. and Rochon, P. A. (2006). Preventing pressure ulcers: A systematic review. *JAMA* **296,** 974-984.

Reid, R. R., Said, H. K., Mogford, J. E. and Mustoe, T. A. (2004). The future of wound healing: Pursuing surgical models in transgenic and knockout mice. *J. Am. Coll. Surg.* **199,** 578-585.

Reigle, K. L., Di Lullo, G., Turner, K. R., Last, J. A., Chervoneva, I., Birk, D. E., Funderburgh, J. L., Elrod, E., Germann, M. W., Surber, C. et al. (2008). Non-enzymatic glycation of type I collagen diminishes collagen-proteoglycan binding and weakens cell adhesion. *J. Cell. Biochem.* **104,** 1684-1698.

Reis, S. R., Medrado, A. P., Marchionni, A. M., Figueira, C., Fracassi, L. D. and Knop, L. A. (2008). Effect of 670-nm laser therapy and dexamethasone on tissue repair: A histological and ultrastructural study. *Photomed. Laser Surg.* **26,** 307-313.

Rhodes, J. M. and Simons, M. (2007). The extracellular matrix and blood vessel formation: Not just a scaffold. *J. Cell. Mol. Med.* **11,** 176-205.

Ribeiro, M. A., Albuquerque, R. L.,Jr, Ramalho, L. M., Pinheiro, A. L., Bonjardim, L. R. and Da Cunha, S. S. (2009). Immunohistochemical assessment of myofibroblasts and lymphoid cells during wound healing in rats subjected to laser photobiomodulation at 660 nm. *Photomed. Laser Surg.* **27,** 49-55.

Riley, K. N. and Herman, I. M. (2005). Collagenase promotes the cellular responses to injury and wound healing in vivo. *J. Burns Wounds* **4,** e8.

Riley, K. N., Maldonado, A. E., Tellier, P., D'Souza-Schorey, C. and Herman, I. M. (2003). Betacap73-ARF6 interactions modulate cell shape and motility after injury in vitro. *Mol. Biol. Cell* **14,** 4155-4161.

Robinet, A., Fahem, A., Cauchard, J. H., Huet, E., Vincent, L., Lorimier, S., Antonicelli, F., Soria, C., Crepin, M., Hornebeck, W. et al. (2005). Elastin-

derived peptides enhance angiogenesis by promoting endothelial cell migration and tubulogenesis through upregulation of MT1-MMP. *J. Cell. Sci.* **118,** 343-356.

Robson, M. C., Phillips, L. G., Heggers, J. P., McPherson, M. A. and Heiner, L. S. (1991). Clinical studies on growth factors in pressure sores: Preliminary report. *Prog. Clin. Biol. Res.* **365,** 95-102.

Robson, M. C., Phillips, T. J., Falanga, V., Odenheimer, D. J., Parish, L. C., Jensen, J. L. and Steed, D. L. (2001). Randomized trial of topically applied repifermin (recombinant human keratinocyte growth factor-2) to accelerate wound healing in venous ulcers. *Wound Repair Regen.* **9,** 347-352.

Rosdahl, C. B. and Kowalski, M. T. (2008). *Textbook of Basic Nursing*, pp. 1741. Philadelphia: Lippincott Williams & Wilkins.

Rosenberg, L., Lapid, O., Bogdanov-Berezovsky, A., Glesinger, R., Krieger, Y., Silberstein, E., Sagi, A., Judkins, K. and Singer, A. J. (2004). Safety and efficacy of a proteolytic enzyme for enzymatic burn débridement: A preliminary report. *Burns* **30,** 843-850.

Roy, R., Zhang, B. and Moses, M. A. (2006). Making the cut: Protease-mediated regulation of angiogenesis. *Exp. Cell Res.* **312,** 608-622.

Sabatier, L., Chen, D., Fagotto-Kaufmann, C., Hubmacher, D., McKee, M. D., Annis, D. S., Mosher, D. F. and Reinhardt, D. P. (2009). Fibrillin assembly requires fibronectin. *Mol. Biol. Cell* **20,** 846-858.

Schultz, G. S., Sibbald, R. G., Falanga, V., Ayello, E. A., Dowsett, C., Harding, K., Romanelli, M., Stacey, M. C., Teot, L. and Vanscheidt, W.

(2003). Wound bed preparation: A systematic approach to wound management. *Wound Repair Regen.* **11 Suppl 1,** S1-28.

Seidman, C., Raffetto, J. D., Marien, B., Kroon, C., Seah, C. C. and Menzoian, J. O. (2003). bFGF-induced alterations in cellular markers of senescence in growth-rescued fibroblasts from chronic venous ulcer and venous reflux patients. *Annals of Vascular Surgery* **17,** 239-244.

Seifert, O. and Mrowietz, U. (2009). Keloid scarring: Bench and bedside. *Arch. Dermatol. Res.* **301,** 259-272.

Senger, D. R., Claffey, K. P., Benes, J. E., Perruzzi, C. A., Sergiou, A. P. and Detmar, M. (1997). Angiogenesis promoted by vascular endothelial growth factor: Regulation through alpha1beta1 and alpha2beta1 integrins. *Proc. Natl. Acad. Sci. U. S. A.* **94,** 13612-13617.

Senger, D., Galli, S., Dvorak, A., Perruzzi, C., Harvey, V. and Dvorak, H. (1983). Tumor cells secrete a vascular permeability factor that promotes accumulation of ascites fluid. *Science* **219,** 983-985.

Senior, R. M., Griffin, G. L. and Mecham, R. P. (1980). Chemotactic activity of elastin-derived peptides. *J. Clin. Invest.* **66,** 859-862.

Sennoune, S. R., Bakunts, K., Martinez, G. M., Chua-Tuan, J. L., Kebir, Y., Attaya, M. N. and Martinez-Zaguilan, R. (2004). Vacuolar H+-ATPase in human breast cancer cells with distinct metastatic potential: Distribution and functional activity. *Am. J. Physiol. Cell. Physiol.* **286,** C1443-52.

Shah, M., Foreman, D. M. and Ferguson, M. W. (1995). Neutralisation of TGF-beta 1 and TGF-beta 2 or exogenous addition of TGF-beta 3 to cutaneous rat wounds reduces scarring. *J. Cell. Sci.* **108 (Pt 3),** 985-1002.

Shai, A. and Halevy, S. (2005). Direct triggers for ulceration in patients with venous insufficiency. *Int. J. Dermatol.* **44,** 1006-1009.

Sharma, A., Singh, A. K., Warren, J., Thangapazham, R. L. and Maheshwari, R. K. (2006). Differential regulation of angiogenic genes in diabetic wound healing. *J. Invest. Dermatol.* **126,** 2323-2331.

Shi, L., Ermis, R., Garcia, T., Telgenhoff, D. and Aust, D. (2009). *Wound Repair and Regeneration. Abstracts of 19th Annual Meeting of the Wound Healing Society SAWC/WHS Joint Meeting.* **17,** A34.

Shiva, S. and Gladwin, M. T. (2009). Shining a light on tissue NO stores: Near infrared release of NO from nitrite and nitrosylated hemes. *J. Mol. Cell. Cardiol.* **46,** 1-3.

Sieggreen, M. Y. and Kline, R. A. (2004). Arterial insufficiency and ulceration: Diagnosis and treatment options. *Nurse Pract.* **29,** 46-52.

Simon, H. U., Haj-Yehia, A. and Levi-Schaffer, F. (2000). Role of reactive oxygen species (ROS) in apoptosis induction. *Apoptosis* **5,** 415-418.

Singer, A. J. and Clark, R. A. (1999). Cutaneous wound healing. *N. Engl. J. Med.* **341,** 738-746.

Singer, A. J. and Dagum, A. B. (2008). Current management of acute cutaneous wounds. *N. Engl. J. Med.* **359,** 1037-1046.

Skinner, S. M., Gage, J. P., Wilce, P. A. and Shaw, R. M. (1996). A preliminary study of the effects of laser radiation on collagen metabolism in cell culture. *Aust. Dent. J.* **41,** 188-192.

Smith, K. C. (2005). Laser (and LED) therapy is phototherapy. *Photomed. Laser Surg.* **23,** 78-80.

Smith, R. J., Birndorf, M., Gluck, G., Hammond, D. and Moore, W. D. (1992). The effect of low-energy laser on skin-flap survival in the rat and porcine animal models. *Plast. Reconstr. Surg.* **89,** 306-310.

Sobanko, J. F. and Alster, T. S. (2008). Efficacy of low-level laser therapy for chronic cutaneous ulceration in humans: A review and discussion. *Dermatol. Surg.* **34,** 991-1000.

Stojadinovic, O., Brem, H., Vouthounis, C., Lee, B., Fallon, J., Stallcup, M., Merchant, A., Galiano, R. D. and Tomic-Canic, M. (2005). Molecular pathogenesis of chronic wounds: The role of beta-catenin and c-myc in the inhibition of epithelialization and wound healing. *Am. J. Pathol.* **167,** 59-69.

Stojadinovic, O., Pastar, I., Vukelic, S., Mahoney, M. G., Brennan, D., Krzyzanowska, A., Golinko, M., Brem, H. and Tomic-Canic, M. (2008). Deregulation of keratinocyte differentiation and activation: A hallmark of venous ulcers. *J. Cell. Mol. Med.*

Sun, G. and Tuner, J. (2004). Low-level laser therapy in dentistry. *Dent. Clin. North Am.* **48,** 1061-76, viii.

Sussman, C. and Bates-Jensen, B. M. (2007). *Wound Care : A Collaborative Practice Manual for Health Professionals*, pp. 720. Philadelphia, PA: Lippincott Williams & Wilkins.

Sutherland, J. C. (2002). Biological effects of polychromatic light. *Photochem. Photobiol.* **76,** 164-170.

Suzuma, K., Takagi, H., Otani, A. and Honda, Y. (1998). Hypoxia and vascular endothelial growth factor stimulate angiogenic integrin expression in bovine retinal microvascular endothelial cells. *Invest. Ophthalmol. Vis. Sci.* **39,** 1028-1035.

Tam, C. C. and Elston, D. M. (2006). Allergic contact dermatitis caused by white petrolatum on damaged skin. *Dermatitis* **17,** 201-203.

Tamm, E. R., Siegner, A., Baur, A. and Lutjen-Drecoll, E. (1996). Transforming growth factor-beta 1 induces alpha-smooth muscle-actin expression in cultured human and monkey trabecular meshwork. *Exp. Eye Res.* **62,** 389-397.

ten Dijke, P. and Arthur, H. M. (2007). Extracellular control of TGFbeta signalling in vascular development and disease. *Nat. Rev. Mol. Cell Biol.* **8,** 857-869.

Tomasek, J. J., Gabbiani, G., Hinz, B., Chaponnier, C. and Brown, R. A. (2002). Myofibroblasts and mechano-regulation of connective tissue remodelling. *Nat. Rev. Mol. Cell Biol.* **3,** 349-363.

Tomic-Canic, M., Ayello, E. A., Stojadinovic, O., Golinko, M. S. and Brem, H. (2008). Using gene transcription patterns (bar coding scans) to guide wound debridement and healing. *Adv. Skin Wound Care* **21,** 487-92; quiz 493-4.

Tran, K. T., Lamb, P. and Deng, J. S. (2005). Matrikines and matricryptins: Implications for cutaneous cancers and skin repair. *J. Dermatol. Sci.* **40,** 11-20.

Tuner, J. and Hode, L. (1998). It's all in the parameters: A critical analysis of some well-known negative studies on low-level laser therapy. *J. Clin. Laser Med. Surg.* **16,** 245-248.

Turkmen, A., Graham, K. and McGrouther, D. A. (2009). Therapeutic applications of the larvae for wound debridement. *J. Plast. Reconstr. Aesthet. Surg.*

Usui, M. L., Mansbridge, J. N., Carter, W. G., Fujita, M. and Olerud, J. E. (2008). Keratinocyte migration, proliferation, and differentiation in chronic ulcers from patients with diabetes and normal wounds. *J. Histochem. Cytochem.* **56,** 687-696.

Vacca, R. A., Marra, E., Passarella, S., Petragallo, V. A. and Greco, M. (1996). Increase in cytosolic and mitochondrial protein synthesis in rat hepatocytes irradiated in vitro by he-ne laser. *J. Photochem. Photobiol. B.* **34,** 197-202.

van Horssen, R., Janssen, E., Peters, W., van de Pasch, L., Lindert, M. M., van Dommelen, M. M., Linssen, P. C., Hagen, T. L., Fransen, J. A. and Wieringa, B. (2009). Modulation of cell motility by spatial repositioning of enzymatic ATP/ADP exchange capacity. *J. Biol. Chem.* **284,** 1620-1627.

Vasilenko, T., Slezak, M., Kovac, I., Bottkova, Z., Jakubco, J., Kostelnikova, M., Tomori, Z. and Gal, P. (2010). The effect of equal daily dose achieved by different power densities of low-level laser therapy at 635 and 670 nm on wound tensile strength in rats: A short report. *Photomed. Laser Surg.* **28,** 281-283.

Vasquez, R., Marien, B. J., Gram, C., Goodwin, D. G., Menzoian, J. O. and Raffetto, J. D. (2004). Proliferative capacity of venous ulcer wound fibroblasts in the presence of platelet-derived growth factor. *Vasc. Endovascular Surg.* **38,** 355-360.

Viegas, V. N., Abreu, M. E., Viezzer, C., Machado, D. C., Filho, M. S., Silva, D. N. and Pagnoncelli, R. M. (2007). Effect of low-level laser therapy on inflammatory reactions during wound healing: Comparison with meloxicam. *Photomed. Laser Surg.* **25,** 467-473.

Vladimirov, Y., Borisenko, G., Boriskina, N., Kazarinov, K. and Osipov, A. (2000). NO–hemoglobin may be a light-sensitive source of nitric oxide both in solution and in red blood cells. *Journal of Photochemistry and Photobiology B: Biology* **59,** 115-122.

Walker, D. J. (1999). Venous stasis wounds. *Orthop. Nurs.* **18,** 65-74, 95.

Wang, H. and Keiser, J. A. (1998). Vascular endothelial growth factor upregulates the expression of matrix metalloproteinases in vascular smooth muscle cells: Role of flt-1. *Circ. Res.* **83,** 832-840.

Weintraub, M. I. (1997). Noninvasive laser neurolysis in carpal tunnel syndrome. *Muscle Nerve* **20,** 1029-1031.

Welch, A. Y. and Herman, I. M. (2002). Cloning and characterization of betaCAP73, a novel regulator of beta-actin assembly. *Int. J. Biochem. Cell Biol.* **34,** 864-881.

Werdin, F., Tenenhaus, M. and Rennekampff, H. O. (2008). Chronic wound care. *Lancet* **372,** 1860-1862.

Werner, S., Breeden, M., Hubner, G., Greenhalgh, D. G. and Longaker, M. T. (1994). Induction of keratinocyte growth factor expression is reduced and delayed during wound healing in the genetically diabetic mouse. *J. Invest. Dermatol.* **103,** 469-473.

Werner, S. and Grose, R. (2003). Regulation of wound healing by growth factors and cytokines. *Physiol. Rev.* **83,** 835-870.

Weyrich, A. S. and Zimmerman, G. A. (2004). Platelets: Signaling cells in the immune continuum. *Trends Immunol.* **25,** 489-495.

Wijelath, E. S., Rahman, S., Namekata, M., Murray, J., Nishimura, T., Mostafavi-Pour, Z., Patel, Y., Suda, Y., Humphries, M. J. and Sobel, M. (2006). Heparin-II domain of fibronectin is a vascular endothelial growth factor-binding domain: Enhancement of VEGF biological activity by a singular growth factor/matrix protein synergism. *Circ. Res.* **99,** 853-860.

Wilgus, T. A., Ferreira, A. M., Oberyszyn, T. M., Bergdall, V. K. and Dipietro, L. A. (2008). Regulation of scar formation by vascular endothelial growth factor. *Lab. Invest.* **88,** 579-590.

Wilchek, M. and Bayer, E. A. (1990). Introduction to avidin-biotin technology. *Methods Enzymol.* **184,** 5-13.

Wolcott, R. D., Rhoads, D. D. and Dowd, S. E. (2008). Biofilms and chronic wound inflammation. *J. Wound Care* **17,** 333-341.

Wong-Riley, M. T., Liang, H. L., Eells, J. T., Chance, B., Henry, M. M., Buchmann, E., Kane, M. and Whelan, H. T. (2005). Photobiomodulation directly benefits primary neurons functionally inactivated by toxins: Role of cytochrome c oxidase. *J. Biol. Chem.* **280,** 4761-4771.

Xie, J., Bian, H., Qi, S., Xu, Y., Tang, J., Li, T. and Liu, X. (2008). Effects of basic fibroblast growth factor on the expression of extracellular matrix and matrix metalloproteinase-1 in wound healing. *Clin. Exp. Dermatol.* **33,** 176-182.

Xu, J., Rodriguez, D., Petitclerc, E., Kim, J. J., Hangai, M., Moon, Y. S., Davis, G. E. and Brooks, P. C. (2001). Proteolytic exposure of a cryptic site within collagen type IV is required for angiogenesis and tumor growth in vivo. *J. Cell Biol.* **154,** 1069-1079.

Yao, J., Liu, Y., Wang, X., Shen, Y., Yuan, S., Wan, Y. and Jiang, Q. (2009). UVB radiation induces human lens epithelial cell migration via NADPH oxidase-mediated generation of reactive oxygen species and up-regulation of matrix metalloproteinases. *Int. J. Mol. Med.* **24,** 153-159.

Yates, J. R.,3rd, Eng, J. K., McCormack, A. L. and Schieltz, D. (1995). Method to correlate tandem mass spectra of modified peptides to amino acid sequences in the protein database. *Anal. Chem.* **67,** 1426-1436.

Ye, J., Lee, S. Y., Kook, K. H. and Yao, K. (2008). Bone marrow-derived progenitor cells promote corneal wound healing following alkali injury. *Graefes Arch. Clin. Exp. Ophthalmol.* **246,** 217-222.

Yost, J. C. and Herman, I. M. (1990). Substratum-induced stress fiber assembly in vascular endothelial cells during spreading in vitro. *J. Cell. Sci.* **95 (Pt 3),** 507-520.

Yu, W., Naim, J. O. and Lanzafame, R. J. (1997). Effects of photostimulation on wound healing in diabetic mice. *Lasers Surg. Med.* **20,** 56-63.

Zhang, R., Mio, Y., Pratt, P. F., Lohr, N., Warltier, D. C., Whelan, H. T., Zhu, D., Jacobs, E. R., Medhora, M. and Bienengraeber, M. (2009). Near infrared light protects cardiomyocytes from hypoxia and reoxygenation injury by a nitric oxide dependent mechanism. *J. Mol. Cell. Cardiol.* **46,** 4-14.

Zhang, Y., Song, S., Fong, C. C., Tsang, C. H., Yang, Z. and Yang, M. (2003). cDNA microarray analysis of gene expression profiles in human fibroblast cells irradiated with red light. *J. Invest. Dermatol.* **120,** 849-857.

Zheng, Y., Zhao, Y. D., Gibbons, M., Abramova, T., Chu, P. Y., Ash, J. D., Cunningham, J. M. and Skapek, S. X. Tgfβ signaling directly induces arf promoter remodeling by a mechanism involving smads 2/3 and p38 mapk. *Journal of Biological Chemistry*.